Advances in the Photovoltaic Field through Light Manipulation

IVANA VALIDŽIĆ

Advances in the Photovoltaic Field through Light Manipulation

Advances in the Photovoltaic Field through Light Manipulation

By

Ivana Validžić

Cambridge Scholars Publishing

Advances in the Photovoltaic Field through Light Manipulation

By Ivana Validžić

This book first published 2022

Cambridge Scholars Publishing

Lady Stephenson Library, Newcastle upon Tyne, NE6 2PA, UK

British Library Cataloguing in Publication Data
A catalogue record for this book is available from the British Library

ISBN (10): 1-5275-8263-9
ISBN (13): 978-1-5275-8263-7

Diversity is another name for science because it leads to innovation.
Through innovation, people have been able to recognize and better understand many natural phenomena throughout history.
This is one such story.

TABLE OF CONTENTS

PREFACE

The term "discovery" in science in the past has usually been called the product of successful investigation. The tests were mainly performed with the help of constructions or aids in science, which today we call innovations in that aspect. Many scientific phenomena and effects in the past were unknown, so researchers were able to observe and try to explain them with the help of a designed and engineered aid (i.e., the whole experiment). People had to be much more inventive in performing experiments and designing the various aids mentioned in performing scientific experiments due to the lack of today's technologies and scientific instruments. This difference in the performance of scientific experiments has contributed to the possibility of looking at discoveries from diverse perspectives (we often say the possibility of looking at a problem from a completely different angle than usual), and this is exactly what leads to a better understanding of science and discoveries in general. As science developed, so did the new generation of instruments for their performance and measurement. With the development of instruments and digitalization, there was a need for uniformity in science. Uniformity has largely eliminated the innovative element of scientific research in terms of the fact that uniformity stands on the opposing side of diversity.

NOTES FOR THE READER

Through this part of the text, I would like to take you through a story whose meaning should be the will and desire to do something, as well as the fact that when you own it, then other mostly material things that you do not have will work in your favor and not to your detriment. In this part of the text, I will try to write in the simplest possible way without going into scientific details as much as possible, in the hope that this note can be understood by the general population, anyone interested in science and research, as well as anyone wanting to learn more about the use of solar energy.

This story related to work in the photovoltaic field began approximately decades ago with syntheses of the semiconductor antimony sulfide, Sb_2S_3. This semiconductor, which belongs to the V-VI group, is well-known to be suitable and quite promising as a material for application in the solar cell. We were extremely surprised concerning the insufficient knowledge about the mentioned semiconductor, which is considered, according to the scientific literature, to be promising for application in every respect of the electronic and optical properties relevant to the application. So, the first steps were to perform high-temperature organic synthesis for the purpose of understanding the growth mechanism and obtaining non-doped and doped Sb_2S_3 amorphous and crystalline nanoparticles of different shapes. Both the growth mechanism and the nanoparticle morphology are quite important for solar device applications. The kinetic control of the reaction allowed tuning of the electronic properties such as the optical bandgap of the nanoparticles, while the shape of the synthesized nanoparticles can play a significant role in electron transfer in the designed solar devices. For example, high aspect ratio nanowires are desirable for industrial applications, whereas small bandgap energy-designed materials are suitable as absorbers for solar cells (the main issue with this material is the optical band gap (found in the literature ranging from 1.7–2.2 eV), which is slightly higher than the ideal value (~1.4 eV) for a solar cell absorber). As a result, Sb_2S_3 with a small bandgap could be an intriguing semiconductor with unique optoelectronic properties. Unfortunately, as we already mentioned, many electronic and optical properties were not known at that time, nor were any reported syntheses of doped antimony sulfide nanoparticles. Therefore, our research related to the synthesis of applicable nanoparticles of this semiconductor, as well as the experimental characterization of the obtained material, had to go hand in hand with theoretical derivations. The theory had to be confirmed and help the experiments better understand the obtained material, i.e., the mentioned material in general. By combining experimental and theoretical results, confirmations, and help from both sides, we can know we are on the right track to learning things about materials for which we have insufficient knowledge. We will give just one example of the importance of the above-written piece in an understandable way to a broader audience of readers. Generally speaking, nanoparticles are synthesized in the domain of materials not only to have smaller dimensions but also to distinguish their unique electronic properties from those of bulk material. For those synthesized nanoparticles to fulfill the demand for different electronic properties compared to bulk materials, they must reach certain nano dimensions, which are different for different semiconductors. That effect is named the quantum confinement or size effect. In theory, quantum confinement effects become significant when one dimension of the nanocrystal approaches the de Broglie wavelength of electrons and holes in bulk semiconductors, $\lambda_e = h / (2m_{eff}\,kT)^{1/2}$, where m_{eff} is the effective mass of the electron (or hole for λ_h). λ_e and λ_h are typically 10–100 nm for most semiconductors. Unfortunately, we were unable to locate effective mass values for Sb_2S_3 in the literature. We discovered a lot of literature claiming to have observed quantum size effects when one dimension of a nanocrystal is quite large (50–100 nm, and even larger) and it receives a band-gap energy value of more than 1.7–1.8 eV. We are adamant that this problem be resolved. Furthermore, the excitons' Bohr radius, a_{ex}, which describes the characteristic separation of a bound electron-hole pair in a bulk semiconductor, is an important length scale. Excitons are quasiparticles composed of bound electron–hole pairs that are attracted to one another via the Coulomb potential. Because the exciton binding energy in most bulk semiconductors is low in comparison to kT at room temperature, electrons and holes are not bound. However, when the dimensions of the synthesized semiconductor nanoparticles are reduced to less than the a_{ex}, quantum size effects begin to play an important role. It was the theory combined with the experiments that provided us with the answer about the critical particle size that we have to reach to be able to invoke the effect, while all previous claims about the quantum size effect were reduced to an assumption. At that time, in the infancy of the development of materials for application in solar cells, in 2012 I gave a lecture at an international conference in Rhodes, where I met Prof. Dr. Daniela Vanmaekelberg from the University of Utrecht. Since I was a Ph.D. student and received my doctorate at Utrecht University, I knew the professor from previous collaborations with his group. Because of my work on the development of antimony sulfide semiconductor materials for possible use in solar cells, the professor invited me to attend the Quantsol workshop, organized by the European Society for Quantum Solar Energy Conversion, of which he is president. I was delighted with his invitation and joined the meetings the following year. The group was built by eminent professors who dealt with solar cells, materials, and theoretical physics. Until that time in our research, we mostly dealt with the synthesis and characterization of materials, both experimental and theoretical, and from that point, it was clear that we would have to go a step further toward the application and production of solar cells to show the application side of our synthesized material. Since then, our story related in the first place to the design of solar devices has begun.

Considering that no one in our institute was previously involved in the design of solar cells and that the infrastructure did not exist, in the initial steps, it was difficult. We only had instruments, such as a nano voltmeter and a multimeter, to measure the current-voltage dependence and the dark current. Because our first synthesized materials were crystal samples of antimony sulfide semiconductors, which morphologically included only elongated shapes such as wires, rods, and bars, many methods of film deposition, such as deep and speed coating, were not useful. Having no further infrastructure that could help us, we set out to manually design and build a system for dispersing synthesized nanoparticles and making films on the conductive glass that has been advanced over time. It should be emphasized that making perfect films from a synthesized semiconductor nanoparticle on a conducting glass as one of the electrodes is one of the first steps in making solar cells. Over time, there have been many attempts to improve the design of solar cells, which primarily refer to good contacts in the cell, cheap solutions for the second electrode, an attempt to replace the liquid electrolyte with the synthesis of cheap electrolyte carriers, and the cheaper and more economical synthesis of conductive polymers. We should only mention here in general that cheap technology and the design of solar cells are crucial because the market is always seeking, and always will, more inexpensive solutions than the existing ones. However, it should be emphasized that the ratio of cost to efficiency represents the true measure of an economic solution.

The next problem we encountered was a sun simulator, for which we did not have the resources to provide, so we had to solve the problems of illumination devices as well as cool the surface of the solar cell. We purchased halogen and tungsten lamps, whose spectra closely matched that of outdoor light, to illuminate the solar devices we built. It should be emphasized that in indoor measurements on experimentally made solar cells, various artificial light lamps are used, which simulate outdoor lighting well, xenon, halogen, tungsten, and others. These same types of light lamps are also found in sun simulators. To solve the problem of cooling the surface of the solar cell, we created optics with flowing water in which the water that serves for cooling is not in direct contact with the solar cell. Since the cooling system also contains an optical segment, convex lenses, we could change the intensity of light as well as their spectra, which can affect the current-voltage response of the solar cell. It should be emphasized that cooling the surface of solar cells and panels is extremely important, both at higher intensities and at lower intensities on a longer time scale, because of the devastating effect of temperature on the material from which solar cells and panels are made, and so for their longer life.

In the beginning, we were not even aware of how much this construction of the optics with indirect cooling of the surface of the solar cell or panel would help us manipulate the spectra at higher as well as lower light intensities, nor did we understand the significance of that. In addition, the issue of cooling the surface of the solar panel was significant for the life and durability of solar panels, especially at higher light intensities and concentration effects. At the time when we constructed optics, only sporadic scientific papers showed that even at lower light intensities (depending on the lamp used, which is usually associated with the difference in radiation spectra apart from another possible light effect), we could get better efficiency from solar cells than at higher ones. From that moment, we start working toward manipulating light intensities and spectra to obtain a better photovoltaic response or efficiency and try to comprehend the obtained measurements on different solar cells and understand the possible additional light effects.

ACKNOWLEDGEMENTS

The book was written entirely by the author, but some of the results represented in the book are the cooperation with other scientists and their universities through jointly published scientific papers. Although the book is dedicated to optics and light manipulation as well as reflectance on the solar cell's measurements, the beginning of this research starts with the development of materials for solar cells. That is why everyone with whom the author has worked from the very beginning deserves gratitude. The author wishes to express his heartfelt gratitude to all of the scientists who, directly or indirectly, assisted him in his work or influenced the author's opinion or attitude formation.

The author would like to thank, in the first place, the closest associates from the Vinca Institute of Nuclear Science, the National Institute of the Republic of Serbia, Dr. Vesna Lojpur from the department of atomic physics, and Dr. Miodrag Mitrić from the department of theoretical physics and condensed matter physics for loyalty, support, and faithful follow-up in joint scientific work. The author would like to thank all the associates from my department for atomic physics, especially the coauthors, Dr. Maja Popović, Dr. Mirjana Novaković, Dr. Nenad Bundaleski, Dr. Zlatko Rakočević, Dr. Zorica Kačarević-Popović, and Dr. Nadica Abazović from the department of radiation chemistry and physics, and Dr. Filip Vukajlović and Dr. Zoran Popović from the department of theoretical physics and condensed matter physics. The author would like to thank former Ph.D. student Valentina Janošević from the department of radiation chemistry and physics. Further, the author is sincerely grateful to Prof. Dr. Giuseppe Marco Tina from the department of electrical, electronics, and computer engineering (DIEEI), University of Catania, as well as Dr. Marco Rosa-Clot from Koine Multimedia in Italy for their successful cooperation concerning scientific work on light and optics. The author owes special thanks to Prof. Dr. Daniël Vanmaekelbergh, Chair in Chemistry and Physics of Nanostructures at Utrecht University, and the President of the European Society for Quantum Solar Energy Conversion, as well as the entire society members and their meetings, in which I participate every year in Austria. I want to thank them for inviting and accepting me into their society and for inspiring me and encouraging me to continue further and better in my scientific work. Furthermore, I would like to thank Dr. Marina Freitag from Uppsala

University (department of chemistry, Angstrom Laboratory, Sweden) for producing dye-sensitized solar cells for our optical measurements. And last but not least, I would like to mention and thank my last cooperation through a common project on the further synthesis and improvement of semiconductor nanoparticles for solar cell applications, Prof. Dr. Christina Graf and Joschko Maximilian from the University of Applied Sciences, Hochschule Darmstadt in Germany.

CHAPTER ONE

LIGHT MANIPULATION AND INNOVATION

General introduction and problems in photovoltaics

Environmental exploitation caused by the traditional harvesting of energy (combustion of fossil fuels), as well as the fact that the overall reserves of global energy potential (natural gas, uranium, coal, oil) have been drastically reduced recently, lead to the immediate search for alternative energy sources.[1,2] Sunlight, biomass, wind, and marine energy are vital and renewable energy sources for the twenty-first century.[3-6] Their potential utilization is still unsatisfactory. Among these cost-free renewable sources of energy, solar energy is the most abundant. However, the use of solar energy compared to the potential is still negligible. In a single hour, the amount of power from the sun that strikes the Earth is more than the entire world consumes in a year. Light (or electromagnetic energy) can be harnessed for a variety of applications by converting energy from one form to another, of which the most important ones are generating electricity with photovoltaic (PV) cells and heating water. A solar cell, also called a PV cell, is a device that converts the energy of light into electrical energy through the photoelectric effect. In 2019, only 11% of global primary energy came from renewable technologies, and around 1% of global energy came from solar technologies. It is hard to believe that there is such a powerful source of energy as the sun without us being able to use it more efficiently than we have so far. Logically, there are things we do not understand well enough and, therefore, do not use effectively.

Most scientists in this field agree on a few facts about solar cells. One of them is that the low efficiency and high cost of currently used solar PV systems, a part of their reliability and durability, are one of the primary reasons for their reduced availability and usability.[7] For photovoltaics to become a more mainstream and pragmatic energy source, the efficiency of solar panels will need to improve drastically. This idea is in line with Goal 7 of the Sustainable Development Goals of the United Nations. It should be emphasized here that the reported maximum silicon (Si) solar cell efficiency is 29%, which is quite higher than the most efficient solar cells obtained in a laboratory, that is 25%[8] and large-area commercial, 24%[9,10] cells.[11]

It is clear that the most efficient crystalline Si-solar cells have almost reached their theoretical maximum efficiency, so it is not clear how efficiency could be increased “drastically’’ with today's knowledge. For now, the theoretical solar conversion efficiency maximum is around 33.7% for a single p-n junction with a bandgap of 1.4 eV, determined by the Stockley-Queisser Limit.[12] Apart from the fact that efficiency is not the only limiting parameter, in reality, the efficiency/cost ratio must be considered. Also, the fact that the most efficient crystalline Si-solar cell has almost reached its theoretical maximum efficiency means that the competitive product has to be significantly cheaper, apart from their reliability and durability, with still good efficiency. Further, polycrystalline and monocrystalline Si solar cells are leading the photo-voltaic market, constituting more than 93% of the market with a development history of nearly 70 years. All the other types of cheaper solar cells (dye-sensitized, thin-film PV, organic, perovskite, etc.) that are currently on the market or will appear soon as cheaper products, will hardly manage to compete with Si-solar cells in terms of material abundance, safety, and improved technology. We do not have decades before all fossil fuel reserves disappear to upgrade and improve new solar cells made from a material that is not even remotely represented as silicon. So, any cheaper type of current or new solar cell or module design can serve more as a backup than a replacement for Si-solar cells. Photovoltaic (PV) energy is on the edge of becoming one of the main global sources of energy, and crystalline silicon will dominate the market with no sign of change in the near future. As was mentioned, in the last 20 years of development, the efficiency of crystalline Si cells has increased from approximately 21% to 26%, reaching an almost theoretical maximum.[13,14] After so many years of improvements, it is difficult to find a way in which efficiency can be drastically increased through the design of solar cells or panels. Furthermore, a major issue in photovoltaics is reliability and durability, with material properties such as temperature resistance (cooling the surface of solar panels to maintain room temperature) being required to meet a photovoltaic product's longer lifetime warranty. The exposure of the material from which the solar panels are made to high temperatures (in the absence of a permanent cooling solution) changes the electronic properties of the material, such as the energy gap on which the photo effect depends. Other officially stated problems, such as manufacturability (searching for disruptive new cheap materials), subsidies (a challenge to the photovoltaic industry regarding subsidy problems), and regulation (competitiveness of photovoltaics to other energy sources), have either been mentioned or have an indirect impact on the mentioned challenges.

It should also be noted that the efficiency of solar cells is not the only or most important parameter in designing PV devices (the only parameter by which one should judge whether or not something is promising), particularly when it comes to their performance in low light. We've been attempting to comprehend the significance of low light and how it can be used, primarily for the purpose of comprehending it and then developing efficient PV devices. Standard low-light conditions have yet to be established, but they are required to exist as guidelines for our research. As a result, the efficiency of the PV devices under standard testing conditions (STC) should not be compared to efficiency under conditions that have not established the low light standard testing conditions. If we do not understand why the same solar devices exhibit higher efficiency at lower light intensities than at higher ones, it means that those values are incomparable. In this regard, perhaps the solid efficiency of cells at low light intensities with low-cost technology in the majority of Earth's conditions could compensate for the higher efficiency in rare and extreme conditions of the established standard testing conditions, STC (irradiation of 1000 W/m^2, module temperature of 25°C, and standard spectrum AM 1.5).[15-21] In other words, there is a good chance that cells with the same efficiency as those operating under the extreme conditions of standard testing conditions (STC) can be designed to have a specific spectral distribution of low-intensity light. Light cannot be changed at different intensities, but different designed lens systems can change its distribution at different wavelengths. This knowledge will be incorporated into future cell technology as soon as one understands how to change the spectral light distribution and determines the most optimum one for the fabricated low-light intensity cells with high efficiency.

Therefore, finding ways to improve the operating characteristics and the general efficiency of the available and currently developed technology by expanding our general knowledge, on the one hand, and trying to solve all the other more technical problems mentioned, on the other hand, are the most important tasks.

An optical system for cooling, light manipulation, and improvement of the photovoltage response of solar cells

In this part, it will be explained the significance and importance of light manipulation through innovation (water-flow-lens (WFL) system) for better and more efficient output (enhanced electricity production) of the tested solar devices, presented in this book. Manipulating sunlight spectra and intensity through innovative design to increase the efficiency of solar devices is one way to expand our knowledge of the effects of light and make significant progress toward better solar energy utilization. By the term "manipulation," we primarily allude to light phenomena for which we do not yet have an explanation, such as the dominantly higher efficiency of solar devices than expected at lower light intensities and non-uniform or non-linear basic current and voltage characteristics of the solar cells, which at least depend on the light spectra and intensity as well. Only with a better understanding of the light effects, we will make progress in harnessing the sun's energy. It should be noted that the amount of solar energy flux that reaches Earth is determined by the geographical area's latitude. Annual solar irradiation exceeds 1600 kWh/m^2 in some parts of the United States, Africa, the Middle East, and Australia. Other parts of the Earth receive far less solar irradiation, so it is critical to research and develop solar cells that can operate at lower light intensities. Along with developing new solar cells, the goal of the research is to achieve high efficiency at low light intensities.

Our original construction of the optics, the WFL system, technically solves the manipulation of light spectra and intensities while simultaneously cooling the surface of solar panels. In many published scientific papers[22–34], we explained the necessity of such a construction as well as the importance of manipulating light through the design of the WFL system for more efficient output of existing solar devices, and that is why we consider ourselves pioneers in this field of light manipulation, especially at lower light intensities. The optical systems for cooling, light manipulation, and improving the photovoltaic response of commercial solar panels are designed and built so that certain natural external changes are monitored and controlled by solving several technical problems at the same time. Apart from changes in the light spectra and intensity, there are also additional effects of the interaction of light with different environments on the way light reaches the surface of the solar cells. Usually, each of the above-mentioned issues, such as cooling the surface of solar panels or increasing light intensities to increase electricity production, is considered and solved separately. However, effects in nature related to heating, changes in the angle, intensity, and radiation spectrum of the sun are combined effects that act in nature simultaneously. It should be emphasized here that the designed optical system with a flowing water system allows us to combine several technical solutions into one optical system, the WFL system. This primarily refers to technical solutions, surface cooling, increasing and decreasing light intensities, as well as light spectra manipulations that are achieved after the passage of external light through the optical part with flowing water on the carrier. As was mentioned, additional light effects and the interaction of light with different environments have been studied through different experiments. Cooling of solar panels is extremely important and cannot be left out. Since solar panels are not in direct contact with water, this WFL system is significantly safer for cooling and allows solar panels to live longer since they are covered with optics. Simultaneously, the system enables cooling depending on the speed of water flow and at a concentration effect, i.e., far higher light intensities than standard test conditions. Further, the manipulation of light spectra at lower (lower than the standard test conditions (STC) of 1000 W/m^2) as well as higher light intensities (higher than STC) causes significant increases in the efficiency of solar panels, leading to higher electricity production.

The importance of the essence of this design will be explained in more detail below. We already mentioned that there were two directions for improving the photovoltaic area, i.e., the production of a larger amount of electricity from solar panels. One direction is related to the design of new solar panels or materials from which solar panels are made, as well as the design of photovoltaic devices, in order to achieve cheaper, more reliable, and durable products than today's most commonly used silicon solar cells.[35-37] Because of the still too high price of currently used solar panels, this direction could be called a low-cost approach. As we already mentioned in this chapter, this approach is not realistic to achieve (in a sense of silicon replacing) due to the theoretical maximum efficiency of Si-solar cells in a very extensively developed technology in the last 70 years on one hand, and the abundance of silicon on the other hand.

The second direction covers finding a more effective way to use already designed panels in terms of reducing the cost of electricity production or better utilization. This second direction includes everything required to maintain and use solar panels at their maximum possible use[38], and these are surface cooling systems for panels[39-41], optics to improve the photovoltaic response of solar panels[42-44], and a crucially important segment, which includes manipulating light intensities and light spectra (aside from the additional light effects)[45–47] to produce more electricity. Our designed optics with flowing water belongs to the second described direction of improving the operation of solar panels and the production of a larger amount of electricity. To additionally emphasize, by the term “manipulation of light intensities and spectra”, we primarily allude to light phenomena for which we do not yet have an explanation, such as the higher efficiency of solar devices primarily at lower light intensities, which clearly at least depends on the light spectra. Moreover, when we say there is no explanation, we primarily mean the additional light effects, which we still do not understand, and the real nature of light, both particles and waves, which should be in accordance with the observed effects.

It is widely acknowledged and accepted that one of the requirements for the successful application of solar panels is that the surfaces of the panels be kept at a tested temperature of 25 °C. [48-50] It should be noted that the change in solar panel efficiency is not strongly related to the tested temperature and occurs at temperatures lower or higher than the tested one, expressed as a percentage of temperature coefficients, illustrating the change in solar panel efficiency with increasing or decreasing temperature. As defined by the Standard Test Conditions (STC), an elevated test temperature greater than 25 °C causes a drop in the conversion rate of between 0.40 % and 0.65 % per degree Celsius. [51,52] Apart from the cooling technique, the increase in electrical efficiency is determined by the size and type of solar panel device, as well as the season of the year and geographical location (light intensity, light spectra reaching the surface of the solar panel, and the angle at which light falls) and increases overall efficiency and electricity, respectively. In general, the intensity of solar radiation and the quality of semiconductors from which the solar panel was made are factors we can control, while variations in solar radiation or solar spectra reaching the surface of the solar module cannot be controlled.[53] Broadly speaking, various semiconductors used in solar cell modules have different band gaps, which represent an electronic characteristic of a given material. As a result, the entire spectrum of solar radiation is ineffective for photoelectricity, and only photons with energies equal to or greater than the bandgap of the PV material used are useful. The remaining photons in the solar spectrum will dissipate their energy as heat, lowering the output of the PV cell or module. Therefore, we need to eliminate the unnecessary solar radiation spectrum (to avoid heating) and maintain the cell surface at an ambient temperature. This cannot be done if there is no filter/cooling system with a liquid, which results in changes in light intensity and spectra as light passes through different environments.[26] In this manner, realistic, reduced light intensities and the impact of altered light spectra on the efficiency of commercial solar panels are realities, and we should try to understand them. However, if we want to get higher electricity production and better use of solar energy, we have to manipulate different light intensities and different light spectra and try to understand all the additional light effects. This cannot be implemented without an optical design like the WFL system (or some similar construction), a system with the effect of cooling, reducing and increasing the light intensity, and modifying the light spectra that reach the surface of the solar panels, apart from the additional light effects that it can cause. When we talk about lower light intensities and light spectra, it should be emphasized that their changes are very important, as well as the interaction of light with the environment, which is also sometimes very complex to understand. By constructing an optical system with flowing water, we have shown so far that by modifying the light spectrum, for the same light intensity (both at lower and higher light intensities), the system, therefore, constructed, increases the efficiency of solar cells, in the first place of silicon solar cells, dye-sensitive solar cells, and our designed and based on synthesized doped and undoped antimony-sulfide solar cells.

Apart from intensity reduction and changes in the spectra, there is also an additional relevant issue concerning the fact that when narrowing down the spectral distribution, conversion efficiency increases significantly.[54,55] But when we go down in light intensity, and the fact is that we do that with any filter/cooling system, then things are not so simple and must be viewed from another perspective. Huge changes in the efficiency of the same device at low and lower light intensities can be produced by different artificial light sources that simulate outdoor radiation and which, in fact, have broadly similar spectra. Additionally, most experiments performed at lower light intensities have been carried out by using artificial light sources so far. For this reason, combining outdoor and indoor experiments could be one way of understanding the behavior of PV devices at both realistic, different spectra and low or lower light intensities. Besides, a significant concentration-effect should be mentioned. Broadly speaking, optical components have been used so far to concentrate sunlight and focus it on solar panels, increasing the light intensity several times. In this way, the production of electricity increases[56-58], but the mutual effect with the cooling system at the same time on the surface of the solar panels is not solved. Our designed WFL system enables cooling depending on the water flow velocity and with a concentration effect. The joint effects are very significant because they, as such, combine to exist in reality and work together. In the described construction, we combine everything that has been proven over years of research to be the best way to improve the operation of solar panels and increase electricity production, which is water. As a proven best medium for cooling, water flow because it has been shown to increase the electrical yield, manipulation of light intensity as well as light spectra that produce a better photovoltaic response, and the effect of concentration, which always increases the electrical yield. It is significant to emphasize here that the simulation of combined effects achieved by simulating external conditions leads to the effect of an increase in current production even at lower light intensities with appropriate light spectra. Through experiments, the optical construction made in this way helps us try to go deeper into the nature of light, as well as additional light effects, and try to understand the ambiguity.

For instance, in photovoltaics, light is, in most cases, only discussed in the form of photons as particles. However, because of optics and the fact that light passes through different environments, we have every right to consider the phenomenon from the perspective of a wave point or the photon as a wave. Further, we noticed that the V_{oc} and I_{sc} without the use of the WFL system mostly obeyed the role that decreases with decreasing light intensity independently of spectra (there are also expectations observed for this rule without additional light manipulation). That role drastically changes after passing the light through the optical system. That should not be the case if we look at light only in the form of photons, but we discussed this issue in the last chapter of this book.

The general principle of operation of the WFL system

So how does the optical system operate? Briefly, the WFL system technically solves the manipulation of light or light spectra that reach the surface of solar panels at both higher and lower light intensities while indirectly cooling the surface of solar panels. Since the solar panel is completely covered with optics, the life span of use of solar panels is greatly extended, which is also a significant form of savings. Depending on the position of the optical part through which the cooling water flows (by approaching and moving the optics away from the solar panel, as well as moving the optical part at various angles in relation to the plane of the panel or module), we can manipulate both light intensities and light spectra. Depending on the position of the optical part, we can either have a concentration effect in which the light intensity increases, or a reduced light intensity with simultaneous indirect cooling. At both lower (than the standard testing conditions of 1000 W/m^2) and higher light intensities, when light passes through the optical system, at least the light spectra that reach the surface of the solar panel change. The change of light spectra even at lower light intensities provides a higher efficiency of solar panels, i.e., higher electricity production. Water that flows through the designed optics all the time indirectly cools the surface of the solar panels by cooling the outside environment. Depending on the light intensity, the water flow velocity can be changed, allowing the panel surface to be kept constant at the standard temperature for the panel operation.

In brief, the optical/lens system consists of two curved glass lenses (two convex surfaces in the spherical form) through which cold water circulates continuously, while the thickness of the water layer at the widest central part is the thickest (figure 1). Water pipes are integrated into the lens's inlets and outlets while the system remains completely closed and safe for use. Because the water layer is not in direct contact with the cell's surface, the cooling is related to maintaining an outdoor temperature.

Figure 1 shows photographs of the basic settings for indoor measurement with the WFL system using the halogen (A) and tungsten (B) lamps as the artificial light sources and outdoor measurement with natural radiation (C).

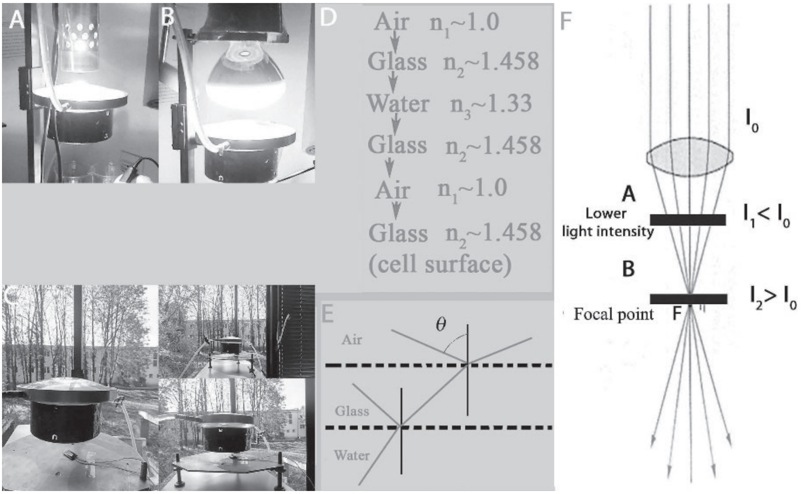

Figure 1. Photos of the basic settings for indoor measurement with the WFL system using the halogen (A) and tungsten (B) lamps as the artificial light sources and outdoor measurements with natural radiation (C). The solar cell is located under the holder of the optical part in the image at a different distance from the optics. The schematic structure is composed of the interface through which light passes, air-glass-water-glass-air glass (cell surface) with corresponding refractive indexes (D), and a ray of light striking the air-glass interface from the upper level, transmitting into the glass and then striking the glass-water interface (E). A schematic view of a lens and the two possible positions of the solar cell compared to the light source, with the lower light intensity than the incident light (A) and a concentration-effect (the higher light intensity) at the focal point (B).

In the figure, photographs of the WFL system used for cooling (flow glass water lens), reducing the intensity of light, and changing the light distribution (spectra) are shown. As well, figure 1D shows the schematic structure composed of the interface through which light passes, composed of the interfaces air/glass/water/glass/air/glass (cell) with a corresponding refractive index. The picture shows (figure 1E) a ray of light striking the air-glass interface from the upper level, transmitting into the glass, and then striking the glass-water interface. It can be noticed that at each interface, some of the rays reflect. Among other things, the behavior is affected by the incidence angle, Θ, which is affected by the reflection losses in the PV system.

Furthermore, it is well known that when a layer of water is hit by a solar ray or light, it selectively filters the various wavelengths of the light, acting as a chromatic filter. Red color (longer wavelengths) absorbs the most strongly, while violet color (shorter wavelengths) absorbs the least.

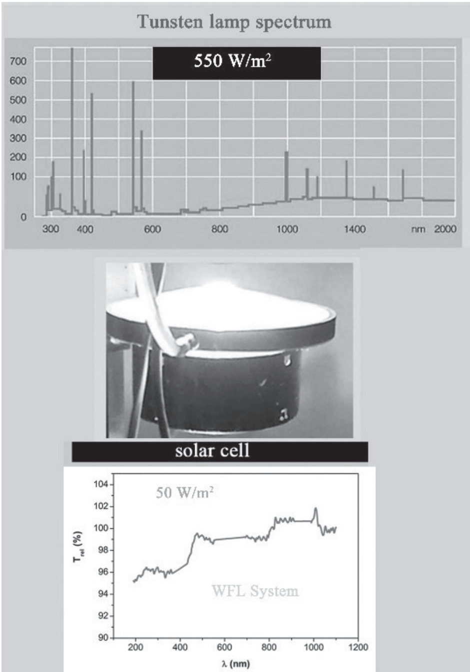

Figure 2. A schematic representation of the spectra of a high-pressure tungsten filament lamp, as well as a photograph of the WFL system used for cooling (flow water glass lens), reducing light intensity (from 550 W/m^2 to 50 W/m^2), and changing light distribution. The figure also depicts the wavelength dependence of the relative transmittance with the use of the WFL system compared to the transmittance of the tungsten lamp without it.

The wavelength dependence of the relative transmittance with the use of the WFL system, compared to the transmittance of the lamp without them, was used to confirm this effect in figure 2. The obtained results show minimal permeability in the UV region (up to 375 nm) and an almost constant value in the visible and NIR regions, with no significant difference in relative transmittance between 460 and 790 nm. It is important to emphasize that the minimum transmittance in the UV regions results in a better match between the tungsten lamp spectrum and the halogen spectrum. More about the evident difference between different artificial lights that have been used for performing indoor experiments and that quite well simulate outdoor radiation is discussed in the last chapter of the book. Here it will be only mentioned that by comparing the spectra of tungsten and halogen lamps, the mismatch is evident in the infrared (IR) and the ultraviolet (UV) parts of the spectrum. [59] We also have additional effects when building the WFL system, one of which is the depth of water in the thickest part of the constructed lenses. Given the thickness of our water layer at 4 cm, it has been proven and demonstrated[26] that the constructed WFL system eliminates a significant portion of the spectrum above 1000 nm. It is also worth mentioning that water causes an increase in the length of the radiation path in water, which is an important parameter for understanding the solar spectrum modification in water. Taking all of the mentioned effects of water into account, we can conclude that the dominant narrow energy part of photons from 550 to 600 nm arrives at the surface of solar cells. Water is also shown to reduce the impendence of incoming radiation and behave like graded glass. Furthermore, it should be noted that it is widely accepted that only water (mostly related to PV panels submerged in water) cannot increase the short-circuit current of the PV cell, regardless of the spectrum of the incoming radiation or the depth of the water. However, it has been reported that increasing water depth results in higher photoelectric efficiency for all tested commercial cells.[60-67] The photoelectric efficiency will differ because each material has a different energy gap, but greater water depth also means a different distribution of light spectra at any depth. So far, our experiments have shown that at low light intensities, the distribution of light cannot be ignored, and appears to be more dominant than the intensity of light itself. To understand this, we must first understand and connect the electronic properties of the material with higher and lower light intensities, as well as the light spectra reaching the surface of the solar cell or module. Furthermore, the behavior of solar radiation through a fluid such as water, heat transfer oils, therminols, fluids[68-71], and so on has been theoretically reported. However, there has been relatively little experimental work to date. About 40 years ago, J. D. Stachiw[72] focused on the possibility of obtaining a significant amount of energy in deep water. In 2010[73] and 2011[60], a systematic study of the behavior of photovoltaic (PV) cells in shallow water was conducted. Morel[74] investigates the effect of water on solar radiation, confirming previous findings and extending the comparison with seawater through numerical simulation.[62,63] These findings were then applied to solar pond technology and water desalination[75], as well as the spectral response and efficiency of silicon solar cells in the presence of a water layer[64]. In 2014, the first direct test of a submerged module's behavior was carried out. There have been reports of attempts to use PV underwater (UW) to increase the long-endurance power sources of UW autonomous systems and sensor platforms.[76] The Naval Research Laboratory (USA) is currently working to reduce the cost of solar cells matched to the UW spectrum by using organic solar cell materials.[67] Other attempts, primarily theoretical in nature, were made to investigate the thermal performance of PV module encapsulation and front covers.[77] Following that, these findings are applied to PV systems to improve their performance. The cooling of a concentrated PV system by immersing the solar cells in liquids[78], as well as the increased electrical yield via water veil on PV modules[79,80], are being investigated. According to the theoretical approach used for submerged PV modules[23], the integrated maximum response of the PV cells versus water depth decreases slightly for lower bandgap materials and increases significantly for higher bandgap materials. The plot of relative efficiency versus water depth, on the other hand, shows a significant increase in lower water depth for low bandgap materials and a slight decrease in lower water depth for higher bandgap materials. Variations in the response of PV modules to water depth may be related to different light distributions that exist at various depths of water. Even for each solar cell, there is either a constant increase or a constant decrease.

In principle, the reflection losses in a PV system are undesirable and affect negatively the efficiency of the solar devices. A ray impinging on the surface between two materials with different refractive indices (n), is divided into a reflected and a transmitted component. Numerous systems have been studied to reduce reflection losses (for instance, anti-reflective coatings (ARC) on the glass), but Krauter[77] by utilizing an optical model, evaluates increased optical transmittance for materials with ideal properties of n = 1.33. These ideal properties cannot be achieved with solid materials, but water, with a refractive index of 1.33, represents the perfect layer to achieve the predicted increase. Further, figure 1F presents a schematic view of a lens and the two possible positions of the solar cell compared to the light source, with the lower light intensity than the incident light (A), and a concentration-effect (the higher light intensity) at the focal point (B). Most of our reported indoor measurements with the WFL system were performed at lower or the same light intensities as the initial light source intensity (marked as I_0) and the position of the solar cell was in the shade ($I_1 < I_0$), away from the focal point. In general, far from the focal point, the intensity of light will always be lower than the initial light source. The distribution of light (spectrum), of course, always changes with the changing position of the WFL system.

Combining all these above-described effects and studying the influence of intensity and spectra, as well as possible additional light effects together with inevitable cooling, at the same time and not separately, is crucially important. In natural conditions, any changes in intensity and spectra have joint consequences, and temperature control of the surface of the solar cell or module is of essential significance in the credibility of the results and the maintenance of the solar system. To understand all those influences, some innovation is needed. The WFL system, handmade in our laboratory, enables cooling, decreasing, and increasing the intensity of light and manipulation of the spectrum. Besides, manipulation on the experimental level with the light intensity and spectra, together with some additional light effects that we do not understand, can help us to expand our knowledge concerning the interaction of light and to perhaps better comprehend the nature of light, for which there are still disagreements over different varieties of theory. The book discusses the possible reasons, such as light intensity reduction, changes in spectral distribution, the effect of interfaces, the effect of water on the solar irradiance spectra, and the fact that light, from our perspective, could be observed as a wave (because it passes through different environments before reaching the solar cell surface), for the better response of different PV devices, using the WFL system, compared with measuring without optics. It is evident that there is a range of energy gaps for all the different solar cells observed, where the use of the WFL system always improves the response of various photovoltaic devices.

In current photovoltaic power research, increasing conversion efficiency has always been a major challenge. As previously stated, this efficiency improvement can refer to designing materials with appropriate electronic properties, improving a photovoltaic device, or optical design. There have been numerous approaches to the design of materials and devices, including the synthesis of new active layer materials with enhanced carrier mobilities[81-83], the optimization of device architectures, the increase of exciton diffusion efficiency[84,85], and the creation of favorable morphologies for charge collection[86-89]. On the contrary, there has been very insufficient research into studying and manipulating incident light coupling into active layers, which has resulted in an increase in conversion efficiency. Micro-lens structures on the solar cell surface have been considered for light trapping.[90-93] Furthermore, a few reports have been published on optical designs to induce light trapping in PV cells, such as manufacturing on prism-shaped substrates[94], V-aligned solar cells[95,96], a patterned mirror-and-lens light trap[97], and the use of a pyramidal rear reflector[98]. It was also reported that a nano-waveguide system was proposed for solar energy conversion and amplification[99], as well as a two-stage dish-style concentration system to increase conversion efficiency.[100] Furthermore, a mixed dye[101] and ascorbic acid system[102] on photogalvanic cells were used to boost energy conversion. In addition, at a water depth of 4 cm[60], an innovative cooling PV technology consisting of submerging PV systems increases photovoltaic efficiency conversion by about 15%. All of these applications effectively increase light absorption in devices and boost performance by 10 to 30%. It should be noted that the designed WFL system has a water layer thickness in the middle of exactly 4 cm.

We mentioned that having such a powerful source of energy as the sun necessitates people's being able to use it more effectively than they currently do. This approach, through innovation, we believe, can broaden our knowledge of how to overcome this issue and more effectively use free energy.

References

[1] Shafiee, S., Topal, E., When will fossil fuel reserves be diminished? (2009) Energy Policy, 37 (1), pp. 181-189.

[2] Karpacheva, M., Malzner, F. J., Wobill, C., Büttner, A., E. Constable, C., Housecroft, C. E., Cuprophilia: Dye-sensitized solar cells with copper(I) dyes and copper(I)/(II) redox shuttles (2018) Dyes and Pigments, 156, pp. 410-416.

[3] Moriarty, P., Honnery, D., What is the global potential for renewable energy? (2012) Renewable & Sustainable Energy Reviews, 16 (1), pp. 244-252.

[4] Jung, S. H., Myung, Y., Kim, B. N., Kim, I. G., You, I.-K., Kim, T. Y., Activated biomass-derived graphene-based carbons for supercapacitors with high energy and power density, Scientific Reports, 8 (1), pp. 1915-1922.

[5] Darvish, A., Rafiee, F. M., Maximum efficiency of wind energy using novel dynamic voltage restorer for DFIG based wind turbine (2018) Energy Reports, 4 (2), pp. 308-322.

[6] Zhang, Y. Q., Sheng, S. W., You, Y. G., Wu, B. J., Liu, Y., Research on energy conversion system of floating wave energy converter (2014) China Ocean Engineering, 28 (1), pp. 105-113.

[7] Almosni, S., Delamarre, A., Jehl, Z., Suchet, D. et all., Material challenges for solar cells in the twenty-first century: directions in emerging technologies (2018) Science and Technology of Advanced Materials, 19 (1), pp. 336-369.

[8] Zhao, J., Wang, A., Green, M. A., 24.5% Efficiency silicon PERT cells on MCZ substrates and 24·7% efficiency PERL cells on FZ substrates (1999) Progress in Photovoltaics 7, pp. 471-474.

[9] Cousins, P. J., Smith, D. D., Luan, H. C., Manning, J., Dennis, T. D., Waldhauer, A., Wilson, K. E., Harley, G., Mulligan, W. P., Generation 3: Improved performance

at lower cost (2010) Proc. Photovoltaics Specialist Conference, San Diego, pp. 275-278.
[10] Smith, D. D., Cousins, P. J., Masad, A., Waldhauer, A., Westerberg, S., Johnson, M., et. al., Generation III high efficiency lower cost technology: Transition to full scale manufacturing (2012) Proc 38th IEEE Photovoltaic Specialists Conference (PVSC), Austin, Texas, pp. 001594-001597.
[11] Blakers, A., Zin, N., McIntosh, K. R., Fong, K., High efficiency silicon solar cells (2013) Energy Procedia, 33, pp. 1-10.
[12] Shockley, W., Queisser, H. J., Detailed balance limit of efficiency of *p-n* junction solar cells (1961) Journal of Applied Physics 32, pp. 510-519.
[13] Yoshikawa, K., Kawasaki, H., Yoshida, W. *et al.* Silicon heterojunction solar cell with interdigitated back contacts for a photoconversion efficiency over 26% (2017) Nature Energy 2, pp. 17032.
[14] Masuko, K., Shigematsu, M., Hashiguchi, T., Fujishima, D., Kai, M., Yoshimura, N., Yamaguchi, T., Ichihashi, Y., Mishima, T., Matsubara, N., Yamanishi, T., Takahama, T., Taguchi, M., Maruyama, E., Okamoto, S., Achievement of more than 25% conversion efficiency with crystalline silicon heterojunction solar cell (2014) IEEE Journal of Photovoltaics, 4, 6, pp. 1433-1435.
[15] Randall, J. F., Jacot, J., Is AM1.5 applicable in practice? Modelling eight photovoltaic materials with respect to light intensity and two spectra (2003) Renewable Energy, 28, pp. 1851–1864.
[16] IEC-904-3, IEC Standard i.e. 1000 W/m2 AM1.5 normal to cell surface at 25 °C, 1989.
[17] Bucher, K., Site dependence of the energy collection of PV modules (1997) Solar Energy Materials & Solar Cell, 47, pp. 85–94.
[18] Roth, W., Schmid, J., Photovoltaically supplied devices of low and intermediate power range (1998) 8th EC Photovoltaic Solar Energy Conference, pp. 263–269.
[19] Pettersson, H., Johansson, H., Johander, P., Gruszecki, T., A design tool for dimensioning mobile solar-driven products, Electronics Goes Green 2000+, pp. 735-739, Berlin, 2000b.
[20] Nakajima, H., Solar array enrich consumer products (1979) JEE, pp. 26–9.
[21] Randall, J. F., Droz, C., Goetz, M., Shah, A., Jacot, J., Comparison of 6 photovoltaic materials over 4 orders of magnitude of intensity (2001) 17th EPVSECE, Munich.
[22] Lojpur, V., Mitrić, M., Validžić, I.Lj., The improved photovoltaic response of commercial monocrystalline Si solar cell under natural and artificial light by using water flow lens (WFL) system (2019) International Journal of Energy Research, 43 (8), pp. 3507-3515.
[23] Tina, G.M., Rosa-Clot, M., Lojpur, V., Validžić, I.Lj., Numerical and experimental analysis of photovoltaic cells under a water layer and natural and artificial light (2019) IEEE Journal of Photovoltaics, 9 (3), art. no. 8643369, pp. 733-740.
[24] Lojpur, V., Validžić, I.Lj., Influence of different light sources, light intensities, and water flow lens (WFL) system on dye-sensitized solar cell performances (2019) IEEE Journal of Photovoltaics, 9 (2), art. no. 8594565, pp. 492-498.

[25] Lojpur, V., Krstić, J., Kačarević-Popović, Z., Filipović, N., Validžić, I.Lj., Flexible and high-efficiency Sb_2S_3/solid carrier solar cell at low light intensity (2018) Environmental Chemistry Letters, 16 (2), pp. 659-664.
[26] Lojpur, V., Mitrić, M., Validžić, I.Lj., The role of low light intensity: A step towards understanding the connection between light, optic/lens and photovoltaic behavior for Sb_2S_3 thin-film solar cells (2018) Optics and Laser Technology, 101, pp. 425-432.
[27] Validžić, I.Lj., Popović, M., Lojpur, V., Bundaleski, N., Rakočević, Z., Confirmation of incorporation of Cu and Se ions in applied p- and n-type-doped Sb_2S_3 by photoemission spectroscopy (2018) Journal of Electronic Materials, 47 (4), pp. 2402-2410.
[28] Lojpur, V., Krstić, J., Kačarević-Popović, Z., Mitrić, M., Rakočević, Z., Validžić, I.Lj., Efficient and novel Sb_2S_3 based solar cells with chitosan/poly(ethylene glycol)/electrolyte blend (2018) International Journal of Energy Research, 42 (2), pp. 843-852.
[29] Lojpur, V., Mitrić, M., Kačarević-Popović, Z., Radosavljević, A., Rakočević, Z., Lj Validžić, I., The role of low light intensity: A cheap, stable, and solidly efficient amorphous Sb_2S_3 powder/hypericin composite/PVA matrix loaded with electrolyte solar cell (2017) Environmental Progress and Sustainable Energy, 36 (5), pp. 1507-1516.
[30] Lojpur, V., Tasić, N., Validžić, I., Different behaviors in current–voltage measurements of undoped and doped Sb_2S_3-based solar cells (2017) Journal of Applied Electrochemistry, 47 (1), pp. 117-124.
[31] Janošević, V., Mitrić, M., Bundaleski, N., Rakočević, Z., Validžić, I.Lj., High-efficiency Sb_2S_3-based hybrid solar cell at low light intensity: Cell made of synthesized Cu and Se-doped Sb_2S_3 (2016) Progress in Photovoltaics: Research and Applications, 24 (5), pp. 704-715.
[32] Validžić, I.Lj., Janošević, V., Mitrić, M., Characterization and current-voltage characteristics of solar cells based on the composite of synthesized Sb_2S_3 powder with small band gap and natural dye (2016) Environmental Progress and Sustainable Energy, 35 (2), pp. 512-516.
[33] Janošević, V., Mitrić, M., Savić, J., Validžić, I.Lj., Structural, optical, and electrical properties of applied amorphized and polycrystalline Sb_2S_3 thin films (2016) Metallurgical and Materials Transactions A: Physical Metallurgy and Materials Science, 47 (3), pp. 1460-1468.
[34] Janošević, V., Mitrić, M., Ležaić, A.J., Validžić, I.Lj., Weak light performance of synthesized amorphous Sb_2S_3-based hybrid solar cell (2016) IEEE Journal of Photovoltaics, 6 (2), art. no. 7347349, pp. 473-479.
[35] Husain, A. A. F., Hasan, W. Z. W., Shafie, S., Hamidon, M. N., Pandey, S. S., A review of transparent solar photovoltaic technologies (2018) Renewable and Sustainable Energy Reviews, 94, pp. 779–791.
[36] Roghabadi, F. A., Ahmadi, N., Ahmadi, V., Di Carlo A., Aghmiuni, K. O., Tehrani A. S., Ghoreishi, F. S., Payandeh, M., Rezaei Fumani, N. M., Bulk heterojunction polymer solar cell and perovskite solar cell: Concepts, materials, current status, and opto-electronic properties (2018) Solar Energy, 173, pp. 407-424.

[37] Gawlinska, K., Iwan, A., Starowicz, Z., Kulesza-Matlak, G., Stan-Glowinska, K., Janusz, M., Lipinski, M., Boharewicz, B., Tazbir, I., Sikora, A., Searching of new, cheap, air- and thermally stable hole transporting materials for perovskite solar cells (2017) Opto-Electronics Review, 25, pp. 274-284.
[38] Inganäs, O., Sundström, V., Solar energy for electricity and fuels (2016) Ambio, 45, pp. 15–23.
[39] Rehan, A., Serdar, C., Effect of cooling on solar panel performance (2017) International Proceedings of Chemical, Biological and Environmental Engineering, 100, pp. 118-123.
[40] Odeh, S., Behnia, M., Improving photovoltaic module efficiency using water cooling (2009) Heat Transfer Engineering, 30(6), pp. 499–505.
[41] Quijano, J. C., Jackson, P. R., Santacruz, S., Morales, V. M., García, M. H., Implications of climate change on the heat budget of lentic systems used for power station cooling: case study clinton lake (2016) Illinois. Environmental Science and Technology, 50 (1), pp. 478–488.
[42] Tadepalli, S., Slocik, S. J., Gupta, M. K., Naik, R. R., Singamaneni, S., Bio-optics and bio-inspired optical materials (2017) Chemical Reviews, 117 (20), pp. 12705–12763.
[43] Alaaeddin, M. H., Sapuan, S. M., Zuhri, M. Y. M., Zainudin, E. S., AL- Oqla, F. M., Photovoltaic applications: Status and manufacturing prospects (2019) Renewable & Sustainable Energy Reviews, 102, pp. 318-332.
[44] López-Escalante, M. C., Fernández-Rodríguez, M., Caballero, L. J., Martín, F., Gabás, M., Ramos-Barrado, J. R., Novel encapsulant architecture on the road to photovoltaic module power output increase (2018) Applied Energy, 228, pp. 1901-1910.
[45] Yang, Z. J., Jiang, R., Zhuo, X., Ya-Ming Xie, Z. M., Jianfang, W., Hai-Qing, L., Dielectric nanoresonators for light manipulation (2017) Physics Reports, 701, pp. 1-50.
[46] Mennucci, C., Muhammad, M. H., Hameed, M. F. O., Mohamed, S. A., Abdelkhalik, M. S., Obayya, S. S. A., Buatier de Mongeot, F., Broadband light trapping in nanotextured thin film photovoltaic devices (2018) Applied Surface Science, 446, pp. 74-82.
[47] Nwoba, E. G., Parlevliet, D. A., Laird, D. W., Alameh, K., Moheimani, N. R., Light management technologies for increasing algal photobioreactor efficiency (2019) Algal Research, 39, pp. 101433.
[48] Mousavi Baygi, S. R., Sadrameli, S. M., Thermal management of photovoltaic solar cells using polyethylene glycol 1000 (PEG1000) as a phase change material (2018) Thermal Science and Engineering Progress, 5, pp. 405-411.
[49] Dupré, O., Physics of the thermal behavior of photovoltaic devices. Thermics [physics.class-ph] (2015) INSA de Lyon, English.
[50] Bai, A., Popp, J., Balogh, P., et al. Technical and economic effects of cooling of monocrystalline photovoltaic modules under Hungar-ian conditions (2016) Renewable and Sustainable Energy Reviews, 60, pp.1086-1099.
[51] Grubišić-Čabo, F., Nižetić, S., Giuseppe Marco, T., Photovoltaic panels: a review of the cooling techniques (2016) Trans FAMENA, 40 (SI-1), pp.63-74.

[52] Emery, K., Burdick, J., Caiyem, Y., Dunlavy, D., Field, H., Kroposki, B., Moriatry, T., Temperature dependence of photovoltaic cells, modules and systems (1996) Proceedings of the 25th IEEE PV specialists conference, Washington DC, USA, May 13–19, pp.1275–1278.
[53] Biwole, P., Eclache, P., Kuznik, F., Improving the performance of solar panels by the use of phase-change materials (2011) World Renewable Energy Congress, 8–13 May, Linköping, Sweden.
[54] Imenes, A. G., Mills, D.R., Spectral beam splitting technology for increased conversion efficiency in solar concentrating systems: a review (2004) Solar Energy Materials & Solar Cells, 84(1-4), pp.19-69.
[55] Reynolds, S., Urbain, F., Smirnov, V., Spectral matching and outdoor solar to electrical conversion efficiency in thin-film silicon multi-junction solar cells (2017) Journal of Physics: Conference Series, 794, pp. 012025.
[56] Apostoleris, H., Stefancich, M., Chiesa, M., Tracking-integrated systems for concentrating photovoltaics (2016) Nature Energy, 1(4), pp.16018.
[57] Baig, H., Sarmah, N., Chemisana, D., Rosell, J., Mallick, T. K., Enhancing performance of a linear dielectric based concentrating photovoltaic system using a reflective film along the edge (2014) Energy, 73, pp.177-191.
[58] Baig, H., Sellami, N., Mallick, T. K., Performance modeling and testing of a building integrated concentrating photovoltaic (BICPV) system (2015) Solar Energy Materials & Solar Cells, 134, pp.29-44.
[59] Aristizabal, J., Omrane, B., Landrock, C., Grayli, S. V., Chuo, Y., Patel, J. N., Kaminska, B., Menon, C., Tungsten lamps as an affordable light source for testing of photovoltaic cells (2011) Journal of Electronic Testing, 27, pp. 403–410.
[60] Tina, G. M., Rosa-Clot, M., Rosa-Clot, P., Scandura, P. F., Optical and thermal behavior of submerged photovoltaic solar panel: SP2 (2012) Energy, 39, pp. 17–26.
[61] Rosa-clot, M., Rosa-clot, P., Lanzafame, R., Nachtmann, S., Rosa-clot, M., Rosa-clot, P., Scandura, P. F., Taddei, S., Tina, G. M., Field experience with performances evaluation of a single-crystalline photovoltaic panel in an underwater environment (2010) IEEE Transactions on Industrial Electronics, 57, pp. 2492-2498.
[62] Muaddi, J. A., Jamal, M. A., Solar spectrum at depth in water (1991) Renewable Energy, 1, pp. 31-35.
[63] Jamal, M. A., Muaddi, J. A., Solar energy at various depths below a water surface (1990) International Journal of Energy Research, 14, pp. 859-867.
[64] Muaddi, J. A., Jamal, M. A., Spectral response and efficiency of a silicon solar cell below water surface (1992) Solar Energy, 49, pp. 29-33.
[65] Kong, J., Nordlund, D., Sung Jin, J., Yup Kim, S., Jin, S. M., Huang, D., Zheng, Y., Karpovich, C., Sertic, G., Wang, H., Li, J., Weng, G., Antonio, F., Mariano, M., Maclean, S., Goh, T. H., Kim, J. Y., Taylor, A. D., Underwater organic solar cells via selective removal of electron acceptors near the top electrode (2019) ACS Energy Letters, 4, pp. 1034-1041.
[66] Messenger, S., Jenkins, P. P., Hoheisel, R., Walters, R. J., Trautz, K. M., Goldstein, D., Maximenko, S. I., Scheiman D., High-bandgap solar cells for underwater photovoltaic applications (2014) IEEE Journal of Photovoltaics, 4, pp. 202-207.

[67] Walters, R. J., Yoon, W., Placencia, D., Scheiman, D., Lumb, M. P., Strang, A., Stavrinou, P. N., Jenkins, P. P., Multijunction organic photovoltaic cells for underwater solar power (2015) IEEE 42nd Photovoltaic Specialists Conference (PVSC), pp. 3, DOI: 10.1109/PVSC.2015.7355644.
[68] Sandeep, S. J., Ashwinkumar, S. D., Experimental investigation of solar photovoltaic thermal system using water, coconut oil and silicon oil as spectrum filters (2017) Journal of the Brazilian Society of Mechanical Sciences and Engineering, 39, pp. 3227–3236.
[69] Hamdy, M. A., El-Hefnawi, S. H., Effect of spectrally selective liquid absorption-filters on silicon solar-cells (1990) Applied Energy, 35, pp. 177– 188.
[70] Kaluza, J., Funken, K. H., Groer, U., Neumann, A., Riffelmann, K. J., Properties of an optical fluid filter: Theoretical evaluations and measurement results (1999) Journal de Physique, 9, pp. Pr3-655–Pr3-660.
[71] Joshi, S. S., Dhoble, A. S., Jiwanapurkar, P. R., Investigations of different liquid-based spectrum beam splitters for combined solar photovoltaic thermal systems (2016) The Journal of Solar Energy Engineering, 138, pp. 0210030.
[72] Stachiw, J., Performance of photovoltaic cells in an undersea environment (1980) Journal of Engineering for Industry, 102, pp. 51–59.
[73] Rosa-Clot, M., Rosa-Clot, P., Tina, G. M., Submerged photovoltaic module: SP2 (2010) Renewable Energy, 35, pp. 1862–1865.
[74] Morel, A., Optical Properties of Pure Water and Pure Sea Water (1974) Jerlov, N. G., Steenman, N. E., Eds. London, U.K.: Academic.
[75] Jamal, M., Junaidi, T., Muaddi, J., A step forward towards an ideal absorber for solar energy (1991) International Journal of Energy Research, 15, pp. 367–375.
[76] Jenkins, P. P., Messenger, S., Trautz, K., Maximenko, S., Goldstein, D., Scheiman, D., Walters, R., High-band gap solar cells for underwater photovoltaic applications (2014) IEEE Journal of Photovoltaics, 4, pp. 202–207.
[77] Krauter, S., Hanitsch, R., Actual optical and thermal performance of PV-modules (1996) Solar Energy Materials & Solar Cells, 41/42, pp.557-574.
[78] Wang, Y., Fanga, Z., Zhub, L., Huanga, Q., Zhanga, Y., Zhanga, Z., The performance of silicon solar cells operated in liquids (2009) Applied Energy, 16, pp. 1037–1042.
[79] Krauter, S., Increased electrical yield via water flow over the front of photovoltaic modules (2004) Solar Energy Materials and Solar Cells, 82, pp. 131–137.
[80] Abdolzadeh, M., Ameri, M., Improving the effectiveness of a photovoltaic water pumping system by spraying water over the front of photovoltaic cells (2009) Renewable Energy, 34, pp. 91–96.
[81] Zhou, H., Yang, L. Q., Price, S. C., Knight, K. J., You, W., Enhanced photovoltaic performance of low-bandgap polymers with deep LUMO levels (2010) Angewandte Chemistry International Edition 49, pp. 7992–7995.
[82] Muhlbacher, D., Scharber, M., Morana, M., Zhu, Z. G., Waller, D., Gaudiana, R., Brabec, C., High photovoltaic performance of a low-bandgap polymer (2006) Advanced Materials, 18, pp. 2884–2889.
[83] Boudreault, P. L. T., Najari, A., Leclerc, M., Processable low-bandgap polymers for photovoltaic applications (2011) Chemistry of Materials, 23, pp. 456–469.
[84] Xue, J., Rand, B. P., Uchida, S., Forrest, S. R., A hybrid planar–mixed molecular heterojunction photovoltaic cell (2005) Advanced Materials, 17, pp. 66–71.

[85] Zheng, Y., Bekele, R., Ouyang, J., Xue, J., Organic photovoltaic cells with vertically aligned crystalline molecular nanorods (2009) Organic Electronics, 10, pp. 1621–1625.
[86] Li, G., Shrotriya, V., Huang, J. S., Yao, Y., Moriarty, T., Emery, K., Yang, Y., High efficiency solution processable polymer photovoltaic cells by self-organization of polymer blends (2005) Nature Materials, 4, pp. 864–868.
[87] Kim, Y., Cook, S., Tuladhar, S. M., Choulis, S. A., Nelson, J., Durrant, J. R., Bradley, D. D. C., Giles, M., Mcculloch, I., Ha, C. S., Ree, M., A strong regioregularity effect in self-organizing conjugated polymer films and high-efficiency polythiophene: fullerene solar cells (2006) Nature Materials, 5, pp. 197–203.
[88] Peet, J., Kim, J. Y., Coates, N. E., Ma, W. L., Moses, D., Heeger, A. J., Bazan, G. C., Efficiency enhancement in low-bandgap polymer solar cells by processing with alkane dithiols (2007) Nature Materials, 6, pp. 497–500.
[89] Yang, X., Loos, J., Veenstra, S. C., Verhees, W. J. H., Wienk, M. M., Kroon, J. M., Michels, M. A. J., Janssen, R. A. J., Nanoscale morphology of high-performance polymer solar cells (2005) Nano Letters, 5, pp. 579–583.
[90] Xie, J., Wu, K., Cheng, J., Li, P., Zheng, J., The micro-optic photovoltaic behavior of solar cell along with microlens curved glass substrate (2015) Energy Conversion and Management, 96, pp. 315–321.
[91] Li, P., Xie, J., Cheng, J., Jiang, Y. N., Study on weak-light photovoltaic characteristics of solar cell with a microgroove lens array on glass substrate (2015) Optics Express, 23, pp. A192–A203.
[92] Zhang, L., Xie, J., Guo, R. B., Wu, K. K., Li, P., Zheng, J. H., Precision and mirror micro grinding of micro-lens array on macro-freeform glass substrate for micro photovoltaic performances (2016) The International Journal of Advanced Manufacturing Technology, 86, pp. 87–96.
[93] Myers, J. D., Cao, W., Cassidy, V., Eom, S. H., Zhou, R., Yang, L., You, W., Xue, J., A universal optical approach to enhancing efficiency of organic-based photovoltaic devices (2012) Energy & Environmental Science, 5, pp. 6900–6904.
[94] Niggemann, M., Glatthaar, M., Lewer, P., Muller, C., Wagner, J., Gombert, A., Functional microprism substrate for organic solar cells (2006) Thin Solid Films, 511, pp. 628–633.
[95] Rim, S. B., Zhao, S., Scully, S. R., McGehee, M. D., Peumans, P., An effective light trapping configuration for thin-film solar cells (2007) Applied Physics Letters, 91, pp. 243501.
[96] Zhou, Y., Zhang, F. L., Tvingstedt, K., Tian, W. J., Inganas, O., Multi folded polymer solar cells on flexible substrates (2008) Applied Physics Letters, 93, pp. 033302.
[97] Tvingstedt, K., Dal Zilio, S., Inganas, O., Tormen, M., Trapping light with micro lenses in thin film organic photovoltaic cells (2008) Optics Express, 16, pp. 21608–21615.
[98] Cao, W., Myers, J. D., Zheng, Y., Hammond, W. T., Wrzesniewski, E., Xue, J., Enhancing light harvesting in organic solar cells with pyramidal rear reflectors (2011) Applied Physics Letters 99, pp. 023306.

[99] Mitatha, S., Kamoldilok, S., Yupapin, P. P., White light generation and amplification using a soliton pulse within a nano-waveguide for the potential of solar energy conversion use (2010) Energy Conversion and Management, 51, pp. 2340–2344.
[100] Wang, Y. L., Zhang, H., Wen, D. S., Zhao, W., Yhou, Z., Characterization of the InGaP/InGaAs/Ge triple-junction solar cell with a two-stage dish-style concentration system (2013) Energy Conversion and Management, 76, pp. 177–184.
[101] Yadav, S., Lal, C., Optimization of performance characteristics of a mixed dye-based photo galvanic cell for efficient solar energy conversion and storage (2013) Energy Conversion and Management, 66, pp. 271–276.
[102] Genwa, K. R., Sagar, C. P., Energy efficiency, solar energy conversion and storage in photo galvanic cell (2013) Energy Conversion and Management, 66, pp. 121–126.

CHAPTER TWO

AN OVERVIEW OF TESTED SOLAR CELLS

In this part of the book, we will present various types of solar cells, dye-sensitized, different types of silicon (Si) solar cells, as well as some types of Sb_2S_3-based solar cells, on which we performed measurements with and without the WFL system. Since our research began with insufficiently studied semiconductors of group V-VI, antimony sulfide, and the development of methods for the synthesis of doped and non-doped Sb_2S_3 nanoparticles for use in different cells made and developed in our laboratory, these diverse types of devices will also be presented apart from commercial cells. We already pointed out at the beginning of the book that our first research related to solar energy began with the development of materials as well as solar cells themselves, while we were not even aware of the possibility to extend our knowledge with light manipulation and the use of WFL systems. We must emphasize here that at the time of semiconductor material development, obtaining our first solar cells and the construction of optics, there were only sporadic scientific papers that demonstrated the remarkable characteristics of different solar devices at lower light intensities, obtained mainly by using different light lamps without going into details. Unfortunately, the most limited number of experiments comparing the responses of solar devices with and without WFL systems, in which we best monitored the impact of light manipulation, were performed on Sb_2S_3 solar cells. At the same time, the largest number of experiments at lower light intensities by using the WFL system were performed on the mentioned solar devices. Further experiments with light manipulation were applied to laboratory-obtained dye-sensitized solar cells. Last but not least, various crystalline and amorphous silicon solar cells have been studied as cells with the most advanced technology and the largest presence on the market, for which this application would be the most interesting and significant.

Application of the WFL system and light manipulation to dye-sensitized solar cells

Solar cells are classified into silicon, semiconductor compounds, and novel materials, which include dye-sensitized, colloidal quantum dots, organic, and perovskite solar cells, based on the primary active material.[1] So, in addition to the antimony sulfide cells discussed in the last title of this chapter, which are broadly classified as semiconductor solar cells, as well as the Si solar cells whose results will be presented in the following title in this section, here we will review the results of dye-sensitized solar cells, which are classified as the third and final classification of solar cells based on new materials. Dye-sensitized solar cells has been thoroughly investigated over the last 20 years, and research interest is continuing due to their very appealing attributes, such as low-cost production and fabrication with relatively high conversion efficiency, which make them a strong candidate to compete with conventional Si-solar cells.[2-6] The importance of understanding the influence of the spectral distribution of a light source that comes to the surface of solar cells was emphasized[7-11] in this chapter using various light sources (xenon, halogen, tungsten), using them as standards that best match outdoor radiation at standard testing conditions (STC) (temperature of 25° C and irradiance of 1000 W/m^2 with an AM 1.5 spectra), as well as the influence of the WFL system. Unfortunately, there are only a few reports that look into the impact of low light intensity and different spectra, and they show that the spectral mismatch between different artificial lamps and outdoor radiation has a significant impact on the experimental performance of solar water-splitting devices.[12] As previously stated, the spectrum and intensity of light can be changed without changing the light source by using the described water flow lens (WFL) system. This WFL system was applied to various types of cells, and all tested cells (described in this chapter) demonstrated improved photovoltaic performance. As a result, the confirmation that diverse spectra and intensities can result in different performances for the same solar cell is extremely significant.

In this section of the chapter, we present a dye-sensitized solar cell that was tested with three different lamps (xenon, halogen, and tungsten) at various light intensities reached by using the WFL system. For each measurement and each light intensity, we also compared the results without using the WFL system. The most significant results are obtained at lower light intensities (below STC, 1000 W/m^2), and the power generation at lower intensities is extremely important for indoor applications and cloudy locations. Conditions for measurements at lower intensities (standard testing conditions at low light intensity) are not yet established and are heavily dependent on measurement parameters. Until now, the majority of investigated cells (organic, dye-sensitized, etc.) have demonstrated better performance at lower light intensities in the scientific literature.[13-18] The dye-sensitized solar cells in this chapter were observed using xenon, halogen, and tungsten lamps, as well as the WFL system, to improve the efficiency of the made solar devices and investigate the impact of light spectra and intensity. The dyes and solvents were used to divide the dye-sensitized solar cells into four groups, as explained in the following section. These cells have been thoroughly investigated[19-21], and we wanted to demonstrate and emphasize how important it is to be aware of light intensities and spectra (and possible additional light effects that will be studied more in the next chapter) and how we can manipulate them to improve the performance of solar cells.

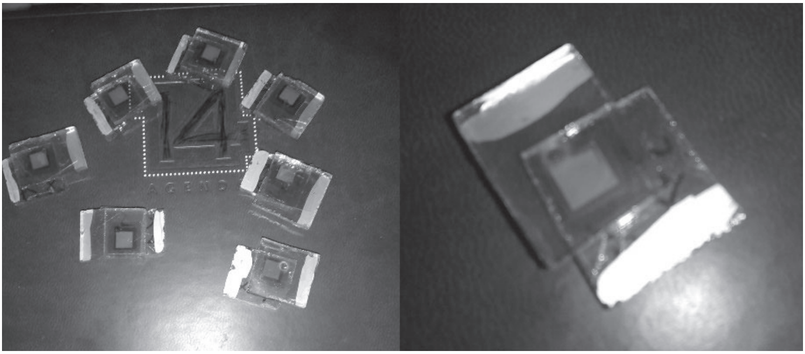

Figure 1. Photos of the experimentally made dye-sensitized solar cells.

We will not consider here the experimental details of making solar cells or details of the measurements[22], because the focus of this book is on the results obtained by manipulating light and the conclusions that emerge. Figure 1 shows a photo of experimentally made dye-sensitized solar cells. Further, under this subject, we will follow results with and without employing the WFL system observed under lower light intensities and results obtained under standard testing conditions (STC), 1000 W/m^2 without light manipulation. Measurements under STC were made by using a xenon lamp, while measurements with light manipulation were performed by using halogen and tungsten lamps. All these different lamps are frequently used for experimental laboratory measurements since their spectra simulate quite well the AM 1.5G global irradiance standard spectrum. Figure 2 illustrates the spectral distributions of three different lamps, xenon, halogen, and tungsten, as well as the AM 1.5G global irradiance standard spectrum, and the distinctions in their spectra are evident. All of these light sources are used to examine solar cells, but we

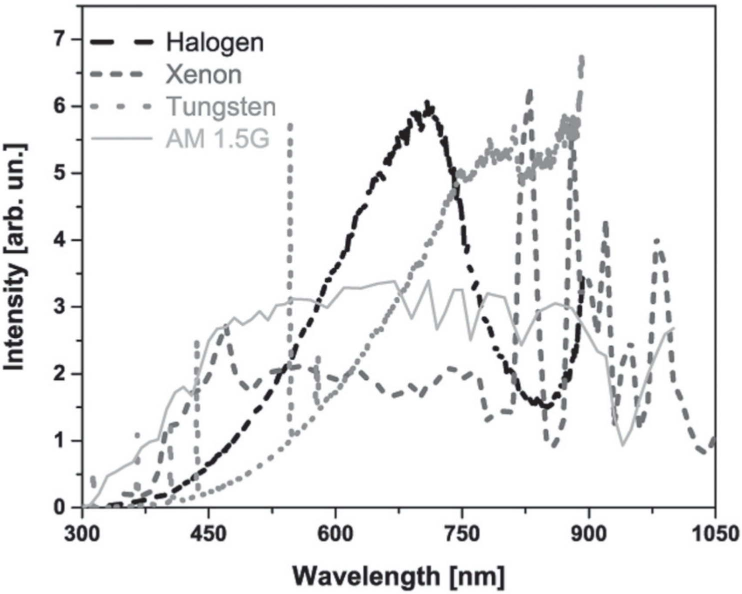

Figure 2. Spectral distributions of the Philips ELH 120V 300W halogen lamp, the xenon lamp, the high-pressure tungsten filament lamp, and the AM 1.5G global irradiance spectrum.

realized through various experiments that even minor changes in the spectrum cause significant variations in voltage, current, efficiency, and overall solar cell performance. So, regardless of whether we consider each of these lamps to be a light source that accurately simulates outdoor radiation, their spectra differ, and these differences can have a significant impact on photovoltaic device performance. In brief, solar cells are labeled using dyes and solvents. XA represents the cell group XY1: D35 with acetonitrile, XP represents XY1: D35 with 3-methoxy-propionitrile, YA represents Y123 with acetonitrile, and YP represents Y123 with 3-methoxy-propionitrile. More than ten solar cells in each of the mentioned groups were measured in each group to identify if the results were repeatable, though only some of the results were presented here. The characteristics of the current-voltage (*I-V*) curves for XA, XP, YA, and YP solar cells measured

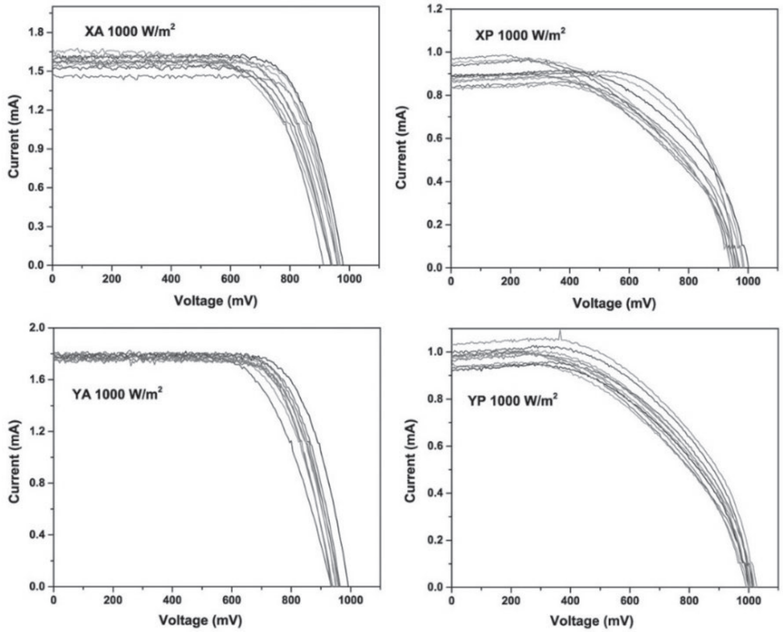

Figure 3. *I-V* curves for XA, XP, YA, and YP solar cells, measured with the xenon lamp in a solar simulator under standard testing conditions (STC) and without light manipulation.

with the xenon lamp in a solar simulator under standard testing conditions (STC) and without light manipulation were presented in figure 3. As can be seen, the resulting curves are very similar within the same group of cells; there are no measurements that differ. The results presented under standard testing conditions (STC, 1000 W/m^2) should be the best in terms of voltage and current values, efficiency, as well as the shape of the curves obtained by measuring these solar cells. Significantly, after the involvement of light manipulation in measurements and experiments, we will see that this is not the case. Table 1 shows the values for short-circuit current I_{sc}, open-circuit voltage V_{oc}, fill factor FF, and efficiency PCE for all different groups of solar cells measured under standard testing conditions (STC) and with a xenon lamp. The efficiencies are calculated relative to the surface of the observed cells, and the entire surface of the cell (1 cm^2) was illuminated during the measurements. The fill factors were calculated using the formula $FF = I_m V_m / I_{SC} V_{OC}$, where I_m and V_m are the maximum current and voltage, respectively. The efficiency η was calculated from the relationship η =

Table 1. All different groups of solar cells with appropriate characteristics (open-circuit voltage (V_{oc}), short circuit current (I_{sc}), fil factor (*FF*) and efficiency (*PCE*)) measured at standard testing conditions (STC) and with a xenon lamp.

1000 W/m² Xenon lamp				
Sample	V_{oc} (mV)	I_{sc} (mA)	*FF*	*PCE* (%)
XA1	939	1.60	0.75	1.13
XA2	940	1.57	0.75	1.11
XA3	960	1.62	0.69	1.07
XA4	939	1.54	0.71	1.01
XA5	911	1.57	0.72	1.03
XA6	943	1.53	0.77	1.11
XP1	982	0.86	0.53	0.45
XP2	951	0.94	0.51	0.45
XP3	972	0.88	0.50	0.43
XP4	955	0.84	0.57	0.47
XP5	949	0.83	0.56	0.44
XP6	941	0.95	0.52	0.47
YA1	993	1.80	0.73	1.30
YA2	953	1.80	0.72	1.23
YA3	964	1.75	0.73	1.23
YA4	934	1.77	0.73	1.21
YA5	940	1.81	0.72	1.22
YA6	930	1.78	0.74	1.22
YP1	1000	0.92	0.53	0.49
YP2	1013	0.97	0.52	0.51
YP3	991	0.98	0.51	0.50
YP4	1014	0.99	0.54	0.54
YP5	998	0.93	0.54	0.50
YP6	1003	0.97	0.50	0.49

$V_{oc}I_{sc}FF/P_{input}$ x100, where P_{input} is the input light energy. These parameters are discussed in more detail in the next chapter. It is well known that results under standard testing conditions (STC) and without light manipulation (or without using the WFL system) should be the best in terms of the solar cell parameters mentioned above, and the next figure 4 shows measurements which reveal that this is not the case. As can be seen in figure 4, short-circuit current as well as short-circuit voltage decrease with decreasing light intensity within the same lamp (the same spectra) without light manipulation as expected. However, the decrease in the light intensity is much more pronounced with the fill factor that remains almost constant, which overall gives higher efficiency at the lower light intensities without light spectra changes. Those measurements were performed at the sun simulator by using filters to change the light intensities that ensure that the spectrum after passing through the filter does not change.[19-21] It is quite an important fact that, without spectra changes, dye-sensitized solar cells can exhibit higher efficiencies at lower light intensities. This could be one more confirmation that measurements of the solar cells at not yet established standard testing conditions at lower light intensity should not be compared with established standard testing conditions at higher light intensity (1000 W/m^2). Further results and comments are discussed in the following chapter.

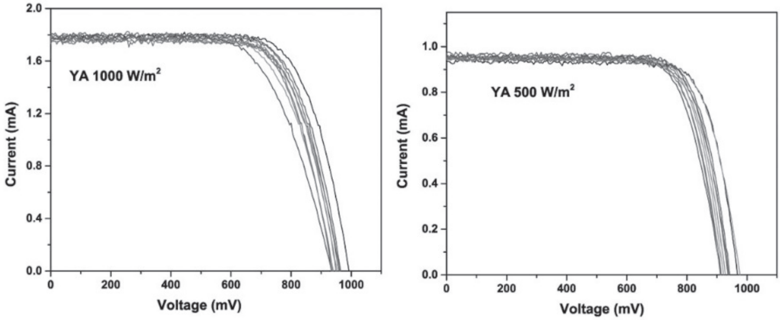

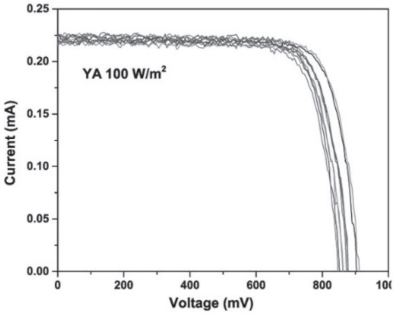

Solar cell	Voc [mV]	Isc [mA]	FF	PCE [%] cell surface
1000 W/m^2 – Xenon lamp				
YA	964	1.75	0.73	1.23
500 W/m^2 – Xenon lamp				
YA	926	0.95	0.79	1.39
100 W/m^2 – Xenon lamp				
YA	876	0.22	0.80	1.63

Figure 4. *I-V* curves for YA solar cells measured with the xenon lamp in a solar simulator under different light intensities, standard testing conditions (STC) of 1000 W/m^2, 500 W/m^2 and 100 W/m^2 without light manipulation. The figure also contains a table with appropriate characteristics of the measured cell YA, including the calculated efficiencies.

Next, we observe what happens when we change the lamps (spectra) as well as the light intensities (figure 5), intending to emphasize how changes in solar cell characteristics can be influenced at least by light spectra independent of light intensity. No matter how similar the spectra are to us, the small differences between their spectra presented in figure 2 can lead to

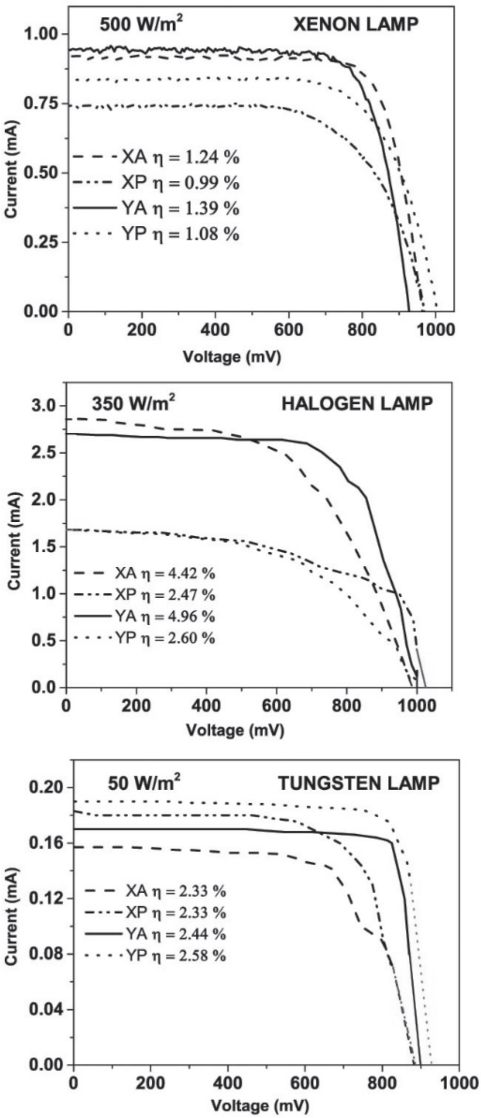

Figure 5. *I-V* curves and efficiency for XA, XP, YA, and YP solar cells at different lamps (spectra) and the light intensity of 500 W/m^2, 350 W/m^2, and 50 W/m^2 recorded with the xenon, halogen, and the tungsten lamp.

quite diverse characteristics of the same solar cell. As is more than clear from figure 5, solar cell characteristics, short-circuit current, and short-circuit voltage, as well as efficiency, don't follow the trend that the above-mentioned characteristics decrease with decreasing light intensity. As can be seen, the lowest efficiency values obtained are typical of cells measured at 500 W/m^2 with the xenon lamp, while the halogen lamp and a light intensity of 350 W/m^2 produce the highest values of I_{sc}, V_{oc}, and efficiency. It should be noted that designed dye-sensitized solar cells generally exhibit better performance at lower light intensities, as was demonstrated in the previous measurements.[19-21]

The use of the WFL system was mentioned in the introduction section of this chapter as a way to change the spectra of light and generally improve the characteristics of solar cells. Hence, in this configuration, we have the same power output and light intensity, but at least the spectra that reach the surface of the solar cell have changed. In figure 6, *I-V* curves and efficiency for all solar cells observed at the same light intensities of 350 W/m^2 and 50 W/m^2 without and with the use of the WFL system are given. As can be seen, the values of I_{sc}, V_{oc}, and efficiency with the WFL system are significantly higher when compared to the same lamp and light intensity without the use of optics with flowing water. The only thing operating here was the WFL system, which at the very least changed the light distribution, one of the facts apart from other additional light effects discussed in greater detail in the following chapter. The values of I_{sc} and efficiency are more than twice as high as for halogen lamps and have an intensity of 350 W/m^2. Also, XA and YA have much higher values (10.2 % and 12.6 % respectively) compared to XP and YP (4.6 % and 5.5 % respectively). The open-circuit voltage maintains very high values, even though there is a noticeable slight increase. The results for all cells obtained at 5% sun and tungsten lamp are impressive and reach the very low light intensity efficiency of the best various solar cells observed at standard testing conditions (STC). Efficiency values for XA and YA are nearly 28 % and 31 %, respectively, while efficiencies for XP and YP are nearly 17 % and 19 %, respectively. Doscher et al.[12] discovered that a tungsten light source can provide a current density of 80 mA/cm^2 for Si at STC, whereas the general current-density limit for Si is only 44.1 mA/cm^2. Hence, apart from the power output, it appears that the light distribution had a considerable influence on I_{sc} in the first set of experiments. After all, in this set of experiments, it seems that the spectrum of the lamp, at least, has a significant impact (more than light intensity) on the characteristics of solar cells. Naturally, the design of the cells experiences a significant impact, as expected. Improvements in short-circuit

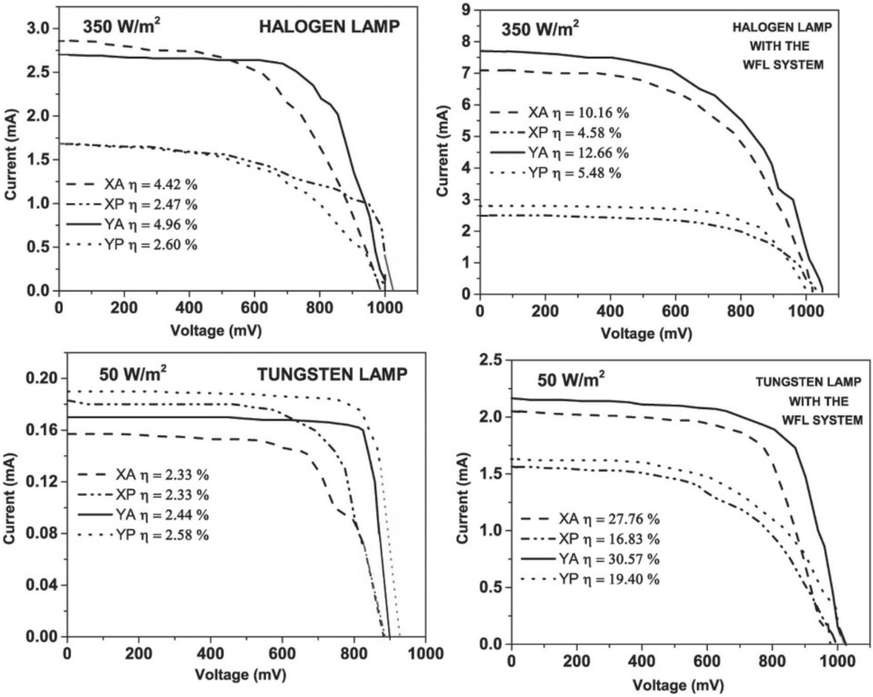

Figure 6. *I-V* curves and efficiency for XA, XP, YA, and YP solar cells observed at the same light intensities of 350 W/m^2, and 50 W/m^2 without and with the use of the WFL system.

current, efficiency, and, in some cases, short-circuit voltage obtained after passing the light through the water and curved glass are at least additional spectra influences, although additional light effects must be taken into account, which were discussed in more detail in the following chapter. It should be emphasized that the processes themselves in designed dye-sensitized solar cells will not be considered here, because they are not made by our group.

Application of the WFL system and light manipulation to monocrystalline, polycrystalline, and amorphous Si-solar cells

Polycrystalline and monocrystalline silicon (Si) cells are the most commonly used types of solar cells in the PV market, accounting for more than 93% of PV cell production in 2016. Because silicon is both environmentally friendly and one of the most abundant resources on the planet, crystalline silicon solar cells are expected to play an important role in the future PV market. The abundance and safety of silicon cells, on the one hand, and the advancement of technology over nearly 70 years, on the other hand, give silicon cells a dominant position over all other types of cells available in the photovoltaic market.[23-27] The reported maximum efficiency of silicon solar cells is 29%,[28-31]while the theoretical maximum solar conversion efficiency is around 33.7% for a single p-n junction with a bandgap of 1.4 eV, as determined by the Stockley-Queisser limit.[32] More about solar cell efficiency and the Stockley-Queisser limit in detail will be discussed in the next chapter. Aside from the fact that efficiency is not the only limiting parameter, the efficiency/cost ratio, apart from durability and reliability, must be considered in reality. In addition, because the most efficient crystalline Si-solar cell has nearly reached its theoretical maximum efficiency, the competitive product must be significantly cheaper while still being efficient. In terms of material abundance, safety, and improved technology, all other types of more inexpensive solar cells (dye-sensitized, organic, perovskite, etc.) that are currently on the market or will appear as cheaper products in the near future will struggle to compete with Si-solar cells. Any less expensive type of current or new solar cell/module design can serve as a backup rather than a replacement for Si-solar cells. As a result, the most important tasks are testing and discovering ways to improve the operating characteristics and overall efficiency of Si-solar cells. On the other hand, in the previous chapter, we emphasized the importance of manipulating light through design optics (the WFL system) to improve and optimize the output of existing solar devices. Specifically, it is widely accepted that changes in the spectra that arrive at the surface of a solar panel are an uncontrollable factor. However, we can deal with light intensity and the quality of the semiconductor used in the solar panel, both of which have a direct impact on efficiency.[33] Indeed, independent of our research, some authors have reported findings that different types of solar cells perform better photovoltaically at lower light intensities[34-39], different artificial light spectra,[12,35,38,40,41] and different water depths[42-48] (different intensities and spectra at each depth). That is why we must and can find a way to manipulate light intensities and spectra in conjunction with the inevitable cooling of the solar surface cell/module to understand additional light effects and why this is happening. For example, for Si-solar cells, many authors have reported higher efficiencies than the theoretical maximum predicted for silicon solar cells, up to 40%–60%, with a dielectric liquid thin-film that can increase the efficiency[49-51] or others who have reported results indicating that the direct liquid-immersion cooling method[52-56] could be an acceptable method for increasing the efficiency. The conversion efficiency of the monocrystalline Si-solar cell, which is 16–18% under standard testing conditions (STC), decreases to 3–6% under artificial LED light, whereas the amorphous Si-solar cell increases from 8% to 20%.[57] Computer simulations and indoor data measurements were used to investigate the significance of the spectral effects of silicon PV devices.[58,59]

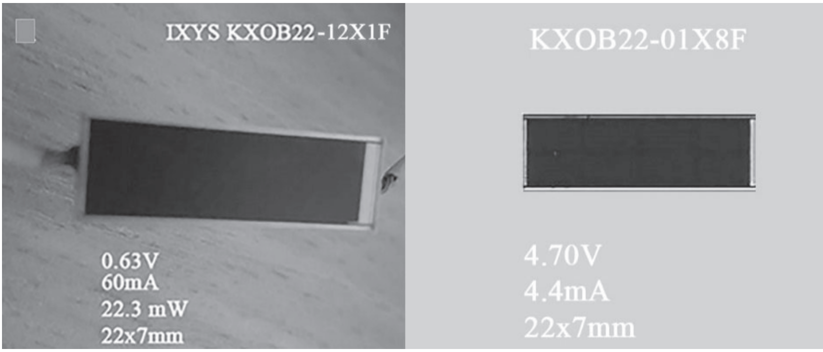

Figure 7. Photos and the main operating characteristics of the monocrystalline Si-solar cells, KXOB22-01X8F and KXOB22-01X8F.

Repeated studies have been conducted on "useful fractions," which are defined as the ratio of measured spectral irradiation to measured global irradiance.[60,61] Ghitas demonstrated that shifting the solar spectrum toward the infrared region produces a negative impact on the device performance of a multicrystalline silicon module.[62] It is critical to combine all of these effects and study the influence of intensity and spectral together with inevitable cooling at the same time, rather than separately. Any changes in intensity, spectra, or some additional light changes, have joined consequences in natural conditions, and temperature control of the surface of the solar cell or module is critical to the credibility of the results and the maintenance of the solar system. To comprehend all of these influences, we must employ some optical design with liquid, such as our design, the WFL system, which was thoroughly described in the previous chapter. Because of the preceding discussion, we demonstrate the results of high-efficiency monocrystalline Si solar cells as well as amorphous Si solar cells for indoor and outdoor applications in the following text. The WFL system is maintained to measure cells under artificial light, with halogen and tungsten lamps, and in natural outdoor conditions.

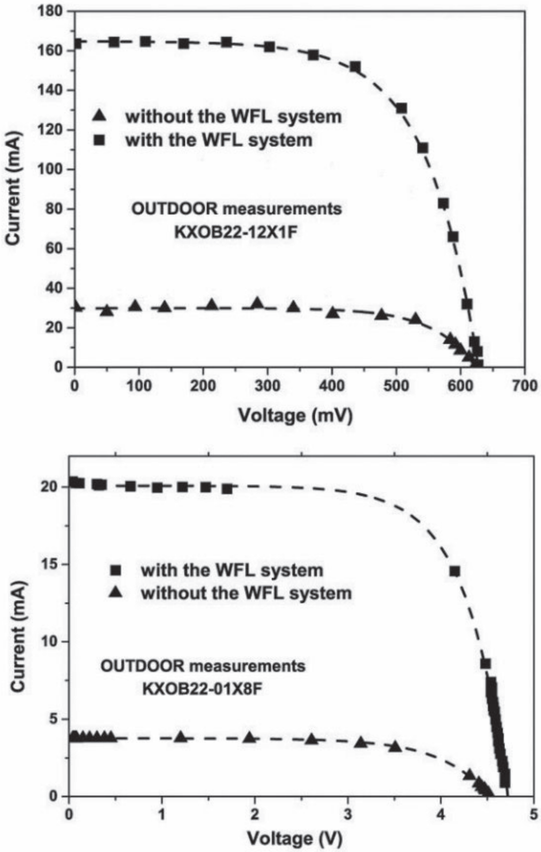

Figure 8. Outdoor *I-V* curves for commercial monocrystalline Si solar cells, IXYS KXOB22-12X1F and KXOB22-01X8F-ND, with and without the use of the WFL system using daily light.

As in previous experiments, we used water as the best cooling liquid in these experiments.[63-65] With changes in spectra, the water flows increase electrical yield while resulting in increased photovoltaic output, independent of any increase or decrease in light intensity. Moreover, a concentration effect with different spectra always improves overall efficiency. Figure 7 depicts the photo and current-voltage characteristics of the monocrystalline Si solar cells used in these tests (indoor and outdoor), IXYS KXOB22-12X1F and KXOB22-01X8F-ND, as provided by the companies (IXYS Korea[66] and Amorton Sanyo[67]). At standard testing conditions (STC) of 1000 W/m^2, the current-voltage and power-voltage characteristics (open-circuit voltage and short-circuit current) of monocrystalline Si-solar cells are given in the same figure. Monocrystalline Si-solar cells have a good response over a wide wavelength area and, as a result, can be used in both indoor and outdoor applications with a cell efficiency of typically 22 %.

We explained in the first chapter of this book that, aside from its cooling effect and spectrum change, the WFL system can be used in two independent regimes depending on the location of the tested solar cell relative to the WFL system and the light source. It means that it can reduce the light intensity if the solar cell is in a different shadow location and increase the light intensity if the solar cell is in or near a focal point, a phenomenon known as the concentration effect.[7,22,68] We can test the influence of different spectra by implementing manipulation regardless of whether the light intensity is increasing or decreasing. Figure 8 depicts the *I/V* curves recorded under outdoor conditions for two commercial monocrystalline Si solar cells, KXOB22-12X1F[66] and KXOB22-01X8F[67], with and without a WFL system and using daily light. The geometry was kept the same for both indoor and outdoor experiments (described in detail in the previous chapter), in the sense that the sun's rays fell vertically on the surface of the WFL system and the hole set-up in general. It should be noted that each expression for determining the efficiency of silicon cells ignores differences in light spectra. Hence, the efficiencies are not given; otherwise, the values would be unrealistically large. More about comparisons of different solar cells' results and understanding the behavior is described in the following chapter. Figure 8 shows that the short-circuit current (I_{sc}) and open-circuit voltage (V_{oc}) measured without the WFL system agree with the results provided by IXYS Korea[66] and Amorton Sanyo[67] at 500 W/m^2 and 1000 W/m^2. The use of the WFL system leads to a significant increase in short-circuit current for both cells, up to 3 to 5 times greater than measured under standard testing conditions. It should be noted that the current-density limit generally for Si is 44.1 mA/cm^2, whereas after use of the WFL system,

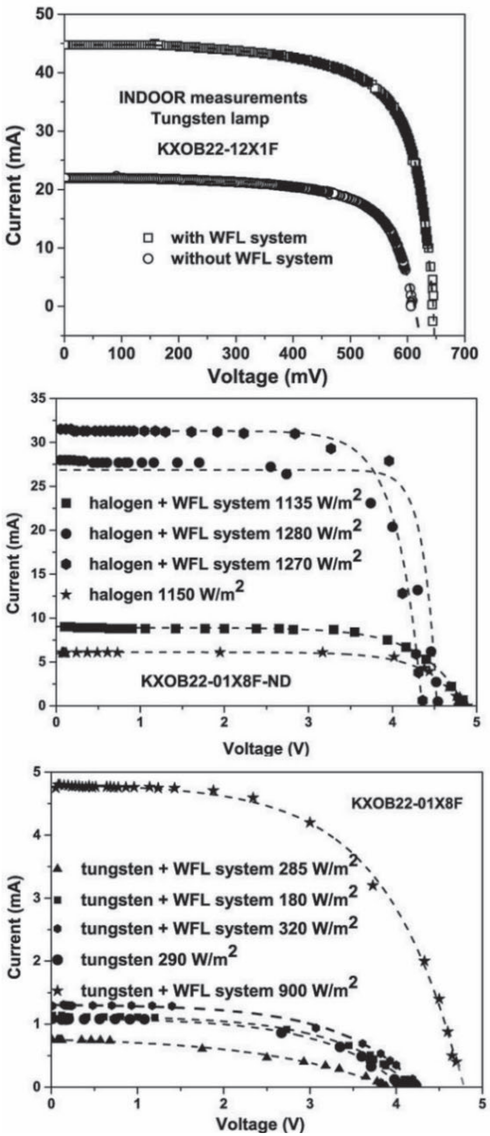

Figure 9. Indoor *I-V* curves for commercial monocrystalline Si solar cells, IXYS KXOB22-12X1F and KXOB22-01X8F-ND, with and without the use of the WFL system, using tungsten and halogen lamps as the initial light source.

current-density increases to 106 mA/cm^2 for the Si-cell, KXOB22-12X1F. Further, the ratios of the I_{sc} and P_{input} are 4.9 and 17.6 without and with the use of the WFL system, respectively, for the Si-cell, KXOB22-01X8F. It seems that a huge increase in I_{sc} cannot be justified by an increase in light intensity, due to the enormously large value of efficiency that overcomes theoretical value and our current knowledge. In figure 9, indoor current-voltage curves for commercial monocrystalline Si-solar cells, IXYS KXOB22-12X1F and KXOB22-01X8F-ND, with and without the use of the WFL system, using tungsten and halogen lamps as the initial light source, are shown. In figure (first dependence), indoor measurements are depicted for an IXYS KXOB22-12X1F Si-solar cell with and without the WFL system, using a tungsten lamp as the initial light source at constant low light intensities of 50 W/m^2 for both presented curves (the solar cell is located far from the focal point and thus in the shade). The results are given for the entire 1.54 cm^2 surface of the solar cell. The ratio of short circuit current (I_{sc}) to input light energy (P_{input}) for measured *I-V* curves is 4.42 for an I_{sc} of 22.5 mA and 8.96 for an I_{sc} of 45 mA without and with the WFL system, respectively. As can be seen, the ratio (I_{sc}/P_{input}) is much higher after passing through the WFL system, implying that short-circuit current is quite high for such low light intensity. Furthermore, the open-circuit voltage (V_{oc}) for the light intensity of 5% of the sun should be 530 mV, according to company data for the silicon solar cell. In our case, it is 620 mV, which increases to nearly 650 mV when the WFL system is employed. On the other hand, the short circuit current (I_{sc}) and open-circuit voltage (V_{oc}) decrease as the light intensity decreases in comparison to 1000 W/m^2 and without the WFL system. The use of the WFL system improves both the open-circuit voltage (V_{oc}) and the short-circuit current (I_{sc}). Further, figure 9 depicts a commercial monocrystalline, KXOB22-01X8F-ND Si-solar cell under artificial light conditions, tungsten, and halogen lamps. It should be noted that the main operating characteristics of the solar cell (dimensions 22x7x1.8 mm), open-circuit voltage (V_{oc}) and short-circuit current (I_{sc}), measured at an STC of 1000 W/m^2, Air Mass of 1.5, and an operating temperature of 25 ^{o}C, are 4.7 V and 4.4 mA, respectively. As can be seen, small changes in the halogen lamp light intensity value resulted in huge changes in I_{sc} and V_{oc}, with up to 7 times higher values of short-circuit current. The short-circuit current (I_{sc}) to input light energy (P_{input}) ratios are 5.2 and 24.8 without and with the WFL system in the measurements, respectively.

Furthermore, in many confirmations thus far, these changes can be attributed to the spectrum effect (or possibly some additional light effects, which we will discuss further in the following chapter) that is always altered by the use of the WFL system. Next, there are no significant oscillations in short-circuit current (I_{sc}) and open-circuit voltage (V_{oc}) for lower light intensities, "shadow position," and a relatively weak tungsten lamp with and without the WFL system. Here it can also be seen that for very small differences in light intensities, I_{sc} and V_{oc} increase or decrease, confirming that the light spectra are dominant at lower intensities.

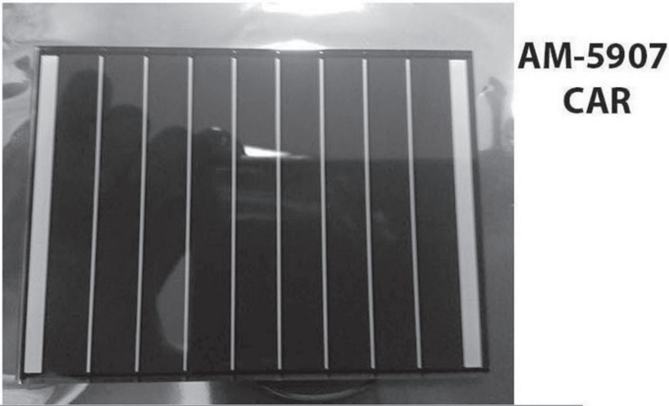

Model	$100 mW/cm^2$		SS-50k-lux		External dimensions (mm)	Weight (g)
	Typical operating characteristics	P_{max} (V_{op}-I_{op})	Typical operating characteristics	P_{max} (V_{op}-I_{op})		
AM-5907	(5.0 V-45.7 mA)	241 mW (5.9 V -40.8 mA)	(5.0 V-20.6 mA)	114 mW (5.9 V-19.3 mA)	75.0 X 55.0	18.3

Figure 10. Photo and the main operating characteristics of the amorphous Si-solar cell for outdoor use, AM-5907 CAR.

At the "focal point position" where intensity increases, there is an obvious huge improvement in I_{sc} and V_{oc}, 4.81 mA and 4.78 V, better than the data for the standard testing conditions (STC) given by the company, which is additional proof of the at least spectra influence. Figure 10 depicts photos and the main operating characteristics provided by the company (Amorton Sanyo) for amorphous for outdoor applications Si-solar cell, AM-5907 CAR. For the same cell, the *I-V* curves at different intensities of the light (artificial as well as outdoor) and with and without the use of the WFL system are presented in figure 11. The typical operating characteristics are given for both standard testing conditions, 1000 W/m^2 and lower light intensity,

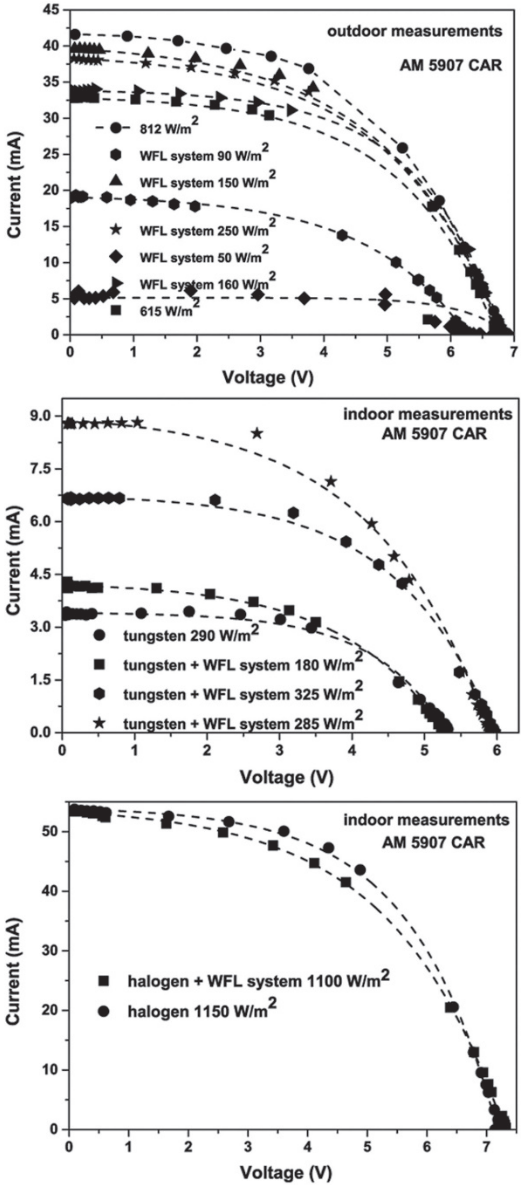

Figure 11. *I-V* curves for the three different light sources: artificial, tungsten, halogen, and natural outdoor light for the amorphous Si-cell for outdoor application (AM-5907 CAR) without and with the use of the WFL system.

50 kLux, which is approximately 500 W/m^2. The values are: the open-circuit voltage (V_{oc}) and short-circuit current (I_{sc}), 5 V and 45.7 mA, measured at 1000 W/m^2, respectively, while for 50 klux they are 5V and 20.6 mA (see figure 10 for details). The outdoor measurements with and without the use of the WFL system as the first *I-V* curve dependence are presented in figure 11. We can see that the current-voltage values are much higher with the used WFL system, and we can measure quite high I_{sc} and V_{oc}, almost matching the values measured under standard testing conditions (STC). The I_{sc} and P_{input} ratios are 5.1-5.3 and 10.5-26.5 without and with the WFL system, respectively. As expected, oscillations at lower light intensities are much more pronounced than in monocrystalline cells. Further, the next dependence in the figure shows that at the lower light intensity (tungsten lamp), the WFL system increases the values of I_{sc} and V_{oc} independent of the light intensity. We mentioned and confirmed in the previous dependence that the efficiency of the monocrystalline Si-solar cell under standard testing conditions (STC), decreases under artificial LED light, whereas the efficiency of the amorphous Si-solar cell, in contrast, increases.[57] As part of at least the spectral influence, this could also explain the larger oscillations in the presented dependences on the values of I_{sc} and V_{oc}, as well as the amorphous cell's better performance at low light intensities than the monocrystalline Si-cell in the previous case. Unlike the monocrystalline Si-solar cell whose surface was very small (1.54 cm^2), the amorphous for outdoor application has a large cell surface area (41.25 cm^2), and therefore the "focal point" measurements were not applied. Apart from the fact that amorphous Si-solar cells show better PV response at lower light intensities, this is an additional reason for not showing results at higher light intensities. The final dependence on figure 11 confirms the previously stated and reveals that there was no real improvement in the higher light intensity obtained using a halogen lamp regardless of the used WFL system and changed spectra, compared to monocrystalline Si-solar cells where oscillations were massive. Overall, for both monocrystalline and amorphous Si-solar cells, it's evident that at least spectra influence causes huge oscillations in operating characteristics, just as for amorphous cells, oscillations are more pronounced at lower light intensities comparable to monocrystalline as we expected. As was stated in the previous title, the processes themselves in commercial amorphous and monocrystalline Si-solar cells will not be considered here, because they are made by solar companies and their processes are known and described.

Application of the WFL system and light manipulation to solar cells based on synthesized doped and undoped Sb_2S_3 semiconductors

This part of the chapter deals with the results of the development of different solar cells based on the synthesized undoped and doped Sb_2S_3 semiconductor nanoparticles.[9,10,69,70] This semiconductor is one of the most interesting and promising materials for use in solar devices because of its high absorption coefficient and low bandgap, among other features.[71-75] Before our report, there had been no report in science on the application of synthesized Sb_2S_3 material in different photovoltaic cell devices entirely based

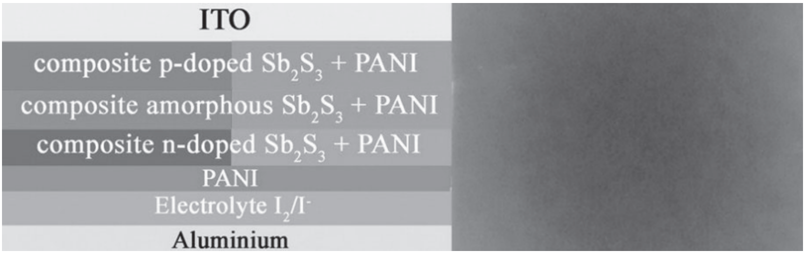

Figure 12. The designed cell's schematic and an image of the thin film made of p-doped Sb_2S_3 + PANI/amorphous/undoped Sb_2S_3 + PANI/n-doped Sb_2S_3 + PANI. PANI stands for polyaniline, a conductive polymer.

based on this semiconductor. The devices are based on extensive reports of quite a number of experimental and theoretical results on the synthesized Sb_2S_3 semiconductor.[74-79] Figure 12 depicts a schematic representation of one of the designed Sb_2S_3-based cell architectures.[9] A thin film of p-doped Sb_2S_3+PANI/amorphous/undoped Sb_2S_3 + PANI/n-doped Sb_2S_3 + PANI deposited on indium tin oxide (ITO) conductive coated glass is also depicted in figure 12. Typical illuminated *I-V* curves for fabricated cells under low illumination of 250 W/m^2 and 50 W/m^2 measured with the WFL system are shown in figure 13. The efficiencies of the manufactured cells are $\eta = 2.12\%$ for the light intensity of 250 W/m^2 and $\eta = 9.03\%$ for the light intensity of 50 W/m^2. It is clear from the figure that the cells are more efficient at lower light intensities. It is important to note that approximately 20 cells with the same characteristics were created, and all of them exhibit the same behavior. Figure 13 shows that the designed solar cell exhibits better efficiency with the use of the WFL system at lower light intensities.[9] Again, the use of the WFL system was found to be one of the possible explanations for the resulting higher efficiency of solar cells at lower intensities.

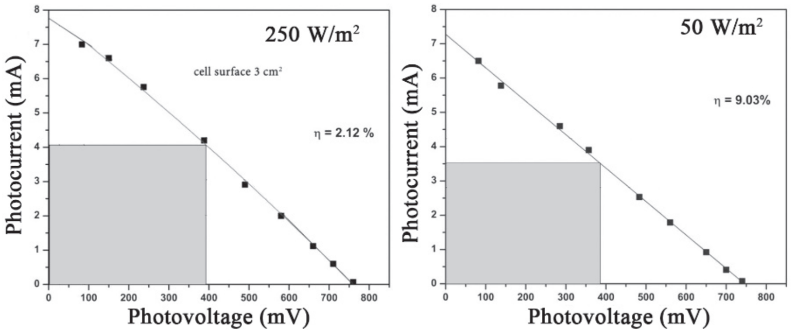

Figure 13. ITO/p-doped Sb_2S_3 + PANI/amorphous/undoped Sb_2S_3 + PANI/n-doped Sb_2S_3 + PANI/PANI/electrolyte (0.5M KI + 0.05MI_2)/Al solar cell: illuminated *I-V* curves for two different low-light intensities of 50 W/m^2 and 250 W/m^2, measured with the WFL system and a tungsten lamp.

Further, in figure 14, current-voltage characteristics of the same cell under standard testing conditions (STC) and without using the WFL system were measured using a halogen lamp. It should be emphasized that previous figure 13, which was measured with the WFL system, was taken with a tungsten lamp. It is obvious that the cells exhibit far higher efficiency

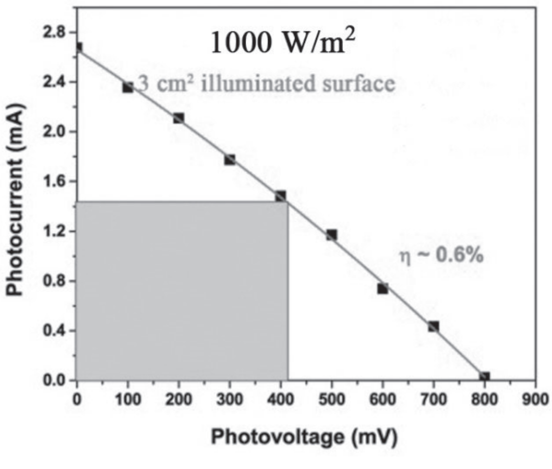

Figure 14. The illuminated *I-V* curve for the designed solar cell, ITO/p-doped Sb_2S_3 + PANI/amorphous/undoped Sb_2S_3 + PANI/n-doped Sb_2S_3 + PANI/PANI/electrolyte (0.5M KI + 0.05MI_2)/Al, obtained at standard testing conditions (STC) measured with a halogen lamp.

at lower light intensities, with changed spectra, and when using the WFL system. Further results and explanations of the design and commercial solar cells are given in the next chapter. The illuminated surfaces of the designed cells shown in the preceding figures measure 3 cm^2. It is critical to understand the dimensions of the cell because their size affects the efficiency value. Figures 13 and 14 show efficiency calculations for the illuminated surfaces of the cells. Different shapes of the illuminated *I-V* curve are discussed in scientific papers when we characterize each cell individually, [9,69,75,80] and will not be covered in this book. Considering that the designed solar cell was made in our group, here, unlike the previous results, we will briefly comment on the processes in the cell. Figure 15 depicts a schematic band diagram of an ITO/p-doped Sb_2S_3/amorphous/ undoped Sb_2S_3/n-doped Sb_2S_3/Al junction. A typical solar cell has a p–a–n (or p–i–n) diode structure, which is similar to that of an amorphous silicon solar cell[81], with p-, n-, and a- (or i-referring to amorphous and intrinsic (undoped)) layers. Light enters the device through the p-layer, which efficiently supports hole collection. The reason for this is that holes have a lower mobility rate than electrons. Experiments and theoretical calculations

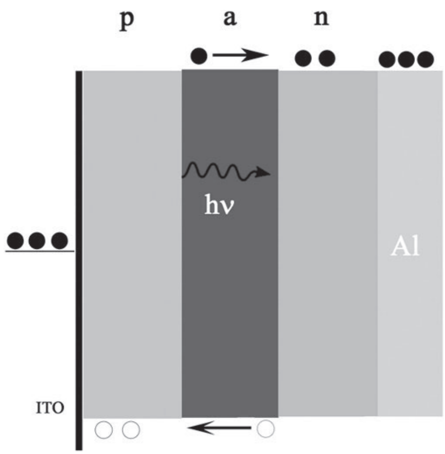

Figure 15. Schematically presented the band diagram of an indium tin oxide (ITO)/p-doped Sb_2S_3/amorphous/undoped Sb_2S_3/n-doped Sb_2S_3/Al junction.

for synthesized Sb_2S_3 revealed significant differences in the effective masses of an electron and a hole ($m_e^* = 1.035\ m_e$ and $m_h^* = 1.843\ m_e$).[74] According to calculations, a hole's effective mass is much greater than that of an electron, implying that holes are less mobile than electrons. A transparent conductive oxide (ITO) film contacts the diode from the front side, and a metal film serves as both a rear contact and a back reflector in the simplest case. An electric field is formed over the intrinsic i- or a- layer by thin (30 nm) p-doped and n-doped layers. Because of their shorter lifetimes in doped samples, electrons and holes generated in doped layers contribute to photocurrent. By the internal electric field, electrons and holes generated in the undoped or amorphous layer are driven to the n-layer and p-layer, respectively.

The charge carrier collection is primarily determined by the quality of the doped and undoped layer materials, the strength and distribution of the electric field, and the presence of PANI, a conductive polymer. It should be noted that the cell made of doped samples without PANI functions as an electricity generator, but with lower photocurrent and efficiency values. It is also important to note that the extra layer of PANI does not affect the cell's efficiency or operation, but only protects the film from electrolyte corrosion. Figure 16 depicts the bandgap (E_g), calculated Rydberg constant (R_x), and Bohr radius (a_x) of free excitons in several direct-gap III–V and II–VI compound semiconductors, as well as the electron effective mass (m_e^*) and hole effective mass (m_h^*). The theoretical and experimental results were "integrated" to yield values for the synthesized Sb_2S_3 semiconductor (the structural, morphological, electronic, and optical properties of the synthesized Sb_2S_3 are combined with the theoretical calculations of the electronic and optical properties of the synthesized powders). According to experimental and theoretical calculations, this semiconductor has different electronic properties than the most well-known and widely used semiconductor. The calculated excitonic effects and effective masses of electrons and holes are important in understanding the physical effects of Sb_2S_3 use in solar cells as well as the fundamental understanding of this semiconductor.[75, 81-84] The calculated high dielectric constant ($\varepsilon \approx 11$), combined with the simultaneous high energy of Wannier–Mott exciton ($E_{ex} \approx 0.1$ eV and radius of exciton $a_x \approx 0.9$ nm ($m_e^* = 1.035m_e$ and $m_h^* = 1.843m_e$), distinguishes this semiconductor from other semiconductors used in solar cells, excitonic solar cells-Frenkel excitons.[85,86] A more in-depth examination revealed that there are arguments for both of the basic types of excitons observed in our case. Wannier-Mott excitons, in particular, are primarily observed in semiconductors with medium-sized band gaps in the range of 1 to 3 eV, which have a large radius (the electron-hole separation is so large) that it encompasses many atoms (hence the alternative name of "free" excitons). These have low exciton energies due to the large electron-hole separation.[85,86] On the other hand, Frenkel excitons, are found in insulator crystals and molecular crystals, which have a much smaller radius, comparable to the size of the unit cell, and thus have higher exciton energies of the order of 0.1 to 1 eV. With an exciton radius of $a_x \approx 0.9$ nm (calculated for synthesized Sb_2S_3 powder), which is three times larger than the smallest distance between Sb-S atoms in the unit cell, it is clear that we have an argument for both basic types of excitons.

Crystal	Eg (eV)	R_x (meV)	a_x (nm)
GaN	3.5	23	3.1
ZnSe	2.8	20	4.5
CdS	2.6	28	2.7
ZnTe	2.4	13	5.5
CdSe	1.8	15	5.4
CdTe	1.6	12	6.7
GaAs	1.5	4.2	13
InP	1.4	4.8	12
GaSb	0.8	2.0	23
InSb	0.2	(0.4)	(100)
Sb_2S_3	1.3-1.5	74	0.8-0.9

Crystal	m_e^*/m_e	m_h^*/m_e
GaN	0.13	0.8
ZnSe	0.13	0.65
CdS	0.19	0.8
ZnTe	0.12	0.5
CdSe	0.06	0.62
CdTe	0.05	0.46
GaAs	0.07	0.2
InP	0.08	0.3
GaSb	0.04	0.1
InSb	0.01	0.25
Sb_2S_3	1.035	1.843

Figure 16. On the left side of the figure are given the bandgap (E_g), the calculated Rydberg constant (R_x), and the Bohr radius (a_x) of free excitons in several direct-gap III-V and II-VI compound semiconductors. The electron effective mass (m_e^*) and hole effective mass (m_h^*) for III-V and II-VI compound semiconductors are given on the right side. All the values for the synthesized Sb_2S_3 semiconductor are obtained by the integration of the theoretical and experimental results.[75]

Figure 17 depicts a schematic of the next designed solar cell made of ITO/composite amorphous Sb_2S_3 + PANI/TiO_2/electrolyte I_2/I^-/Al.[10] Figure 18 depicts typical illuminated *I–V* plots of fabricated cells made of ITO/composite amorphous Sb_2S_3 + PANI/TiO_2/electrolyte I_2/I^-/Al under low illumination of 250 W/m^2 and 50 W/m^2 using a tungsten lamp and the WFL system. The calculated efficiencies of the cells are $\eta = 0.74\%$ for 250 W/m^2 and $\eta = 2.71\%$ for 50 W/m^2 light intensity, respectively. As in the previously designed cell, it is obvious that the cells exhibit higher efficiency at lower light intensities and with the use of the WFL system. The surface of the solar cell is the same as in the previous design, 3 cm^2.

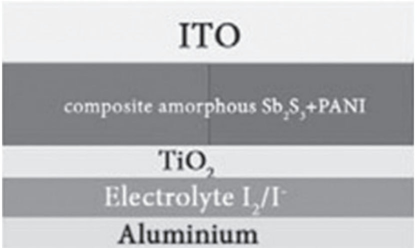

Figure 17. The designed cell's schematic, made of ITO/composite amorphous Sb_2S_3 + PANI/TiO_2/electrolyte I_2/I^-/Al. PANI stands for polyaniline, a conductive polymer.

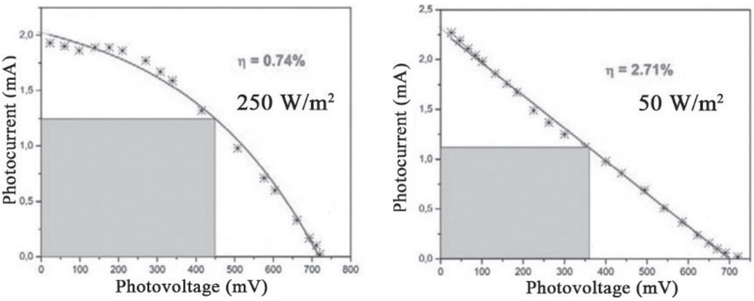

Figure 18. ITO/ composite amorphous Sb_2S_3 + PANI/TiO_2/electrolyte I_2/I^-/Al solar cell: illuminated *I-V* curves for two different low-light intensities of 250 W/m^2 and 50 W/m^2, measured with the WFL system and a tungsten lamp.

Figure 19 shows the illuminated *I-V* curve for the designed solar cell, ITO/composite amorphous Sb_2S_3 + PANI/TiO_2/electrolyte I_2/I^-/Al, measured with a halogen lamp, at standard testing conditions (STC), and without the WFL system. The calculated efficiency of the cell is $\eta = 0.25\%$ for 1000 W/m^2 light intensity. There is obviously a very large difference in efficiencies relative to light intensities in terms of higher efficiencies for lower light intensities. We also see that the WFL system itself has the effect of increasing the efficiency of the designed cells. Some of the results at lower intensities with lower efficiencies without the presence of the WFL system are presented in the next chapter. Also, as we already emphasized here, the designed Sb_2S_3 solar cells are the first PV cells where we employed the WFL system. We were unaware that through light manipulations, we could start to understand the fact that some solar devices exhibited higher efficiencies at lower light intensities. This is the reason for the low number of direct comparisons of results with and without WFL systems at the same light intensities.

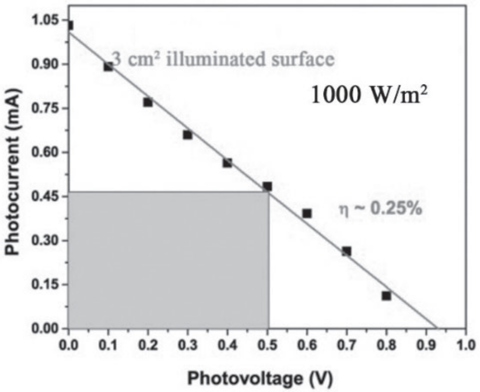

Figure 19. The illuminated *I-V* curve for the designed solar cell, ITO/ composite amorphous Sb_2S_3 + PANI/TiO_2/electrolyte I_2/I^-/Al obtained at standard testing conditions (STC) measured with a halogen lamp.

One more example of the designed cell is presented in figure 20.[8] On the right side of the figure, one side of the cell is lighter in color (it belongs to conductive PANI) and the other side of the cell is darker in color (it belongs to the color of the P3HT polymer). Furthermore, the solid carrier that we used is completely flexible, allowing for good contacts in the cell, which is essential for its properties. On the left-hand side, a schematic presentation of the designed cell and the composition of every layer are given.

In figure 21 are presented *I-V* curves of fabricated cells under illumination of 50 W/m^2 (made with a tungsten lamp and with the WFL system), 350 W/m^2 made with a halogen lamp and with the WFL system, as well as under the illumination of 1000 W/m^2 made with a halogen lamp and without the WFL system. The cell's efficiencies are = 22.1% for 50 W/m^2, = 2.87% for 350 W/m^2, and = 0.7% for 1000 W/m^2. As we can see again, the highest efficiencies are reached at lower light intensities with changed light spectra and with the presence of the WFL system. The impact of different sources of light (different lamps) with respect to diversity in spectra and intensity also has a negligible influence on solar cell characteristics.

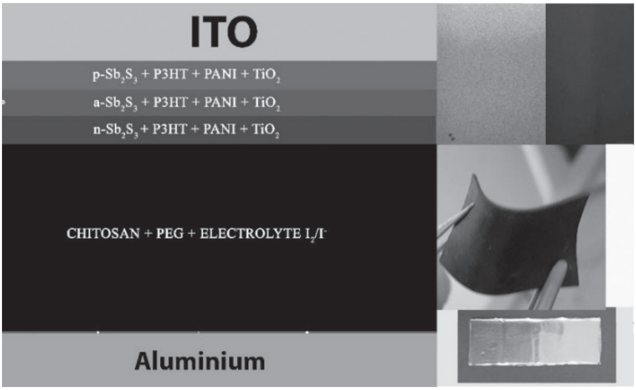

Figure 20. A schematic of the cell, as well as images of the thin film, solid carrier, and counter electrode.

Figure 22 depicts the energy level diagram of one layer. Sb_2S_3 is p-doped in the first layer, then amorphous or undoped, and finally n-doped.

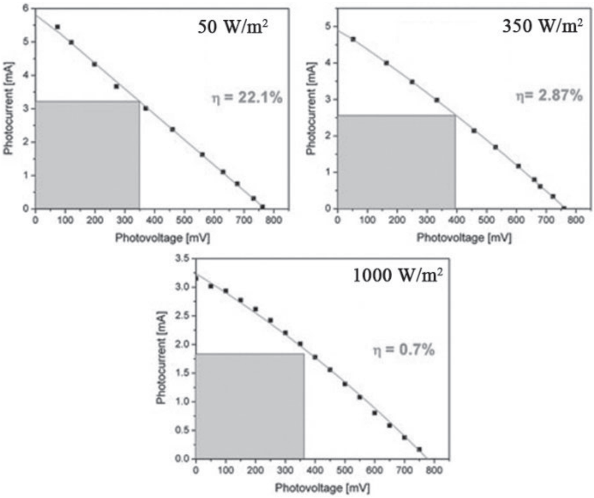

Figure 21. The illuminated *I-V* curves for the designed solar cell, obtained at 50 W/m^2 (tungsten lamp) and 350 W/m^2 (halogen lamp) measured with the WFL system, and at standard testing conditions (STC), 1000 W/m^2 measured with a halogen lamp without the WFL system.

Light is entering through the p layer, which has an excess of holes in the device, while the n- layer has an excess of electrons. An electric field was formed by p-doped and n-doped layers over the intrinsic (undoped) layer. The internal electric field is in charge of directing electrons and holes from the undoped layer to the n- and p- layers. The quality of all Sb_2S_3 materials, the P3HT and PANI conductive polymers responsible for charge carrier collection, and the TiO_2 photon absorber drive solar cell performance. P3HT is a hole-conducting dye with high absorption in the Vis range, which is critical given the use of water lenses. TiO_2-derived electrons can recombine with holes in P3HT or Sb_2S_3. Direct recombination can also occur in the absorber, and holes in P3HT can recombine with negative charge carriers in the Sb_2S_3 layer.[87] Making a composite allows for easier recombination of materials.

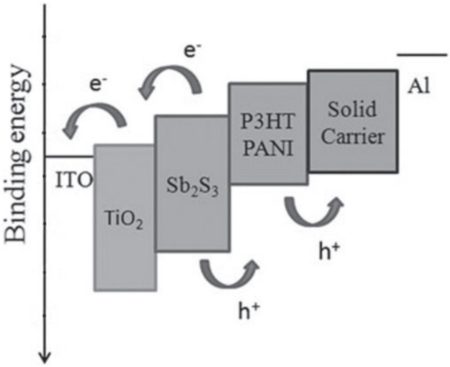

Figure 22. Simplified band energy diagram of the designed solar cell.

As previously stated, the next chapter will address the additional consequences of the WFL system's use. Certainly, using appropriate components in the cell design, as well as the way devices are made in terms of compatibility and stability, improves photon absorption, resulting in better device efficiency. Next, it is reported here that an inexpensive, solid, and stable solar cell is designed and made entirely of synthesized materials: Sb_2S_3/hypericin (dye) thin film on ITO-coated glass (working electrode), aluminum (counter electrode), and PVA matrix (solid carrier) loaded with electrolyte (0.5M KI + 0.05M I_2).[69] Figure 23 depicts the cell architecture schematically. The figure also includes images of an amorphous Sb_2S_3/hypericin composite thin film deposited on ITO glass, a polyvinyl alcohol (PVA) matrix loaded with electrolyte, and an aluminum electrode.

The film's accented dark red color is derived from amorphous sulfide and extracted hypericin, both of which are red. The black color of the PVA matrix is caused by the black color of the electrolyte. Hypericin, a low-cost natural dye, was combined with amorphous Sb_2S_3 as a composite film and absorption layer to increase band gap values and photon absorption. Figure 23 additionally depicts surface phase AFM images of the amorphous Sb_2S_3/hypericin composite film. The presence of two phases is clearly visible; spherical Sb_2S_3 particles immersed in dye. Figure 24 depicts typical illuminated *I–V* plots of fabricated cells based on the synthesized amorphous Sb_2S_3/hypericin composite thin film/PVA matrix loaded with electrolyte/Al under very low, low, and medium illumination levels of 50 W/m^2, 250 W/m^2, and 550 W/m^2. Solar cells are clearly more efficient at lower light intensities.

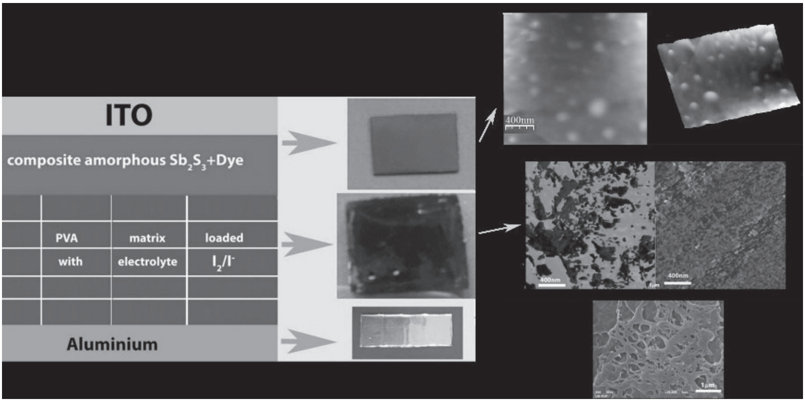

Figure 23. A schematic of the designed cell and images of the thin film made of amorphous Sb_2S_3/hypericin composite, PVA matrix loaded with electrolyte and aluminum electrode. On the right-hand side are given phase and 3D AFM images of the Sb_2S_3 amorphous powder/hypericin composite film and images of the PVA matrix filled with an electrolyte. The last image below is a scanning electron micrograph (SEM) of a lyophilized PVA matrix released from water.

Furthermore, when compared to the expensive dye used in DSSCs, the use of the low-cost natural dye hypericin results in lower power generation, and in this regard, our designed cell achieved an efficiency of about 3.84 % at a light intensity of only 50 W/m^2, which is not bad at all. It is important to note that at least ten cells with the same characteristics were created, and they all exhibit the same behavior. It should also be noted that PVA demonstrated excellent stability over a three-month testing period. There were no changes in PVA during testing at low light levels of 50 W/m^2 and 250 W/m^2. Over the course of a week, the film remained stable. Following that, its structure crumbled as a result of the dye's constant contact with electrolyte-filled PVA.

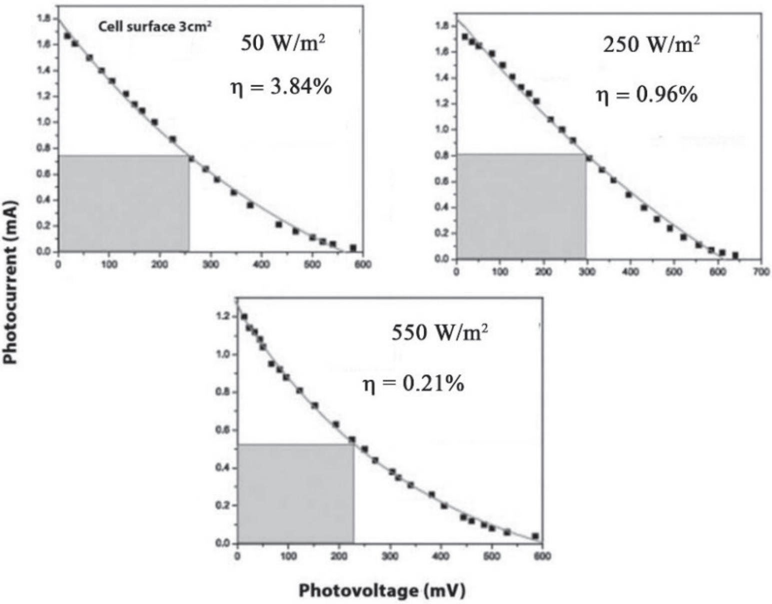

Figure 24. Illuminated *I–V* curves for an ITO/amorphous Sb_2S_3/hypericin composite/PVA matrix loaded with electrolyte (0.5M KI/10.05M I_2)/Al solar cell: plot of power output characteristics for three low-light intensities of 50 W/m^2, 250 W/m^2, and 550 W/m^2. To reach the lowest light intensities of 250 W/m^2 and 50 W/m^2, the WFL system was used.

It has already been stated that the changes in typical illuminated *I-V* curves, which are actually translated from exponential to linear curves, will not be discussed in this book. It is sufficient to state here that the shape of the illuminated *I–V* curves is primarily influenced by the resistance present in the designed solar cell. As previously stated in this chapter for other designed Sb_2S_3-based solar cells, to achieve the low light intensities we used the WFL system (250 W/m^2 and 50 W/m^2 illuminations) interposed between the lamp and the cell, as well to prevent heating. Further, we compare what is happening with the same designed solar cell with and without the use of the WFL system, by keeping the same light intensities.

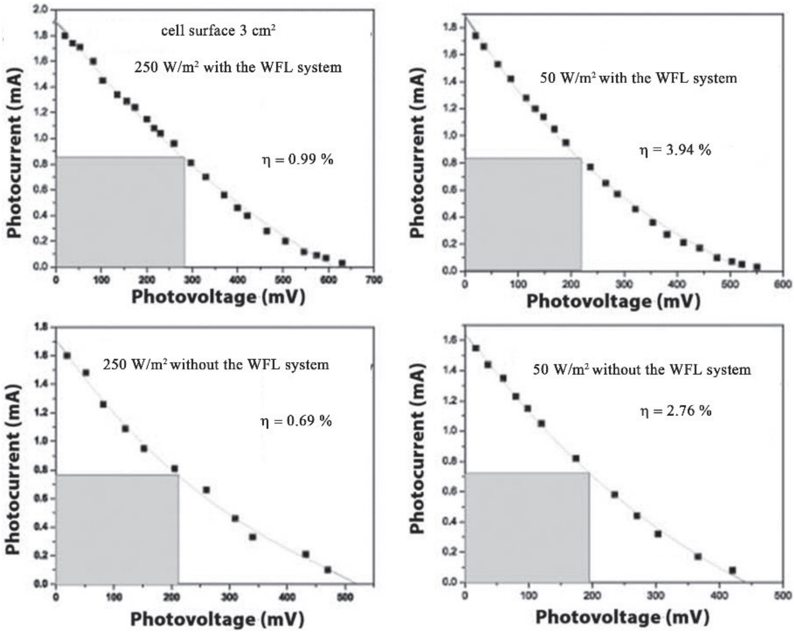

Figure 25. Illuminated *I–V* curves for solar cells made of ITO/amorphous Sb_2S_3/hypericin composite/PVA matrix loaded with electrolyte (0.5M KI/10.05M I_2)/Al: plot of power output characteristics for two low-light intensities, 50 W/m^2 and 250 W/m^2 using the WFL system.

As can be seen, according to results presented in figure 25, the use of the WFL system again increases the efficiency of the designed solar devices at lower and quite low light intensities. Here again, at least the changes in spectra influence the changes in device efficiency. Although the efficiency of this cell is not high because of the cheap components that we tried to use (a low-cost natural dye, hypericin, compared to the expensive dye used in dye-sensitized solar cells, as well as other synthesized components of the solar cell that are cheap while their processes of synthesis are quick and easy), the increase in efficiency due to the use of designed optics is not small. At the lowest light intensity of only 50 W/m^2, that increase is nearly 40%. The designed cell is made of the same materials as the DSSC. The only difference is that instead of TiO_2, we used Sb_2S_3. As a dye, Sb_2S_3 can absorb photons and release electrons. When a photon strikes a composite of hypericin molecules and Sb_2S_3, the photon's energy is absorbed by the dye molecule and sulfide. Both dye molecules and Sb_2S_3 become excited and emit electrons (nano-particles of Sb_2S_3 also allow electronic conduction), which reach the anode via the iodide solution as an indirect transmitter.

The transfer of charge into the electrolyte at the surfaces of the dye, semiconductor, and electrolyte causes charge separation at the particle surface.[88,89] Iodide can replenish the electrons lost by dye molecules. When electrons reach the anode, the iodide molecules oxidize to triiodide, which then contacts the cathode. The triiodide recovers its missing electrons from the cathode, reducing the triiodide back to three iodine molecules. When all of these processes occur at the same time, an electric current is produced.

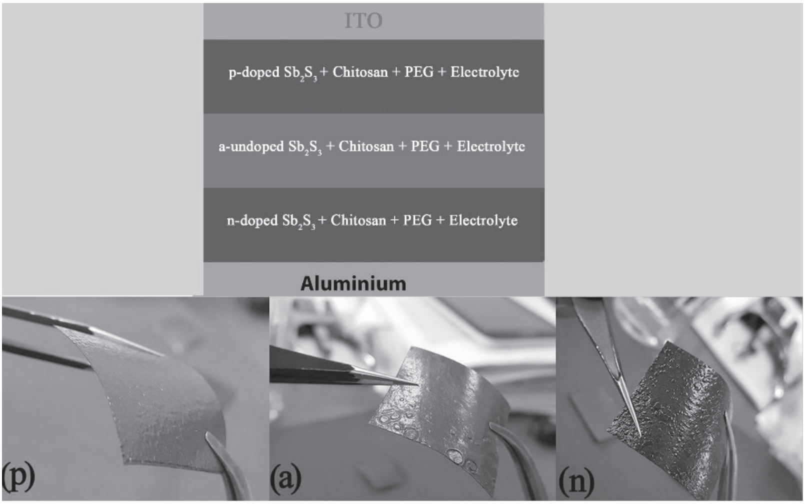

Figure 26. A schematic of a designed cell containing the exact composition of each of the flexible Sb_2S_3/solid layers, as well as photographs of designed flexible layers labeled (p), (a), and (b) (n). Sb_2S_3 solid layers are extremely flexible, and their softness after filing with electrolyte allows for good cell contacts.

The last designed Sb_2S_3-based solar cell we reported here is a flexible solar cell made of p-doped, amorphized, amorphous, undoped, and n-doped Sb_2S_3 solid carriers loaded with electrolyte. The working electrode was indium tin oxide (ITO) glass, and the counter electrode was aluminum.

The corresponding amorphized amorphous undoped and p and n-doped Sb_2S_3 semiconductors (in construction p-a-n) were synthesized using a low-cost casting and solvent evaporation technique from a blend of chitosan, polyethylene glycol, and an electrolyte containing 0.5 M potassium iodide and 0.05 M iodine. The results show that flexible Sb_2S_3 solar cells have good stability and an efficiency of around 10% at 50 W/m^2.

Overall, it has been demonstrated for the first time that flexible solar cells based on the synthesized Sb_2S_3 semiconductor can be manufactured and used for low-light-intensity applications. Figure 26 depicts a schematic representation of the designed cell architecture. A thick (around 1 mm) p-doped, amorphous (a)-undoped, and n-doped (marked with (p), (a), and (n)) flexible Sb_2S_3/solid carrier is also shown in the figure. Solid carriers are extremely flexible, and their softness after filling with electrolyte allows for good contacts within the cell. Figure 27 depicts typical illuminated *I–V* curves for fabricated cells under 50 W/m^2 illumination.

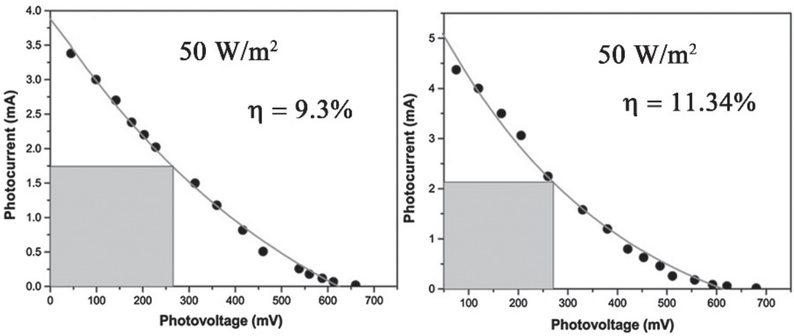

Figure 27. The figure depicts illuminated current-voltage (*I–V*) curves for designed solar cells measured with the WFL system at a very low light intensity of 50 W/m^2. The figure shows the measured results for two different designed solar cells made to be the same.

Two cells with measured results were made to be the same. At 50 W/m^2, the cell efficiency is 9.3% and 11.3%, respectively. A typical solar cell has a p–a–n diode structure, that is similar to that of an amorphous silicon solar cell[90], where p-, n-, and a- (or i- refer to doped and intrinsic (undoped) layers. Light enters the device via the p-layer, which efficiently supports hole collection. A transparent conductive oxide (indium tin oxide, ITO) film contacts the diode from the front side, and a metal film serves as both a rear contact and a back reflector in the simplest case. Over the intrinsic or undoped layer, thick p-doped and n-doped layers create an electric field.

Electrons and holes generated in the undoped layer are driven to the n and p-layers by the internal electric field, respectively. It should be noted that the cell made without extra electrolyte loaded into every layer functions as an electricity generator, but with lower photocurrent values and lower efficiency. The handmade WFL system was placed between the lamp and the cell to prevent cell heating, reduce light intensity, and make at least spectral changes. The illuminated surfaces of the cells are 3 cm^2, with a total surface area of 7.5 cm^2. We were able to obtain repeatable results with the same efficiency using no temperature effect and an optical system. As previously mentioned, and discussed in this book, the use of a lens/optic system with a flowing water layer that at least changes the spectrum enables the application of these solar cells in the majority of conditions present on Earth with low light irradiation.

Conclusion

In this chapter of the book, different solar cells, dye-sensitized, different types of Si-solar cells, as well as different types of designed solar devices based on synthesized doped and non-doped Sb_2S_3 semiconductors are presented. The common behavior of all the described solar devices is to give better photo-voltaic characteristics and hence efficiency with the use of WFL systems. The influence of different spectra as well as different light intensities by light manipulation is a very important factor in furthering understanding of the utilization of designed and commercial solar devices. The deviation of artificial light spectra from standard test conditions (STC), although small, cannot be ignored. Such manipulations of light (apart from the cooling effect) allow us to better understand the operation of solar devices and the changes in the influence of spectrum and intensity, as well as possible additional influences related to the nature of light or additional light effects. In addition, such experiments may allow us to understand and approach the answers to questions such as our negligible use of free solar energy, better performance of solar devices at lower light intensities, as well as set theoretical limits on the maximum efficiency of the solar device. Furthermore, the most important conclusions for every separate solar cell presented here will be emphasized.

Based on measurements on dye-sensitized solar cells, the results show that it is critical to emphasize the type of light source in the characterization. Because the differences in obtained parameters can be significant, it is critical to pay close attention to the type of light source, i.e., spectrum, used. Furthermore, it was observed that by using the same light source and varying the intensity of light, the highest efficiency was achieved at the lowest intensity of light (100 W/m^2~1.5%). Measurements at various intensities and spectra revealed that solar cells with an efficiency of ~4.4% measured with a halogen lamp at 350 W/m^2 produced the best results, while all cells measured with a xenon lamp produced the worst results (1% at 500 W/m^2). It should be noted here that when it is discussed concerning the best-reached efficiency here, it is always meant to be the best numerical number. For instance, in the mentioned case, we said that the best efficiency was reached with a halogen lamp, while with a tungsten lamp and intensity of only 50 W/m^2, we obtained nearly 2.6% efficiency. This intensity is seven times lower than the intensity reached with a halogen lamp, so in general, obtaining efficiency at a lower light should be considered a better result. We also demonstrated an intriguing aspect of using the WFL system to change light distribution without changing a light source. These analyses revealed that the designed dye-sensitized solar cells performed twice as well with a halogen lamp at 350 W/m^2 and more than ten times better with a tungsten lamp at 50 W/m^2. Efficiencies ranged from 2.3% to 2.4% without the WFL system, and 27.8% and 30.5% with used optics, respectively. It is critical that we all understand that even minor changes in the spectra (apart from the possible additional light effects) cause significant changes in the properties of solar cells, which will be attempted to explain in the following chapter.

The performances of the presented high-efficiency commercial monocrystalline Si solar cells, IXYS KXOB22-12X1F and KXOB22-01X8F-ND, were evaluated under artificial and natural light, as well as with and without the use of the WFL system for cooling, which increases and decreases light intensity with changes in the spectrum. It has been discovered that using the WFL system improves the PV performance of the device in all conditions. The basic function of the WFL system is to cool and increase and decrease the light intensity with unavoidable oscillations in the spectrum, but that manipulation actually helps us better understand the nature of light itself. In an indoor environment with an artificial light source, the results show that spectra are more dominant than light intensity for both tested cells at low and lower light intensities. Higher efficiency was obtained in an outdoor environment by using the WFL system, this time as a lens system that can increase the intensity of light. Further experiments are performed on amorphous Si-solar cells for application in outdoor and indoor conditions. The outdoor measurements with and without the use of the WFL system reveal that the current-voltage values are much higher with the WFL system, and we can measure quite high I_{sc} and V_{oc}, almost matching the values measured under standard testing conditions (STC). Furthermore, at lower light intensities (tungsten lamps), the WFL system increases I_{sc} and V_{oc} values independently of light intensity. Overall, it is clear that spectral influence causes huge oscillations in operating characteristics in both monocrystalline and amorphous Si-solar cells, and that oscillations are more pronounced in amorphous cells at lower light intensities comparable to monocrystalline, as expected. It is possible that because the described WFL system combines all of the effects (that is, cooling with flowing water in a closed system with no evaporation), as well as the fact that we can simultaneously adjust the intensity and influence the spectrum due to the lens system, it could be a possible solution for cooling and improving the PV response of solar cells and modules. All of the findings described above provide useful insights into many unsolved and hot problems in PV applications. Additionally, because of the many realistic effects that the designed WFL system has, such as the possibility to test at the same time the influence of intensity and spectral change as well as the cooling effect, this design could be a possible solution for improving the solar module response. It should also be noted that experiments are carried out both inside and outside, and that because all-optical construction is limited in size and degree of freedom of the designs, we are also very limited in the types of measurements that this type of improved optics could perform on a larger scale. It should also be noted that the cost of such designed optics is very low (hole construction is done in our lab) and that the possibilities on a larger scale with small advancements are unknown.

It was demonstrated that inexpensive p-doped and n-doped Sb_2S_3-based hybrid solar cells made entirely of synthesized material work as electricity generators and exhibit very high efficiency (around 8–9%) at a very low light intensity of 50 W/m^2. The efficiency of the designed cell is higher at lower light intensities, most likely due to the different distribution of the visible part of the spectrum at the wavelengths achieved with a biconvex lens filled with water, the WFL system. Investigations at low light intensities are found to be very important, just as they were for the previously described solar cells, but comparable data for solar cells at low light intensities, particularly for synthesized Sb_2S_3-based hybrid solar cells, is lacking. The Sb_2S_3-based hybrid solar cell, which was reported to be inexpensive and entirely made of synthesized Sb_2S_3 nanomaterial, also demonstrated improved cell efficiency at lower intensities. Apart from the light intensity changes, additional shifts in the light spectra were made by changing the used lamps. Cheap hybrid solar cells with a solid efficiency at very low light intensities should have good prospects for the exploitation of solar energy. The measured properties of a novel solar cell made of ITO, composite Sb_2S_3 (p-doped, a-undoped, and n-doped), P3HT, PANI, and TiO_2, a solid carrier, and a counter electrode were also presented. A new low-cost solid carrier, as well as a new absorption layer composition, were created. A combination of the polymers P3HT and PANI with the semiconductor Sb_2S_3 enabled photon absorption to be broadened while also improving conductivity. An excellent efficiency value of 23.1% at a low light intensity, 50 W/m^2, as a result of the appropriate WFL system permeability and the tungsten filament lamp's irradiation spectrum. Following that, we observed a low-cost, solid Sb_2S_3 powder/hypericin dye-based solar cell made entirely of synthesized nano-material that could generate electric current at very low, low, and medium-light intensities. Because of the different distributions of the light spectrum, the efficiency, short-circuit current, and open-circuit voltage of the designed cell are higher at lower light intensities, as shown. However, the shape of the illuminated *I–V* curves of the solar cell at low light intensity appears to be primarily governed by resistance. The efficiency of solid cells of 3.9% at 50 W/m^2 is a promising result, especially given the use of a low-cost natural dye, hypericin, as opposed to the expensive dye used in DSSCs. Furthermore, all of the synthesized solar cell components presented are inexpensive, and their synthesis processes are quick and simple. The first measurement was made on a solar cell composed of indium tin oxide/p and n-doped and amorphized (a) undoped flexible Sb_2S_3/solid carrier loaded with electrolyte/aluminium as the counter electrode. Each layer was created using a low-cost casting/solvent evaporation technique. The cell has a high efficiency of more than 10% at a very low light intensity of 50 W/m^2 and a suitable distribution, which is achieved by using an optics/lens system.

References

[1] Ibn-Mohammed, T., KohI, S. C. L., Reaney, M., Acquaye, A. Schileo, G., Mustapha, K. B., Greenough, R., Perovskite solar cells: An integrated hybrid lifecycle assessment and review in comparison with other photovoltaic technologies (2017) Renewable and Sustainable Energy Reviews, 80, pp. 1321–1344.

[2] Zhao, Z., Lin, C. Y., Tang, J., Xi, Z., Catalytic mechanism and design principles for heteroatom-doped graphene catalysts in dye-sensitized solar cells (2018) Nano Energy, 49, pp. 193–199.

[3] El-Said, W. A., Abdel-Shakour, M., Abd-Elnaiem, A. M., An efficient and low-cost photoanode for backside illuminated dye-sensitized solar cell using 3D porous alumina, Materials Letters, 222, pp. 126–130.

[4] Kim, J. K., Lee, C. S., Lee, S. Y., Cho, H. H., Kim, J. H., Bimodal porous TiO_2 structures templated by graft copolymer/homopolymer blend for dye-sensitized solar cells with polymer electrolyte (2016) Journal of Power Sources, 336, pp. 286–297.

[5] Sansongsiri, S., Kaewmanee, T., Boonyawan, D., Yu, L. D., Thongtem, S., Effect of titanium dioxide blocking layer deposited by cathodic arc plasma on the energy

conversion efficiency of dye-sensitized solar cells (2016) Surface and Coatings Technology, 306, pp. 257–261.
[6] Ho, C. Y., Wang, H. W., Characteristics of thermally reduced graphene oxide and applied for dye-sensitized solar cell counter electrode (2015) Applied Surface Science, 357, pp. 147–154.
[7] Lojpur, V., Mitrić, M., Validžić, I. Lj., The role of low light intensity: A step towards understanding the connection between light, optic/lens and photovoltaic behavior for Sb_2S_3 thin-film solar cells (2018) Optics & Laser Technology, 101, pp. 425–432.
[8] Lojpur, V., Krstić, J., Kačarević-Popović, Z., Mitrić, M., Rakočević, Z., Validžić, I. Lj., Efficient and novel Sb_2S_3 based solar cells with chitosan/poly (ethylene glycol)/electrolyte blend (2018) International Journal of Energy Research, 42, pp. 843–852.
[9] Janošević, V., Mitrić, M., Bundaleski, N., Rakočević, Z., Validžić, I. Lj., High-efficiency Sb_2S_3-based hybrid solar cell at low light intensity: Cell made of synthesized Cu and Se-doped Sb_2S_3 (2016) Progress in Photovoltaics: Research and Applications, 24, pp. 704-715.
[10] Janošević, V., Mitrić, M., Ležaić, A. J., Validžić, I. Lj., Weak light performance of synthesized amorphous Sb_2S_3-based hybrid solar cell (2016) IEEE Journal of Photovoltaics, 6, pp. 473–479.
[11] Lojpur, V., Krstić, J., Kačarević-Popović, Z., Filipović, N., Validžić, I. Lj., Flexible and high-efficiency Sb_2S_3/solid carrier solar cell at low light intensity (2018) Envionmental Chemistry Letters, 9, pp. 1–6.
[12] Doscher, H., Young, J. L., Geisz, J. F., Turner, J. A., Deutsch, T. G., Solarto-hydrogen efficiency: Shining light on photoelectrochemical device performance (2016) Energy & Environmental Science, 9, pp. 74–80.
[13] Kawata, K., Tamaki, K., Kawaraya, M., Dye-sensitised and perovskite solar cells as indoor energy harvestors (2015) Journal of Photopolymer Science and Technology, 28, pp. 415–418.
[14] Dharani, S., Mulmudi, H. K., Yantara, N., Trang, P. T. T., Park, N. G., Graetzel, M., Mhaisalkar, S., Mathews, N., Boix, P., High efficiency electrospun TiO_2 nanofiber based hybrid organic–inorganic perovskite solar cell (2014) Nanoscale, 6, pp. 1675–1679.
[15] Chen, C. Y., Chang, J. H., Chiang, K. M., Lin, H. L., Hsiao, S. Y., Lin, H. W., Perovskite photovoltaics for dim-light applications (2015) Advanced Functional Materials, 25, pp. 7064–7070.
[16] Peng, J. S. S., Pei, J., Liang, Y., Cheng, F., Chen, J., Quasi-solid-state dye-sensitized solar cells with polymer gel electrolyte and triphenylaminebased organic dyes (2009) ACS Applied Materials & Interfaces, 1, pp. 944–950.
[17] Kakiage, K., Aoyama, Y., Yano, T., Oya, K., Fujisawa, J. I., Hanaya, M., Highly-efficient dye-sensitized solar cells with collaborative sensitization by silyl-anchor and carboxy-anchor dyes (2015) Chemical Communications, 51, pp. 15894–15897.
[18] Steim, R., Ameri, T., Schilinsky, P., Brabec, C. J., Organic photovoltaics for low light applications (2011) Solar Energy Materials & Solar Cells, 95, pp. 3256–3261.
[19] Freitag, M., Teuscher, J., Saygili, Y., Zhang, X., Giordano, F., Liska, P., Hua, J., Zakeeruddin, S. M., Moser, J. E., Grätzel, M., Hagfeldt, A., Dye-sensitized solar

cells for efficient power generation under ambient light (2017) Nature Photonics, 11, pp. 372–378.
[20] Saygili, Y., Söderberg, M., Pellet, N., Giordano, F., Cao, Y., Muñoz-García, A. B., Zakeeruddin, S. M., Vlachopoulos, N., Pavone, M., Boschloo, G., Kavan, L., Moser, J. E., Grätzel, M., Hagfeldt, A., Freitag, M., Copper bipyridyl redox mediators for dye-sensitized solar cells with high photovoltage (2016) Journal of the American Chemical Society, 138, pp. 15087–15096.
[21] Freitag, M., Giordano, F., Yang, W., Pazoki, M., Hao, Y., Zietz, B., Grätzel, M., Hagfeldt, A., Boschloo, G., Copper phenanthroline as a fast and high-performance redox mediator for dye-sensitized solar cells (2016) The Journal of Physical Chemistry C, 120, pp. 9595–9603.
[22] Lojpur, V., Validžić, I., Influence of different light sources, light intensities, and water flow lens (WFL) system on dye-sensitized solar cell performances (2019) IEEE Journal of Photovoltaics, 9, pp. 492-498.
[23] Saga, T., Advances in crystalline silicon solar cell technology for industrial mass production (2010) NPG Asia Materials, 2, pp. 96-102.
[24] Ranabhat, K., Patrikeev, L., Revina, A. A., Andrianov, K., Lapshinsky, V., Sofronova, E., An introduction to solar cell technology (2016) Journal of Applied Engineering Science, 14, pp. 481-491.
[25] Green, M. A., Crystalline and thin film silicon solar cells: state of the art and future potential (2003) Solar Energy, 74, pp. 181-192.
[26] Kondrotas, R., Chen, C., Tang, J., Sb_2S_3 solar cells (2018) Joule, 2, pp. 857-878.
[27] Heuberger, C. F., Rubin, E. S., Staffell, I., Shah, N., Mac Dowell, N., Power capacity expansion planning considering endogenous technology cost learning (2017) Applied Energy, 204, pp. 831-845.
[28] Zhao, J., Wang, A., Green, M. A., 24·5% Efficiency silicon PERT cells on MCZ substrates and 24·7% efficiency PERL cells on FZ substrates (1999) Progress in Photovoltaics, 7, pp. 471-474.
[29] Cousins, P. J., Smith, D. D., Luan, H. C., Manning, J., Dennis, T. D., Waldhauer, A., Wilson, K. E., Harley, G., Mulligan, W. P., Generation 3: Improved performance at lower cost (2010) Photovoltaic Specialists Conference (PVSC), San Diego, pp. 275-278.
[30] Smith, D. D., Cousins, P. J., Masad, A., Waldhauer, A., Westerberg, S., Johnson, M., et. al., Generation III high efficiency lower cost technology: Transition to full scale manufacturing (2012) 38th IEEE Photovoltaic Specialists Conf (PVSC), Austin, Texas, pp. 001594-001597.
[31] Blakers, A., Zin, N., McIntosh, K. R., Fong, K., High efficiency silicon solar cells (2013) Energy Procedia, 33, pp. 1-10.
[32] Shockley, W., Queisser, H. J., Detailed balance limit of efficiency of *p-n* junction solar cells (1961) Journal of Applied Physics, 32, pp. 510-519.
[33] Águas, H., Mateus, T., Vicente, A., Gaspar, D., Mendes, M. J., Schmidt, W. A., Pereira, L., Fortunato, E., Martins, R., Thin film silicon photovoltaic cells on paper for flexible indoor applications (2015) Advanced Functional Materials, 25, pp. 3592-3598.
[34] De Rossi, F., Pontecorvo, T., Brown, T. M., Characterization of photovoltaic devices for indoor light harvesting and customization of flexible dye solar cells to

deliver superior efficiency under artificial lighting (2015) Applied Energy, 156, pp. 413-422.
[35] Freeman, D., Sridhar, N., A study of dye sensitized solar cells under indoor and low-level outdoor lighting: comparison to organic and inorganic thin film solar cells and methods to address maximum power point tracking (2011) Proceedings of the 26th European Photovoltaic Solar Energy Conference and Exhibition, pp. 232-236.
[36] Freunek, M., Freunek, M., Reindl, L. M., Maximum efficiencies of indoor photovoltaic devices (2013) IEEE Journal of Photovoltaics, 3, pp. 59-64.
[37] Andrews, R. W., Pearce, J. M., The effect of spectral albedo on amorphous silicon and crystalline silicon solar photovoltaic device performance (2013) Solar Energy, 91, pp. 233-241.
[38] Mathews, I., King, P. J., Stafford, F., Frizzell, R., Performance of III–V solar cells as indoor light energy harvesters (2016) IEEE Journal of Photovoltaics, 6, pp. 230-235.
[39] Cornaro, C., Bartocci, S., Musella, D., Strati, C., Lanuti, A., Mastroianni, S., Penna, S., Guidobaldi, A., Giordano, F., Petrolati, E., Brown, T. M., Reale, A., Di Carlo, A., Comparative analysis of the outdoor performance of a dye solar cell mini-panel for building integrated photovoltaics applications (2015) Progress in Photovoltaics, 23, pp. 215-225.
[40] Yoon, S., Tak, S., Kim, J., Jun, Y., Kang, K., Park, J., Application of transparent dye-sensitized solar cells to building integrated photovoltaic systems (2011) Building and Environment, 46, pp. 1899-1904.
[41] Mehrotra, S., Rawat, P., Debbarma, M., Sudhakar, K., Performance of a solar panel with water immersion cooling technique (2014) International Journal of Environmental Science and Technology, 3, pp. 1161-1172.
[42] Sheeba, K. N., Madhusudhana, Rao R., Jaisankar, S., A study on the underwater performance of a solar photovoltaic panel (2015) Energy Sources, Part A: Recovery, Utilization, and Environmental Effects, 37, pp. 1505-1512.
[43] Abdulgafar, S. A., Omar, O. S., Yousif, K. M., Improving the efficiency of polycrystalline solar panel via water immersion method (2014) International Journal of Innovative Research in Science, Engineering and Technology, 3, pp. 8127-8132.
[44] Grubišić-Čabo, F., Nižetić, S., Giuseppe Marco, T., Photovoltaic panels: A review of the cooling techniques (2016) Transactions of Famena XL, 1, pp. 63-74.
[45] Rosa-Clot, M., Rosa-Clot, P., Tina, G. M., Scandura, P. F., Submerged photovoltaic solar panel: SP2 (2010) Renew Energy, 35, pp. 1862-1865.
[46] Hosseini, R., Hosseini, N., Khorasanizadeh, H., An experimental study of combining a photovoltaic system with a heating system (2011) World Renewable Energy Congress, Sweeden. 57, pp. 2993-3000.
[47] Du, B., Hu, E., Kolhe, M., Performance analysis of water cooled concentrated photovoltaic (CPV) system (2012) Renewable and Sustainable Energy Reviews, 16, pp. 6732-6736.
[48] Akbarzadeh, A., Wadowski, T., Heat pipe-based cooling systems for photovoltaic cells under concentrated solar radiation (1996) Applied Thermal Engineering, 16, pp. 81-87.

[49] Han, X., Wang, Y., Zhu, L., Electrical and thermal performance of silicon concentrator solar cells immersed in dielectric liquids (2011) Applied Energy, 88, pp. 4481-4489.
[50] Abramyan, Y. A., Karamyan, G. G., Murodyan, A. A., Stafeev, V. I., Serago, V. I., Effect of liquid dielectrics on the efficiency of silicon solar cells (1999) Semiconductors, 33, pp. 1320-1321.
[51] Abrahamyan, Y. A., Serago, V. I., Aroutiounian, V. M., Anisimova, I. D., Stafeev, V. I., Karamian, G. G., et al., The efficiency of solar cells immersed in liquid dielectrics (2002) Solar Energy Materials and Solar Cells, 73, pp. 367-375.
[52] Wang, Y. P., Fang, Z. L., Zhu, L., Huang, Q. W., Zhang, Y., Zhang, Z. Y., The performance of silicon solar cells operated in liquids (2009) Applied Energy, 86, pp. 1037-1042.
[53] Zhu, L., Wang, Y. P., Fang, Z. L., Sun, Y., Huang, Q. W., An effective heat dissipation method for densely packed solar cells under high concentrations (2010) Solar Energy Materials and Solar Cells, 94, pp. 133-140.
[54] Tanaka, K., Solar energy converter using optical concentration through a liquid (2003) Patent US 2003/0029497A1.
[55] Tanaka, K., Solar energy converter using a solar cell in a shallow liquid–gel layer (2007) Patent US7244888B1.
[56] Christian, K. H., Cooling photovoltaic (PV) cells during concentrated solar radiation in specified arrangement in coolant with as low electric conductivity as possible (2000) Patent DE19904717.
[57] Reich, N. H., van Sark, W. G. J. H. M., Turkenburg, W. C., Charge yield potential of indoor-operated solar cells incorporated into product integrated photovoltaic (PIPV) (2011) Renewable Energy, 36, pp. 642-647.
[58] Gottschalg, R., Infield, D. G., Kearney, M., Experimental study of variations of the solar spectrum of relevance to thin film solar cells (2003) Solar Energy Materials and Solar Cells, 79, pp. 527-537.
[59] Kenny, R. P., Ioannides, A., Ullejans, H. M., Zaaiman, W., Dunlop, E. D., Performance of thin film PV modules (2006) Thin Solid Films, 511–512, pp. 663-672.
[60] Durisch, W., Urban, J., Smestad, G., Characterisation of solar cells and modules under actual operating conditions (1996) Proceedings of World Renewable Energy Congress, vol. 1, Pergamon Press, Oxford, Denver, CO, USA, pp. 359-366.
[61] Emery, K. A., Solar simulators and *I-V* measurement methods (1986) Solar Cells, 18, pp. 251-260.
[62] Elsayed, Ghitas A., Studying the effect of spectral variations intensity of the incident solar radiation on the Si solar cells performance (2012) NRIAG Journal of Astronomy and Geophysics, 1, pp. 165-171.
[63] Chaniotakis, E., Modelling and analysis of water-cooled photovoltaics (2001) M.Sc. thesis, Faculty of Energy System and Environment, Department of Mechanical Engineering, University of Strathclyde, Glasgow, Scotland.
[64] Moharram, K. A., Abd-Elhady, M. S., Kandil, H. A., El-Sherif, H., Enhancing the performance of photovoltaic panels by water cooling (2013) Ain Shams Engineering Journal, 4, pp. 869-877.

[65] Krauter, S., Increased electrical yield via water flow over the front of photovoltaic panels (2004) Solar Energy Materials and Solar Cells, 82, pp. 131-137.
[66] http://ixapps.ixys.com/DataSheet/KXOB22- 01X8F_Nov16.pdf
[67] https://panasonic.co.jp/ls/psam/en/produc ts/pdf/Catalog_Amorton_ENG.pdf
[68] Tina, G. M., Rosa-Clot, M., Lojpur, V., Validžić, I. Lj., Numerical and experimental analysis of photovoltaic cells under a water layer and natural and artificial light (2019) IEEE Journal of Photovoltaics, 9, pp. 733-741.
[69] Lojpur, V., Mitrić, M., Kačarević-Popović, Z., Radosavljević, A., Rakočević, Z., Lj Validžić, I., The role of low light intensity: A cheap, stable, and solidly efficient amorphous Sb_2S_3 powder/hypericin composite/PVA matrix loaded with electrolyte solar cell (2017) Environmental Progress and Sustainable Energy, 36 (5), pp. 1507-1516.
[70] Validžić, I.Lj., Janošević, V., Mitrić, M., Characterization and current-voltage characteristics of solar cells based on the composite of synthesized Sb_2S_3 powder with small band gap and natural dye (2016) Environmental Progress and Sustainable Energy, 35 (2), pp. 512-516.
[71] Benda, V., Černá, L., PV cells and modules – State of the art, limits and trends (2020) Heliyon, 6, e05666.
[72] Wang, Q., Chen, Z., Wang, J., Xu, Y., Wei, Y., Wei, Y., Qiu, L., Lu, H., Ding, Y., Zhu, J., Sb_2S_3 solar cells: functional layer preparation and device performance (2019) Inorganic Chemistry Frontiers, 6, pp. 3381-3397.
[73] Miao, T., Li-na, Z., Hong-xiu, T., Meng-di, G., Research progress of Sb_2S_3 solar cells (2016) Journal of synthetic crystals, 45 (8), pp. 2125-2129.
[74] Validžić, I. Lj., Mitrić, M., Abazović, N. D., Jokić, B. M., Milošević, A. S., Popović, Z. S., Vukajlović, F. R., Structural analysis, electronic and optical properties of the synthesized Sb_2S_3 nanowires with small band gap (2014) Semiconductor Science and Technology, 29, pp. 035007.
[75] Janošević, V., Mitrić, M., Savić, J., Validžić, I.Lj., Structural, optical, and electrical properties of applied amorphized and polycrystalline Sb_2S_3 thin films (2016) Metallurgical and Materials Transactions A, 47, pp.1460–1468.
[76] Validžić, I. Lj., Abazović, N. D., Mitrić, M., Growth of Sb_2S_3 nanowires synthesized by colloidal process and self-assembly of amorphous spherical Sb_2S_3 nanoparticles in wires formation (2012) Metals and Materials International, 18, pp. 989–995.
[77] Validžić, I. Lj., Abazović, N. D., Ahrenkiel, S. P., Janković, I. A., Structural and morphological dependences of Sb_2S_3 nanobars synthesised by organo-colloidal process on precursor concentrations and reaction times (2012) Journal of Crystal Growth, 354, pp. 157–163.
[78] Validžić, I. Lj., Abazović, N. D., Mitrić, M., Organic synthesis with different OA/EHA ratios of Sb_2S_3 nanowires of flowerlike organization and [010] orientation (2012) Metallurgical and Materials Transaction A, 43A, pp. 1405–1409.
[79] Validžić, I. Lj., Mitrić, M., Colloidal synthesis of Sb_2S_3 nanorods/bars with strong preferred orientation (2011) Materials Letters, 65, pp.1919–1922.
[80] Lojpur, V., Tasić, N., Validžić, I. Lj., Different behaviors in current–voltage measurements of undoped and doped Sb_2S_3-based solar cells (2017) Journal of Applied Electrochemistry, 47, pp. 117-124.

[81] Zhang, Y., Mascarenhas, A., Deb, S., Effects of excitons on solar cells (1998) Journal of Applied Physics, 84, pp. 3966–3971.
[82] Burgelman, M., Minnaert, B., Including excitons in semiconductor solar cell modelling (2006) Thin Solid Films, 511–512, pp. 214–18.
[83] Gregg, B. A., Excitonic solar cells (2003) Journal of Physical Chemistry B, 107, pp. 4688–4698.
[84] Corkish, R., Chan, D. S. P., Green, M. A., Excitons in silicon diodes and solar cells: A three-particle theory (1996) Journal of Applied Physics, 79, pp. 195–203.
[85] Fox, M., Optical properties of solids (2001) University Press, Oxford, ISBN 0-19-850613- 9 (hardback); ISBN 0-19-850612-0 (paperback).
[86] Knox, R. S., Theory of Excitons (1963) Academic Press INC, New York and London.
[87] Godel, K. C., Roose, B., Sadhanala, A., Vaynzof, Y., Pathake, S. K., Steiner, U., Partial oxidation of the absorber layer reduces charge carrier recombination in antimony sulphide solar cells (2017) Physical Chemistry Chemical Physics, 19, pp. 1425-1430.
[88] Bard, A. J., Design of semiconductor photoelectrochemical systems for solar energy conversion (1982) Journal of Physical Chemistry, 86, pp. 172–177.
[89] Mane, R. S., Lokhande, C. D., Photoelectrochemical cells based on nanocrystalline Sb_2S_3 thin films (2002) Materials Chemistry and Physics, 78, pp. 385–392.
[90] Rech, B., Wagner, H., Potential of amorphous silicon for solar cells (1999) Applied Physics A, 69, pp. 155–167.

CHAPTER THREE

LIGHT EFFECTS FROM THE PERSPECTIVE OF EXPERIMENTAL RESULTS

As was described in this book, the optical WFL system overcomes several problems in photovoltaics simultaneously. The problem of cooling solar panel surfaces is solved by water flowing through designed optics located above the surface of solar panels, which cools the surroundings and, indirectly, the solar panel surface. The manipulation of light intensities and light spectra is enabled by the different positions and angles of the WFL system compared to the used solar panel, where a better current-voltage response and higher current production are achieved. At the same time, the optics covering the solar panel protect the panel and allow its longer use. By the term manipulation of light intensities and spectra, we primarily allude to additional light effects for which we do not yet have an explanation, such as the higher efficiency of solar devices at lower as well as higher light intensities and non-uniform or non-linear basic current and voltage characteristics, which, at least, depend on the light spectra and intensities.

This section will not cover all aspects of the known facts concerning light and its impact on solar cells, but only those that are essential for comparing and trying to understand our research results.

The solar spectrum and particle photon approach

The spectral mismatch between solar cells (that is, bandgap as an electronic characteristic of the material, which is defined as the energy difference between the top of the valence band and the bottom of the conduction band from which the solar cell/panel was made) and incident radiation represents a fundamental factor limiting their efficiency, at least from the point where light is mainly discussed in the form of particles or photons, as is the case in photovoltaics.[1-5] The solar radiation spectrum presented in figure 1 is described as the number of photons with a distribution of energies. Depending on their energy, these photons may have enough energy to create free electrons and holes, and the most suitable material for the solar cell or panel has a bandgap at the maximum curve of the presented distribution.[6-8] Generally, AM0 radiation represents the extraterrestrial spectrum of solar radiation (not presented in figure 1) outside the earth's atmosphere.[9,10] In contrast to the situation outside the earth's atmosphere, more complex terrestrial solar radiation varies both in intensity and in spectral distribution depending on the earth's position and the position of the sun in the sky. To allow comparison between the performances of solar cells tested at diverse locations and terrestrial solar radiation, the standard has to be defined, and measurements are referred to this standard. At present, AM1.5 radiation serves as the standard spectral distribution. The irradiance of the AM1.5 radiation is 827 W/m^2, and the value of 1000 W/m^2 was typically incorporated to become a standard.[6-10]

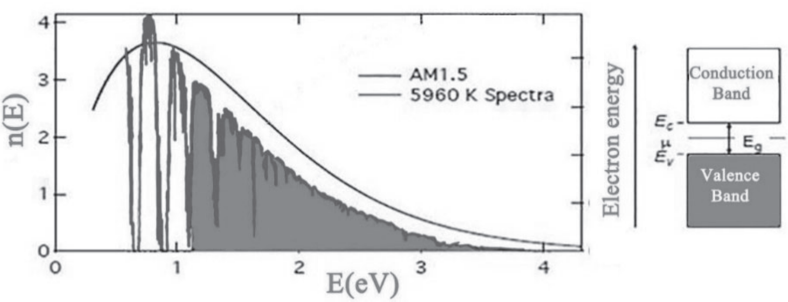

Figure 1. The solar spectrum is presented as the number of photons with a distribution of energies. In the same figure, the spectra of a black body (5960 K) and AM 1.5 normalized to a total irradiance of 1000 W/m^2 are given. On the right hand side, the bandgap (Eg) is presented as the energy difference between the top of the valence (outer electron) band and the bottom of the conduction (free electron flow) band.

This irradiance value is comparable to the limit received on the earth's surface. The peak power of a photovoltaic device is expressed in peak watts and is generated under standard AM1.5 (1000 W/m^2) radiation. Further, in figure 1, the black-body radiation spectrum has a characteristic, continuous energy spectrum that depends solely on the body's temperature, called the Planck spectrum. The Sun is also an approximate black body with an emission spectrum peaking in the middle, a yellow-green portion of the visible spectrum, but with reasonable power in the ultraviolet as well, with an effective temperature of 5960 K.[11-15] Further, the key property of photovoltaic material is to convert light energy to electric current[16,17] which becomes conductive when the energy of the photons absorbed by the solar cell material is sufficient to raise the electron state from the valence band (the lower energy level of a semiconductor) to the conduction band (the energy level at which an electron can be considered free) as shown in figure 1. It should be noted that the excitation of an electron into the conduction band results in the formation of both an electron and a hole in the valence band. As a result, both the electron and the hole can participate in conduction and are referred to as carriers. The amount of energy needed to excite an electron is known as the bandgap, which is an electronic property of semiconductors that has a direct impact on the photovoltaic cell voltage. Generally, an electron is in a high energy state when it gets enough energy to participate in conduction (i.e., is "free"). When an electron is bound and thus unable to participate in conduction, it is in a low energy state (figure 1). As a result of the presence of the bond between the two atoms, the electrons have two distinct energy states. The electron cannot achieve energy values that are intermediate between these two levels; it is either in a low energy position in the bond or has gained enough energy to break free and thus has a certain minimum energy. This minimum energy is known as a semiconductor's "bandgap," and the number and energy of these free electrons, or electrons participating in conduction, is essential to the operation of electronic devices. The photon energy's proximity to the material's bandgap, as well as whether the photon energy is sufficient to cover or overcome the bandgap, will decide how suitable the materials are for photovoltaic applications.[18-22] That is why, for example, a crystalline silicon solar cell with an energy gap of 1.1 eV represents an ideal applicative material.[23,24]

When a photon with an energy of 2 eV interacts with a crystalline silicon surface, 1.1 eV of that energy is used to transfer an electron into the conduction band, while the remaining energy (0.9 eV) is lost as heat. While using a material with a larger bandgap, such as copper oxide (bandgap of 2.1 eV), 2 eV is insufficient to free the electron. We would need a higher energy photon, and we can see from the distribution that there is a limited number of photons with such high energy. It is important to note that, no matter how large the photon energy is in comparison to the bandgap, only one electron can be freed by a single photon.[25,26] This is the explanation for the photovoltaic cells' reduced performance and low efficiency. To overcome this problem, it is common to combine materials with different bandgap energies, mostly through the doping process.[27-33] Doping is the process of introducing impurities into a semiconductor crystal, by varying the number of electrons and holes in semiconductors in order to increase their electrical conductivity.[34] Semiconductors may be doped to provide a surplus or deficit of valence electrons. The two types of dopants are the n-type ("n" for negative) and the p-type ("p" for positive). Extra valence electrons with energies

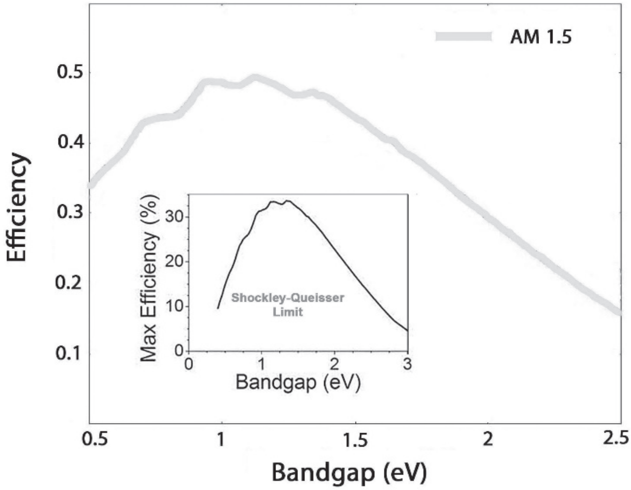

Figure 2. The maximum solar efficiency for the AM 1.5 solar radiation spectra of one p-n junction solar cell is according to the Shockley-Queisser Limit. Efficiency was expressed in percentages (inset) and through the losses due to the spectral mismatch of almost 50% for a crystalline silicon solar cell (Eg = 1.1 eV).

similar to the conduction band are found in n-type dopants, which serve as electron donors. When incorporated into the atomic lattice of a semiconductor, the valence electrons of n-type dopants can easily be excited into the conduction band. By accepting electrons, p-type dopants assist in conduction. When a p-type dopant is introduced into a semiconductor's atomic lattice, it can host electrons from the conduction band, allowing positive holes to form easily.[35] Figure 2 shows how the bandgap affects the maximum efficiency of one p-n junction solar cell.[36] When an n-type material and a p-type material are fused to form a semiconductor diode, a p-n junction is formed. Most photons will not cause a photovoltaic effect if the band gap is too large; if it is too small, most photons will have more energy than required to excite electrons across the bandgap, and the rest will be lost.[35,36] Reflection and transmission are typically regarded as loss mechanisms in photovoltaic devices because photons that are not absorbed do not generate power. The most widely used semiconductor in commercial solar cells, silicon (which contributes to 96 % of the market[37]), has a bandgap near the peak of this curve. The Shockley–Queisser limit[38] refers to the measurement of a single p-n junction solar cell's maximal theoretical efficiency (the peak of the curve has been exceeded experimentally by combining materials with different bandgap energies). The theoretical maximum limit, assuming a single p - n junction with a bandgap of 1.34 eV, was estimated to be around 33% using an AM 1.5 solar spectrum (inset in figure 2). However, not all fractions of the AM 1.5 spectrum cannot be converted into usable energy by a crystalline silicon solar cell[39-43] (see further in the book). Figure 2 demonstrates that in the case of a crystalline silicon solar cell (Eg = 1.1 eV), the losses due to the spectral mismatch account for almost 50%.[44,45]

Solar cell efficiency

So far, taken from the angle of light particle photons, we see the efficiency of solar cells strongly depends on the energy gap of the material through light photons of particular energies. The part related to the definition of particle photon nature is discussed later in the book with respect to our measurement results without and with the presence of the WFL system. In the previous chapter, we have already described the different solar cells that we examined: commercial amorphous and crystalline Si-solar cells, dye-sensitized solar cells, as well as different types of designed Sb_2S_3-based-on solar cells. Because all tested solar devices show significantly higher efficiency using the described WFL system compared to measurements and calculated efficiencies without a WFL system, the appropriate values of the energy gaps of various tested solar cells are summarized in Table 1. Of course, here we will not forget the results that, even without light manipulation and changes in light spectra, give better efficiencies at lower light intensities than higher ones. The values of the energy gaps are given in order to see the range of the energy gaps, within which our designed WFL system operates in the sense of increasing the efficiency of the designed solar devices for some light intensities and spectra presented in the previous chapter. The fact is that for all tested cells with energy gaps ranging between 1.1 and 2.0 eV, using an optic/lens system almost always improves (for higher as well as lower light intensities) the photovoltaic response of the designed devices (depending at least on radiation spectra).

We'll get back to this issue and comment on the results later, but first we need to say something general about efficiency. One of the most common metrics used to compare the performance of different solar cells is efficiency, in the sense that photovoltaics is the direct conversion of light to electricity, so it produces current and voltage, which are directly proportional to efficiency.[46-50] Put differently, the most general method for determining a solar cell's efficiency is to examine its parameters to obtain values that can then be translated into a ratio of energy output from the solar cell to input

Table 1. The values of the bandgap for all tested commercial amorphous and crystalline Si-solar cells, dye-sensitized solar cells, as well as different types of designed Sb_2S_3-based solar cells.

All various tested solar cells and absorption layers	Energy gap (eV)
Crystalline silicon (c-Si)	1.1
Amorphous silicon (a-Si)	1.84
Amorphous/undoped Sb_2S_3 (a- Sb_2S_3)	1.57 1.91
Cu-doped Sb_2S_3 (p-doped)	1.47
Se-doped Sb_2S_3 (n-doped)	1.61
a- Sb_2S_3/hypericin	1.75 1.6
a- Sb_2S_3/ betanin	2.0
a- Sb_2S_3/PANI composite	2.0
XY1/D35/Y123	~1.8-2.0

energy from the sun. However, if the specific spectrum that corresponds to the measured intensity of incident sunlight (the same light intensity that reaches the solar cell surface can have different corresponding light spectra) is not included[51,52], the efficiency of solar cells is not complete and well defined. In the previous chapter, we showed that different artificial light sources that simulate outdoor radiation and which have generally similar spectra, if applied to the same solar cells at lower light intensities, can cause huge changes in the efficiency of the same device.[53] However, we will come back to this issue later in this chapter. As a result, to compare various solar cells, the conditions under which efficiency is calculated must be carefully monitored and preserved. As it is firmly established that terrestrial solar cells are tested under AM1.5 conditions and at a temperature of 25ºC, while the ambient conditions for building a spatial solar power plant or spacecraft powered by solar energy would be AM0.[54]

The efficiency of a solar cell is determined as the fraction of incident power that is converted to electricity and is defined as[55]:

$$P_{max} = V_{oc}\, I_{sc}\, FF \qquad [1]$$

$$\eta = V_{oc}\, I_{sc}\, FF / P_{in} \qquad [2]$$

where V_{oc} is the open-circuit voltage, I_{sc} represents the short-circuit current, *FF* is the fill-factor, and η is the efficiency, which is determined from *I-V* measurements. P_{max} describes the maximum power generated by a solar cell and the incident power, $P_{in.}$ The incident power is equal to the AM 1.5 spectrum irradiance normalized to 1000 W/m^2.

$$FF = V_{mp} I_{mp} / V_{oc} I_{sc} \qquad [3]$$

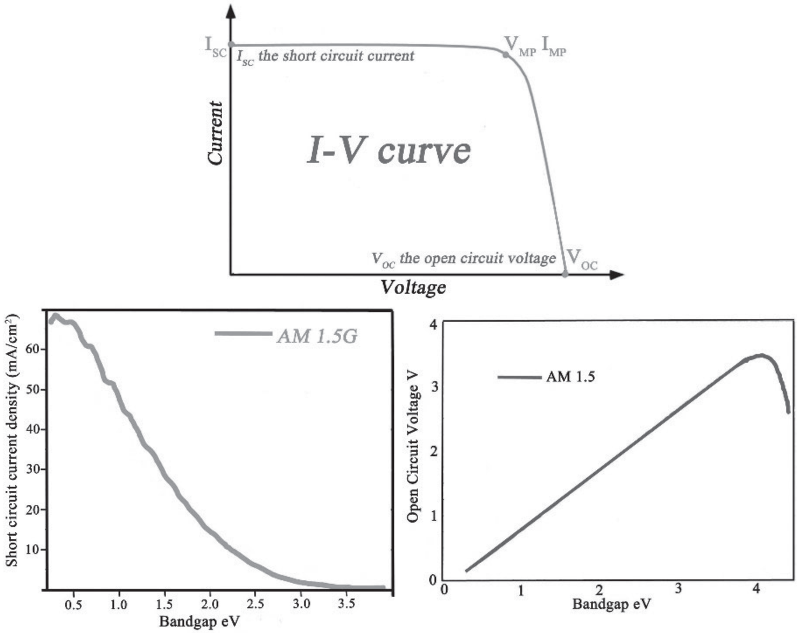

Figure 3. The *I-V* characteristic curve with the meaning of *Isc* and *Voc* and the limits for short-circuit current density and open-circuit voltage of a solar cell within the Shockley-Queisser model.

The "fill factor" is a parameter that defines the maximum power output of a solar cell (presented schematically in figure 3) when combined with V_{oc} and I_{sc}. It is known as the ratio of the solar cell's maximum power to the product of V_{oc} and I_{sc}.[8, 56-61] Figure 3 describes and connects several important parameters that are used to describe solar cells. The *I-V* curve provides information on the short-circuit current (I_{sc}), open-circuit voltage (V_{oc}), fill factor (*FF*), and efficiency. When the voltage across the solar cell is zero, the short-circuit current flows through the cell. The short circuit current (I_{sc}) is calculated by multiplying the short circuit current density (J_{sc}) (presented in figure 3 as bandgap dependence) by the cell area. This dependence is based on the assumption that each solar photon is converted into an electron that flows through the circuit according to the Shockley-Queisser model.[38] Because there are fewer photons above the bandgap at higher bandgap values, the current density decreases. Further, as can be seen in figure 3, the open-circuit voltage, V_{oc}, is the maximum voltage available from a solar cell when the cell current is zero. As the recombination current decreases, the V_{oc} increases with the bandgap.[62] Shortly, any electron in the conduction band is meta-stable and will eventually stabilize at a lower energy position in the valence band. When this happens, it must enter an empty valence band state. As a result, when the electron returns to the valence band, it effectively removes a hole. This effect is known as recombination. The rate of electron-hole production is limited by recombination. For instance, in silicon, this reduces theoretical performance under normal operating conditions by 10%, in addition to thermal losses.[8, 63-76] V_{oc} is restricted by recombination. Because of the very low I_{sc}, there is a drop in V_{oc} at higher bandgap values, as shown in figure 3.

Experimental results and deviations from conventional measurements caused by light manipulation

In this chapter, we have shown table 1, in which different values of energy bandgaps for various solar cell materials are given and where all solar devices show better efficiency at different light intensities by employing the WFL system regardless of the value of the energy gap (1.1-2.0 eV). To be able to go into the presentation and comments of our results, the following step would be to explain and connect, that is, to present a conventional opinion about the relationship between efficiency, energy gap, and light intensity or power. Unfortunately, the influence of light spectra cannot be related to today's knowledge. It has already been stated that when a photon's energy is equal to or greater than the material's bandgap, the photon is absorbed by the material and excites an electron into the conduction band. When a photon is absorbed, it produces both a minority and a majority carrier. The concept of the generation of charge carriers by photons sets the foundation of photovoltaic energy production. We can calculate the fraction of incident radiation energy absorbed by a single p-n junction solar cell.[8, 77-84] When we express λg as the wavelength of photons that corresponds to the bandgap energy of the absorber of the solar cell, only photons with energy greater than the bandgap are absorbed, implying that photons with $\lambda \leq \lambda g$ are absorbed. P_{in}, the incident power flux from the artificial light/sun expressed in equation 2, can be calculated from the spectral power density, *P(λ)* using the following equation:

$$P_{in} = \int_0^{\infty} P(\lambda) d\lambda \qquad [4],$$

or expressed in terms of photon flux density, Φ(λ)

$$P_{in} = \int_0^{\infty} \Phi\,(\lambda) \frac{hc}{\lambda} d\lambda \qquad [5].$$

The photon flux is defined as the number of photons per second per unit area. The fraction of the incident power p that is absorbed by a solar cell and used for energy conversion is expressed as

$$P_{abs} = \frac{\int_0^{\lambda_G} \Phi\,(\lambda) \frac{hc}{\lambda} d\lambda}{\int_0^{\infty} \Phi\,(\lambda) \frac{hc}{\lambda} d\lambda} \qquad [6].$$

Apart from the absorbed energy, the excess energy of photons is lost because of the thermalization of photo-generated electrons and holes in the absorber material. The equation adequately describes the fraction of absorbed energy that the sun can deliver as useful energy, P_{use}

$$P_{use} = \frac{E_g \int_0^{\lambda_G} \Phi\,(\lambda) d\lambda}{\int_0^{\lambda_G} \Phi\,(\lambda) \frac{hc}{\lambda} d\lambda} \qquad [7],$$

so that the conversion efficiency is limited by the spectral mismatch

$$\eta = P_{abs} P_{use} \qquad [8].$$ [8]

The main figure 2 shows the conversion efficiency of solar cells limited only by spectral mismatch as a function of the bandgap of a semiconductor absorber for a single-junction solar cell, for AM 1.5 solar radiation spectra.

Many authors[85-88] presented the dependence of various solar cell efficiencies on the bandgap of semiconductor materials for various artificial and natural lights. As we expected (from figure 2), those presented dependencies on efficiency as a function of semiconductor bandgap have a maximum energy conversion efficiency. In order to compare our results and

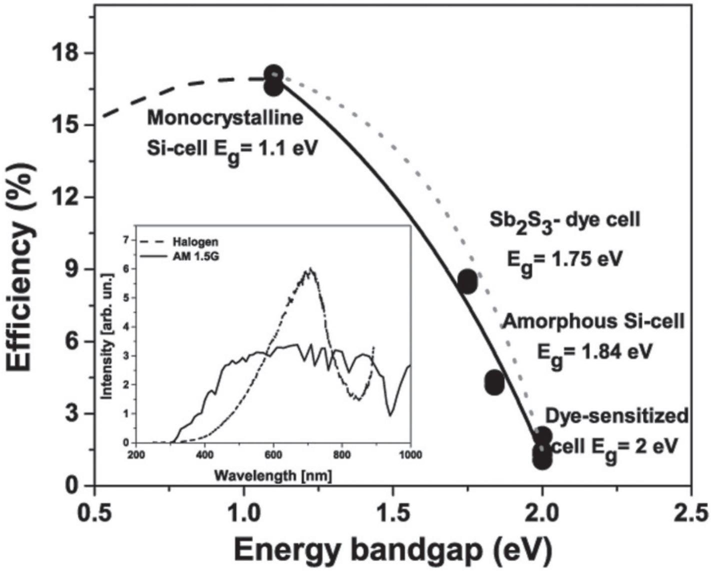

Figure 4. The energy conversion efficiency limits for different solar cells that we measured and made as a function of the bandgap of the semiconductor material, under halogen radiation.

further draw conclusions, in figure 4 the energy conversion efficiency limits for different solar cells that we measured and made, as a function of the bandgap of the semiconductor material, are presented. The results were obtained with an artificial light source, a halogen lamp, due to spectra similarity (presented in the inset of figure 4) with the outdoor 1.5 AM spectrum. It should be emphasized that not all different solar cells were measured under outdoor radiation. Therefore, figure 4 follows a dependence concerning the measurements made with a halogen lamp. As can be seen in figure 4, dependence follows maximum distribution (dotted and dashed fitted lines), as we expected for different single-junction solar cells.

As is evident, the efficiency values that we measured for different solar cells and presented in figure 4 cover one part of the maximum distribution curve, and therefore, the fitted curve of the maximum dependence is marked with a dashed line. The silicon-based devices are usually homojunction, while other devices presented in the same dependencies here and in the literature[89-92] constitute heterojunctions. Although we could discuss whether our different designs of Sb_2S_3-based solar cells (made similar to the design of Si-solar cells with some changes) represent homojunction or heterojunction solar cells, this is not the topic of this book, and we will not deal with it. It should be emphasized that the dependence presented in figure 4 is not given to assess whether we can exceed the Shockley-Queisser limit but to further compare our experimental results obtained using the WFL system. For the purpose of comparison, figure 5 shows the same dependence as figure 4, except that instead of the calculated efficiency, we present the $I_{sc}V_{oc}/P_{input}$ ratio.

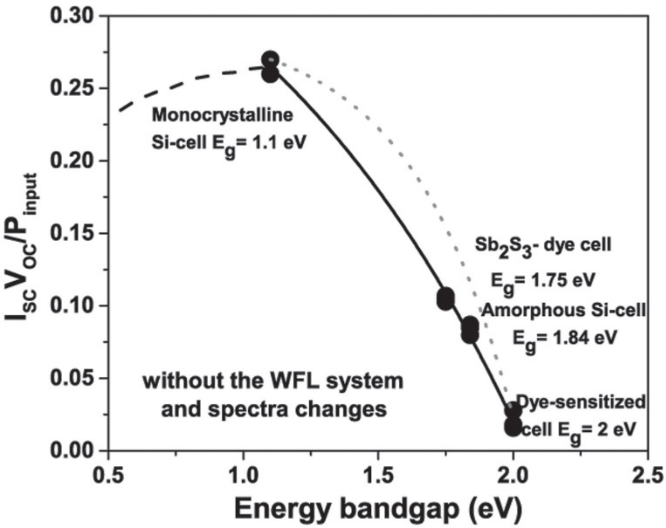

Figure 5. The ratio of $I_{SC}V_{OC}/P_{input}$ for the same different solar cells is presented in figure 4 that we measured and made as a function of the bandgap of the semiconductor material under halogen radiation.

We again stress here that the expression for the efficiency calculation at both higher and lower light intensities than standard testing conditions (STC) does not take into account the different light distributions that reach the solar panel. So, for that reason, in our published results so far[56, 93-96], the efficiency after light manipulation has not been calculated; in contrast, the value would be unreal and very high. As can be seen in figure 5 (the same as in figure 4), dependence follows maximum distribution, and the fitted curve of the maximum dependence is marked with a dashed and dotted line. In this way, we further avoid efficiency calculations in the results with the WFL system and light manipulation for the mentioned reasons. The reported experimental results further in this chapter consider the sun as well as artificial light, halogen (ELH Osram lamp 120 V, 300 W), and tungsten (ULTRA-VITALUX 300-280) lamps as sources of radiation. Note that, independently of the fact that a comparison of the responses of solar devices in the presence and absence of the WFL system is presented on all the solar devices herein described, most of these measurements are performed on different Si-solar cells.

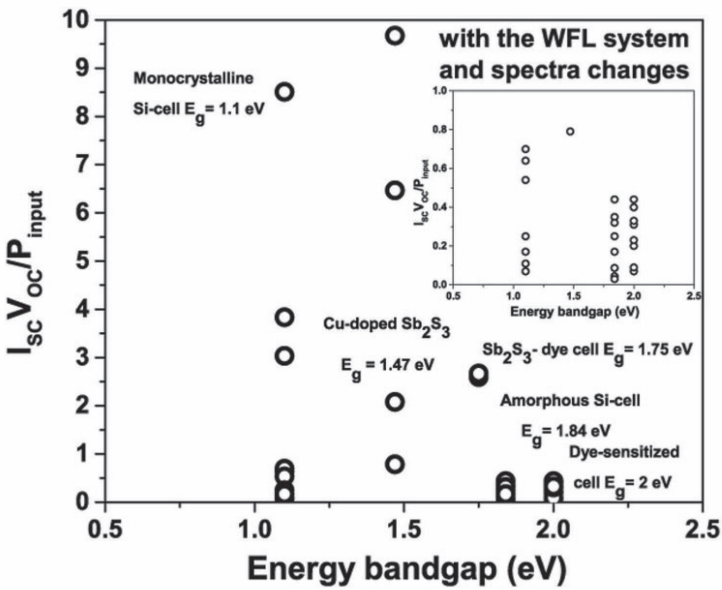

Figure 6. The ratio of $I_{SC}V_{OC}/P_{input}$ for the same different solar cells presented in figures 4 and 5 that we measured and made, as a function of the bandgap of the semiconductor material with the use of the WFL system and spectral changes.

Although it is mentioned in Chapter 1, most authors state that while the intensity of solar radiation and the quality of the semiconductor in use directly affect efficiency and are controllable, variations in solar radiation spectra that reach the surface of the solar cell or panel are not.[97] On the other hand, any designed cooling system/mechanism with liquid or direct immersion of the panel in water results in a reduction in solar ray intensity and spectral changes.[94] As a result, realistic, reduced light intensity and the effect of changed spectra on the efficiency of commercial solar cells and modules are things we need to study and comprehend.

In that respect, the ratio of $I_{sc}V_{oc}/P_{input}$ for the same different solar cells presented in figures 4 and 5 that we measured and made as a function of the bandgap of the semiconductor material with the use of the WFL system and spectral changes is presented in figure 6. As can be seen from dependence, it is quite difficult to find any pattern except the fact that the ratio of $I_{sc}V_{oc}/P_{input}$ generally is much higher after passing through the WFL system, which is at least influenced by the light spectral changes. This follows from previous statements that the WFL system almost always improves the solar device output no matter the measured solar devices with different bandgaps presented in table 1.

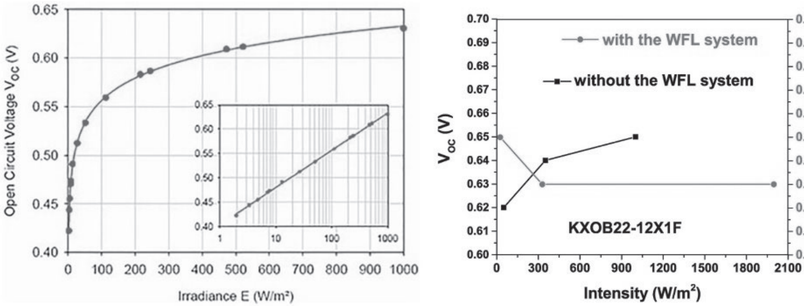

Figure 7. Open-circuit voltage versus irradiance for the commercial monocrystalline Si-solar cell (KXOB22-12X1F, left). The performance data sheet is given by the company. On the right-hand side, the same dependence that was measured without (black) and with the WFL system (red) is shown.

Furthermore, we focus more closely on the separated and most thoroughly tested Si-solar cells. Figures 7, 8, and 9 show photos and the main operating characteristics of commercial monocrystalline for indoor and outdoor applications and amorphous for outdoor applications Si-solar cells used in these experiments, provided by the companies (IXYS Korea[98] and Amorton Sanyo[99]).

If we look at Fig. 7 and the changes in open-circuit voltage versus irradiance for the commercial monocrystalline Si-solar cell (KXOB22-12X1F) and compare the datasheet provided by the company to the data that we measured without the WFL system, we can see that V_{oc} decreases as light

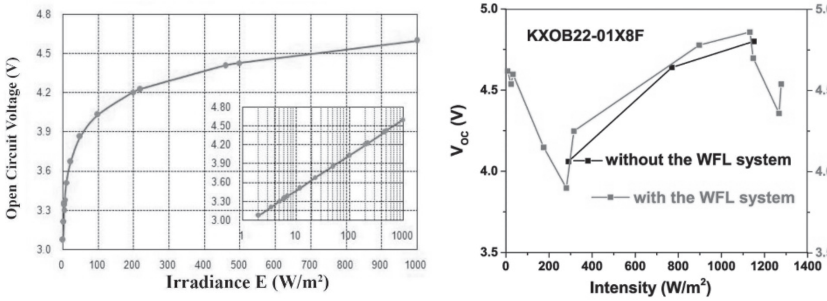

Figure 8. Open-circuit voltage versus irradiance for the commercial monocrystalline Si-solar cell (KXOB22-01X8F, left). The performance data sheet is given by the company. On the right-hand side, the same dependence that was measured without (black) and with the WFL system (red) is shown.

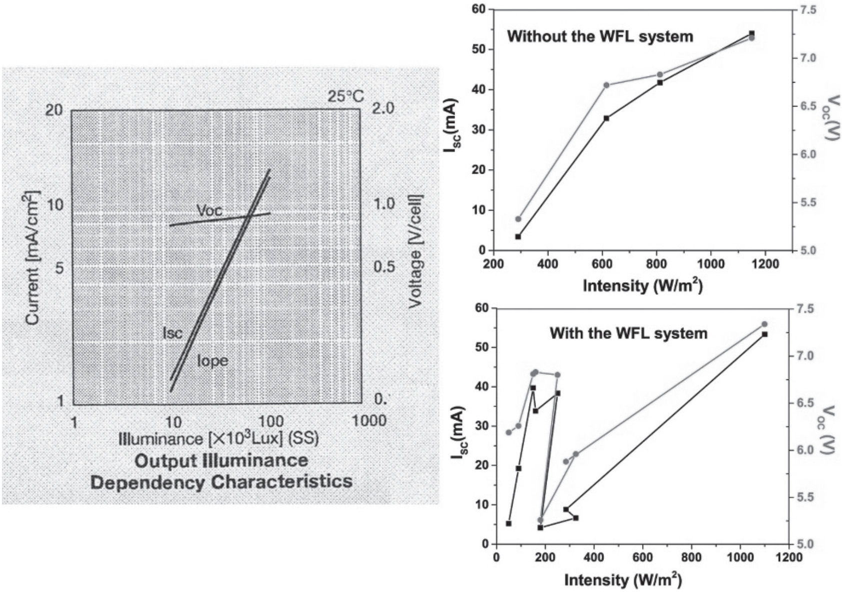

Figure 9. Open-circuit voltage and short-circuit current versus irradiance for the commercial amorphous Si-solar cell for outdoor applications (AM-5907 CAR, left). The performance data sheet is given by the company. On the right-hand side are the same dependences, V_{oc} and I_{sc}, that were measured without (black) and with the WFL system (red).

intensity decreases, as expected. According to company data, that decrease in the open-circuit voltage is not so pronounced as it appears. However, the differences in the spectra of outdoor radiation and artificial light can never be ignored. In the case of V_{oc} dependence in the presence of the WFL/lens system with the same values of intensity, the situation is completely different, and the dependence does not have a decreasing trend.

It is quite visible that V_{oc} maintains a more or less constant value at higher radiation intensities, and at lower intensity values it has an increase in the open-circuit voltage. This is in accordance with the measured results, where high efficiency, or better said, the ratio of $I_{sc}V_{oc}/P_{input}$ was obtained at the low light intensities for all measured solar cells with the altered radiation spectra.

Further, a similar trend was observed for another monocrystalline Si-solar cell, KXOB22-01X8F, presented in figure 8. As in the previous figure, the changes in open-circuit voltage versus irradiance for the commercial monocrystalline Si-solar cell (KXOB22-01X8F) are given by the datasheet provided by the company. If we compare this data with the data that we measured without the WFL system, we can see that V_{oc} decreases as light intensity decreases, as expected. In the case of V_{oc} dependence in the presence of the WFL/lens system, the situation is changing as expected. Now the curve trend at higher light intensities is not constant, but again, at lower intensity values there is an increase in the open-circuit voltage. Oscillations in open-circuit voltage at the higher light intensities are mostly caused by more intensive measurements of this specific type of Si-solar cell. Also, as we emphasized many times, at least the spectral change at particular light intensities causes oscillations in solar cell parameters. Further, in figure 9, open-circuit voltage and short-circuit current versus irradiance (given by the company) for the commercial amorphous Si-solar cell for outdoor application, AM-5907 CAR, are given. On the right-hand side, it is clearly visible that dependences, V_{oc}, and I_{sc} that were measured without the WFL system nicely follow decreasing trends in a function of light intensity. However, the measurements presented with the use of the WFL system exhibit a visible decrease in the open-circuit voltage at the higher light intensities, while at lower light intensities, V_{oc} increases. As a result, in contrast to monocrystalline Si-solar cells, where open-circuit voltage is kept less constant or with smaller oscillations at a still very high voltage, the voltage decreases in amorphous Si-solar cells. Additionally, in table 2, the values of the intensities, short-circuit currents, and open-circuit voltages for different tested Si-solar cells, measured without and with the WFL system and under outdoor as well as artificial light, are summarized.

This oscillation in behavior between two different types of Si-solar cells is not surprising. As mentioned, the conversion efficiency of the monocrystalline Si-solar cells under standard testing conditions (STC) decreases under artificial LED light (lower light intensity), whereas the amorphous Si-solar cell increase, representing the opposite in behavior.[100]

Table 2. The values of the intensities, short-circuit currents, and open-circuit voltages for different tested Si-solar cells, measured without and with the WFL system. The light after passing through the WFL system has changed spectra independently of the same light intensity.

Type of the Si-solar cell	Without the WFL system			With the WFL system		
	Intensity (W/m^2)	I_{SC} (mA)	V_{OC} (V)	Intensity (W/m^2)	I_{SC} (mA)	V_{OC} (V)
KXOB22-12X1F	50 350 1000	21.85 22.21 61.47	0.62 0.64 0.65	50 350 ≥2000 (concentration effect)	44.86 29.82 164.7	0.65 0.63 0.63
KXOB22-01X8F-ND	290 770 1150	1.09 3.8 5.97	4.06 4.64 4.8	13 29 38 180 285 320 900 1135 1150 1270 1280	3.69 3.78 3.87 1.14 0.75 1.29 4.80 8.95 20.27 31.53 27.90	4.62 4.54 4.6 4.15 3.9 4.25 4.78 4.86 4.7 4.36 4.54
AM5907-CAR	290 615 812 1150	3.41 32.87 41.76 53.98	5.33 6.72 6.83 7.21	50 90 150 160 180 250 285 325 1100	5.26 19.21 39.70 33.86 4.19 38.33 8.83 6.67 53.33	6.19 6.26 6.81 6.83 5.26 6.80 5.88 5.96 7.34

The significance of the spectral effects of silicon PV devices has been examined on the basis of computer simulations and indoor data measurements.[101,102] Repeated investigations have been established on "useful fractions", defined as the ratio of the measured spectral irradiation with respect to the measured global irradiance.[103,104]

References

[1] Jošt, M., Topič, M., Efficiency limits in photovoltaics-case of single junction solar cells (2014) Electronics and Energetics, 27, pp. 631 – 638.
[2] Araujo, G., Marti, A., Absolute limiting efficiencies for photovoltaic energy-conversion (1994) Solar Energy Materials & Solar Cells, 33, pp. 213–240.
[3] Kosyachenko, L. A., Solar cells: new approaches and reviews (2015) Intech Open DOI: 10.5772/58490, ISBN: 978-953-51-2184-8.
[4] Lincot, D., The new paradigm of photovoltaics: From powering satellites to powering humanity (2017) Comptes Rendus Physique, 18, pp. 381-390.
[5] Ushasree, P. M., Bora, B., CHAPTER 1:Silicon solar cells , in *Solar Energy Capture Materials* (2019), pp. 1-55, DOI: 10.1039/9781788013512-00001
eISBN: 978-1-78801-351-2.
[6] Jarosz, G., Marczyński, R., Signerski, R., Effect of band gap on power conversion efficiency of single-junction semiconductor photovoltaic cells under white light phosphor-based LED illumination (2020) Materials Science in Semiconductor Processing, 107, pp. 104812.
[7]Gueymard, C. A., Solar Radiation Spectrum (2013) In: Richter C., Lincot D., Gueymard C.A. (eds) Solar Energy. Springer, New York, NY.
https://doi.org/10.1007/978-1-4614-5806-7_445.
[8]Zeman, M., Introduction to photovoltaic solar energy, Solar Cells Miro Zeman.pdf (uson.mx).
[9] Saiprasad, N., Castelletto, S., Boretti A., Optoelectronics modelling of thin film solar cells (2016) In: Jazar R., Dai L. (eds) Nonlinear Approaches in Engineering Applications. Springer, Cham. https://doi.org/10.1007/978-3-319-27055-5_11.
[10] Mazzio, K. A., Luscombe, C. K., The future of organic photovoltaics (2015) Chemical Society Reviews, 44, pp. 78-90.
[11] Smets, A., Jäger, K., Olindo, I., van Swaaij, R., Zeman, M., Solar energy : the physics and engineering of photovoltaic conversion, technologies and systems (2016) Uit Cambridge Ltd, Cambridge, United Kingdom, ISBN10 1906860327.
[12] Tyagi, H., Chakraborty, P. R., Powar, S., Kumar Agarwal, A., Solar energy (2020) Springer, Singapore, ISBN: 978-981-15-0674-1.
[13] Ringstad, A., The science of solar energy (2018) Reference Point Press, ISBN: 9781682823071.
[14] Wu, W., Liu, Y., Radiation entropy flux and entropy production of the Earth system (2010) Reviews of Geophysics, 48, pp. RG 2003 (1-27).
[15] Severn, G., Physics 272 Laboratory Experiments (2016)
blackbody_radiation_p272_s16_v2.dvi (sandiego.edu).

[16] Zaidi, B., Solar Panels and Photovoltaic Materials (2018) InTech Open; London, UK, Introductory Chapter: Introduction to Photovoltaic Effect; pp. 1–8.
[17] Luceño-Sánchez, J. A., Díez-Pascual, A. M., Capilla, R. P., Materials for photovoltaics: state of art and recent developments (2019) International Journal of Molecular Sciences, 20, pp. 976.
[18] Hirst, L. C., Principles of solar energy conversion (2012) Comprehensive Renewable Energy, 1, pp. 293-313.
[19] Jestin, Y., Down-shifting of the incident light for photovoltaic applications (2012) Comprehensive Renewable Energy, 1, pp. 563-585.
[20] Bayod-Rújula, A. A., Solar photovoltaics (PV) (2019) Solar Hydrogen Production, Chapter 8, pp. 237-295.
[21] Corkish, R., Solar cells (2013) Reference Module in Earth Systems and Environmental Sciences, https://doi.org/10.1016/B978-0-12-409548-9.01481-0.
[22] Benda, V., Photovoltaics: The basics (2018) A Comprehensive Guide to Solar Energy Systems with Special Focus on Photovoltaic Systems, pp. 151-179.
[23] Würfel, P., Physics of solar cells from principles to new concepts (2005) WILEY-VCH Verlag GmbH & Co. KGaA, Weinheim.
[24] Luque, A., Hegedus, S., Handbook of photovoltaic science and engineering (2003) John Wiley & Sons Ltd, England.
[25] Singh Solanki, C., Solar photovoltaics: fundamentals, technologies and applications, 3rd edition (2015) PHI Learning Pvt. Ltd.
[26] Kasap, S. O., Optoelectronics and Photonics 2nd edition (2013) Pearson publications.
[27] Li, X., Xie, D., Park, H., Zhu, M., Helen Zeng, T., Wang, K., Wei, J., Wu, D., Kong, J., Zhu, H., Ion doping of graphene for high-efficiency heterojunction solar cells (2013) Nanoscale, 5, pp. 1945-1948.
[28] Mahmmod Ahmad, S., Leong Cheow, S., Ludin, N. A., Sopian, K., Zaidi, S. H., In-depth investigation of spin-on doped solar cells with thermally grown oxide passivation (2017) Results in Physics, 7, pp. 2183-2193.
[29] Wolf, M., The influence of heavy doping effects on silicon solar cell performance (1986) Solar Cells, 17, pp. 53-63.
[30] Durose, K., High efficiency for As-doped cells (2019) Nature Energy, 4, pp. 825–826.
[31] Trukhanov, V. A., Bruevich, V. V., Paraschuk, D. Y., Effect of doping on performance of organic solar cells (2011) Physical Review B, 84, pp. 205318.
[32] Sidarth Thirunavukkarasu, G., Seyedmahmoudian, M., Chandran, J., Stojcevski, A., Subramanian, M., Marnadu, R., Alfaify, S., Shkir, M., Optimization of mono-crystalline silicon solar cell devices using PC1D simulation (2021) Energies, 14, pp. 4986.
[33] Jiang, J., Wang, Q., Jin, Z., Zhang, X., Lei, J., Bin, H., Zhang, Z. G., Li, Y., Liu, S. F., Polymer doping for high-efficiency perovskite solar cells with improved moisture stability (2018) Advanced Energy Materials, 8, pp. 1701757.
[34] E-book, Semiconductors: A Comprehensive Guide, Power & Beyond - Mesago Messe Frankfurt GmbH, Rotebühlstr. 83-85, 70178 Stuttgart, Deutschland.
[35] "Chapter 6: Diodes." Fundamentals of Electrical Engineering. 2nd ed. New York, New York: Oxford UP, 1996, pp. 352-54.

[36] Dinçer, F., Meral, M. E., Critical factors that affecting efficiency of solar cells (2010) Smart Grid and Renewable Energy, 1, pp. 47-50.
[37] Gregory Wilson, M., et al., The 2020 photovoltaic technologies roadmap (2020) Journal of Physics D: Applied Physics, 53, pp. 493001.
[38] Shockley, W., Queisser, H. J., Detailed balance limit of efficiency of *p-n* junction solar cells (1961) Journal of Applied Physics, 32, pp. 510-519.
[39] Tawalare, P. K., Optimizing photovoltaic conversion of solar energy (2021) AIP Advances, 11, pp. 100701.
[40] Battaglia, C., Cuevas, A., De Wolf, S., High-efficiency crystalline silicon solar cells: status and perspectives (2016) Energy & Environmental Science, 9, pp. 1552-1576.
[41] Joseph Day S., Mallick, S. T. K., Improving spectral modification for applications in solar cells: A review (2019) Renewable Energy, 132, pp. 186-205.
[42] Aberle, A. G., Mathew, B. B., Hoex, B., Mueller, T., Review industrial silicon wafer solar cells - status and trends (2012) Green, 2, pp. 135-148.
[43] Izatt, R. M., Izatt, S. R., Bruening, R. L., Izatt, N. E., Moy, B. A., Challenges to achievement of metal sustainability in our high-tech society (2014) Chemical Society Reviews, 43, pp. 2451-2475.
[44] Day, J., Senthilarasu, S., Mallick, T. K., Improving spectral modification for applications in solar cells: A review (2019) Renewable Energy, 132, pp. 186-205.
[45] Gouvêa, E. C., Sobrinho, P. M., Souza, T. M., Spectral response of polycrystalline silicon photovoltaic cells under real-use conditions (2017) Energies, 10, pp. 1178.
[46] Dale, B., Rudenberg, H. G., High efficiency silicon solar cells (1960) Proceedings of the 14th Annual Power Sources Conference, pp. 22.
[47] Lindholm, F. A., Fossum, J. G., Burgess, E. L., Application of the superposition principle to solar-cell analysis (1979) IEEE Transactions on Electron Devices, 26, pp. 165–171.
[48] Vant-Hull, L. L., Hildebrandt, A. F., Solar thermal power system based on optical transmission (1976) Solar Energy, 18, pp. 31 - 39.
[49] Tiedje, T., Yablonovich, E., Cody, G. D., Brooks, B. G., Limiting efficiency of silicon solar cells (1984) IEEE Transactions on Electron Devices, vol. ED-31, pp. 711-716.
[50] Sinton, R. A., Cuevas, A., Contactless determination of current–voltage characteristics and minority-carrier lifetimes in semiconductors from quasi-steady-state photoconductance data (1996) Applied Physics Letters, 69, pp. 2510-2512.
[51] Lojpur, V., Mitrić, M., Validžić, I.Lj., The improved photovoltaic response of commercial monocrystalline Si solar cell under natural and artificial light by using water flow lens (WFL) system (2019) International Journal of Energy Research, 43, pp. 3507-3515.
[52] Biwole, P., Eclache, P., Kuznik, F., Improving the performance of solar panels by the use of phase-change materials (2011) World Renewable Energy Congress, Sweden, 8-13 May, Linkoping, Sweden.
[53] Tina, G. M., Rosa-Clot, M., Lojpur, V., Validžić, I.Lj., Numerical and experimental analysis of photovoltaic cells under a water layer and natural and artificial light (2019) IEEE Journal of Photovoltaics, 9 (3), art. no. 8643369, pp. 733-740.

[54] Smith, K. D., Gummel, H. K., Bode, J. D., Cuttriss, D. B., Nielsen, R. J., & Rosenzweig, W., The solar cells and their mounting (1963) Telstar I. NASA SP-32 pp.1765.
[55] Kita, T., Harada, Y., Asahi, S., Energy conversion efficiency of solar cells (2019) Springer Singapore, Springer Nature Singapore Pte Ltd., ISBN: 978-981-13-9088-3.
[56] February 2010. http://alumni.media.mit.edu/~nate/AES/PV_Theory_II.pdf
[57] Neaman, D. A., Semiconductor Physics and devices: Basic Principles (2003) McGraw-Hill.
[58] Green, M. A., Solar Cells; Operating Principles, Technology and System Applications (1982) Prentice-Hall.
[59] van Overstraeten, R. J., Mertens, R. P., Physics, Technology and Use of Photovoltaics (1986) Adam Hilger Ltd.
[60] Sterling, H. F., Swann, R. C. G., Chemical vapour deposition promoted by r. f. discharge (1965) Solid-State Electronics, 8, pp. 653-654.
[61] Spear, W., Le Comber, P., Substitutional doping of amorphous silicon (1975) Solid State Communications, 17, pp. 1193-1196.
[62] Roland, S., Charge carrier recombination and open circuit voltage in organic solar cells: from bilayer-model systems to hybrid multi-junctions (2017) Dissertation, Faculty of Mathematics and Natural Sciences of the University of Potsdam, Berlin, Germany.
[63] Carlson, D. E., Wronski, C. R., Amorphous silicon solar cell (1976) Applied Physics Letters, 28, pp. 671-673.
[64] Yang, J., Banerjee, A., Lord, K., Guha, S., Proceedings of the 2nd World Conference and Exhibition on Photovoltaic Solar Energy Conversion (1998) Vienna, Austria, July 6 – 10, pp. 387-390.
[65] Hamakawa, Y., Okamoto, H., Nitta, Y., A new type of amorphous silicon photovoltaic cell generating more than 2.0 V (1979) Applied Physics Letters, 35, pp. 187-189.
[66] Kuwano, Y., Imai, T., Ohnishi, M., Nakano, S., Proceedings of the 14th IEEE Photovoltaic Specialist Conference (1980), pp. 1402.
[67] Tawada, Y., Okamoto, H., Hamakawa, Y., a-SiC:H / a-Si:H heterojunction solar cell having more than 7.1% conversion efficiency (1981) Applied Physics Letters, 39, pp. 237-239.
[68] Nakamura, G., Sato, K., Yukimoto, Y., Shirahata, K., Proceedings of the 3rd E.C. Photovoltaic Solar Energy Conference (1980), pp. 835.
[69] Deckman, H. W., Wronski, C. R., Witzke, H., Yablonovitch, E., Optically enhanced amorphous silicon solar cells (1983) Applied Physics Letters, 42, pp. 968-969.
[70] Arya, R. R., Carlson, D. E., Amorphous silicon PV module manufacturing at BP solar (2002) Progress in Photovoltaics: Research and Applications, 10, pp. 69-76.
[71] Okamoto, S., Terakawa, A., Maruyama, E., Shinohara, W., Tanaka, M., Kiyama, S., Amorphous and Heterogeneous Silicon-Based Films (2001), (Materials Research Society Symposium - Proceedings, 664, San Francisco, CA), A11.1. 12.

[72] Ichikawa, Y., Yoshida, T., Hama, T., Sakai, H., Harashima, K., Production technology for amorphous silicon-based flexible solar cells (2001) Solar Energy Materials & Solar Cells, 66, pp. 107-115.
[73] Guha, S., Yang, J., Banerjee, A., Amorphous silicon alloy photovoltaic research-present and future (2000) Progress in Photovoltaics: Research and Applications, 8, pp.141-150.
[74] Meier, J., Dubail, S., Flückiger, R., Fischer, D., Keppner, H., Shah, A., Intrinsic microcrystalline silicon (μc-Si:H)—a promising new thin film solar cell material (1994) Proceedings of the 1st IEEE World Conference on Photovoltaic Energy Conversion (WCPEC '94), vol. 1, pp. 409–412, Waikoloa, Hawaii, USA.
[75] Meier, J., Dubail, S., Cuperus, J., Kroll, U., Platz, R., Torres, P., Anna Selvan, J. A., Pernet, P., Beck, N., Pellaton Vaucher, Ch. Hof, N., Fischer, D., Keppner, H., Shah, A., Recent progress in micromorph solar cells (1998) Journal of Non-Crystal Solids, 227-230, pp. 1250-1256.
[76] Yamamoto, K., Yoshimi, M., Tawada, Y., Okamoto, Y., Nakajima, A., Thin film Si solar cell fabricated at low temperature (2000) Journal of Non-Crystal Solids, 266-269, pp. 1082-1087.
[77] Schropp, R. E. I., Zeman, M., Amorphous and microcrystalline solar cells: modeling, materials, and device technology (1998) Kluwer Academic Publishers.
[78] Street, R. A., Doping and the fermi energy in amorphous silicon (1982) Physical Review Letters, 49, pp. 1187-1189.
[79] Staebler, D. L., Wronski, C. R., Reversible conductivity changes in discharge-produced amorphous Si (1977) Applied Physics Letters, 31, pp. 292-294.
[80] Halls, J. J., Friend, R. H., Organic photovoltaic devices, in clean electricity from Photovoltaics (2001) Archer, M. D., Hill, R., Editors, Imperial College Press: London.
[81] Simon, J., Andre, J. J., Molecular semiconductors (1985) Berlin-Heidelberg: Springer Verlag, 142.
[82] Hoppe, H., Sariciftci, N. S., Organic solar cells: An overview (2004) Journal of Materials Research, 19(7), pp. 1924-1945.
[83] Gregg, B. A., Excitonic solar cells (2003) Journal of Physical Chemistry B, 107(20), pp. 4688-4698.
[84] Gregg, B. A., The photoconversion mechanism of excitonic solar cells (2005) MRS Bulletin, 30(1), pp. 20-22.
[85] Fahhad Alharbi, H., Kais, S., Theoretical limits of photovoltaics efficiency and possible improvements by intuitive approaches learned from photosynthesis and quantum coherence (2015) Renewable and Sustainable Energy Reviews, 43, pp. 1073–1089.
[86] Xakalashe, B. S., Tangstad, M., Silicon processing: from quartz to crystalline silicon solar cells (2011) Southern African Pyrometallurgy, Edited by R.T. Jones & P. den Hoed, pp. 73-99.
[87] Girish Kumar, S., Koteswara Rao, K. S. R., Physics and chemistry of CdTe/CdS thin film heterojunction photovoltaic devices: fundamental and critical aspects (2014) Energy & Environmental Science, 7, pp. 45–102.
[88] Masters, G. M., Renewable and efficient electric power systems (2013) 2nd Edition, Wiley-IEEE Press, ISBN: 978-1-118-63350-2.

[89] Ehrler, B., Alarcon-Llado, E., Tabernig, S. W., Veeken, T., Garnett, E. C., Polman, A., Photovoltaics reaching for the Shockley− Queisser limit (2020) ACS Energy Letters, 5, pp. 3029-3033.
[90] Gratzel, M., Dye-sensitized solar cells (2003) Journal of Photochemistry and Photobiology C: Photochemistry Reviews, 4, pp. 145-153.
[91] Bercx, M., Saniz, R., Partoens, B., Lamoen, D., Exceeding the Shockley-Queisser limit within the detailed balance framework (2018) In: Angilella G., Amovilli C. (eds) Many-body Approaches at Different Scales. Springer, Cham. https://doi.org/10.1007/978-3-319-72374-7_15.
[92] Bercx, M., Sarmadian, N., Saniz, R., Partoens, B., Lamoen, D., First-principles analysis of the spectroscopic limited maximum efficiency of photovoltaic absorber layers for CuAu-like chalcogenides and silicon (2016) Physical Chemistry Chemical Physics, 18, pp. 20542-20549.
[93] Lojpur, V., Mitrić, M., Kačarević-Popović, Z., Radosavljević, A., Rakočević, Z., Lj Validžić, I., The role of low light intensity: A cheap, stable, and solidly efficient amorphous Sb_2S_3 powder/hypericin composite/PVA matrix loaded with electrolyte solar cell (2017) Environmental Progress and Sustainable Energy, 36 (5), pp. 1507-1516.
[94] Lojpur, V., Mitrić, M., Validžić, I.Lj., The role of low light intensity: A step towards understanding the connection between light, optic/lens and photovoltaic behavior for Sb_2S_3 thin-film solar cells (2018) Optics and Laser Technology, 101, pp. 425-432.
[95] Lojpur, V., Mitrić, M., Validžić, I.Lj., The improved photovoltaic response of commercial monocrystalline Si solar cell under natural and artificial light by using water flow lens (WFL) system (2019) International Journal of Energy Research, 43 (8), pp. 3507-3515.
[96] Lojpur, V., Validžić, I.Lj., Influence of different light sources, light intensities, and water flow lens (WFL) system on dye-sensitized solar cell performances (2019) IEEE Journal of Photovoltaics, 9 (2), art. no. 8594565, pp. 492-498.
[97] Rhodes, C. J., Solar energy: principles and possibilities (2010) Science Progress, 93, pp. 37–112.
[98] http://ixapps.ixys.com/DataSheet/KXOB22- 01X8F_Nov16.pdf
[99] https://panasonic.co.jp/ls/psam/en/produc ts/pdf/Catalog_Amorton_ENG.pdf
[100] Reich, N. H., Sark, W. G. J. H. M. van, Turkenburg, W. C., Charge yield potential of indoor-operated solar cells incorporated into Product Integrated Photovoltaic (PIPV) (2011) Renewable Energy, 36, pp. 642-647.
[101] Gottschalg, R., Infield, D. G., Kearney, M., Experimental study of variations of the solar spectrum of relevance to thin film solar cells (2003) Solar Energy Materials and Solar Cells, 79, pp. 527-537.
[102] Kenny, R. P., Ioannides, A., Ullejans, H. M., Zaaiman, W., Dunlop, E. D., Performance of thin film PV modules (2006) Thin Solid Films, 511-522, pp. 663-672.
[103] Durisch, W., Urban, J., Smestad, G., Characterisation of solar cells and modules under actual operating conditions (1996) Proceedings of World Renewable Energy Congress, Pergamon Press, Oxford, Denver, CO, USA, 1, pp. 359-366.

[104] Emery, K. A., Solar simulators and I-V measurement methods (1986) Solar Cells, 18, pp. 251-260.

GENERAL CONCLUSION CONCERNING LIGHT EFFECTS

Cooling, decreasing, and increasing the light intensity with unavoidable oscillations in the spectrum is the basic function of the WFL system, but in fact, that manipulation helps us to better understand the additional light effects and, hence, the nature of the light itself, in order to make serious strides towards the use of solar energy. By studying various types of solar devices, such as monocrystalline and amorphous Si-solar cells, differently designed Sb_2S_3-based solar cells made of synthesized undoped and doped semiconductors, and dye-sensitized solar cells, it has been discovered that with the use of the WFL system, PV performance can exhibit large improvements in all tested conditions. It was also observed and proved that small changes in the light intensity values, simultaneously with spectra changes, cause large changes, primarily in the I_{sc} and V_{oc}. Those changes can be attributed at least to the spectrum effect (or some additional effect) that appears significant at the higher light intensity as well as the lower intensity of light, although so far it seems more dominant at low lighting. Because of the many realistic and testing effects that the designed WFL system has, such as the ability to test the influence of intensity and spectral change at the same time, as well as the cooling effect, this design could be a realistic choice for significantly improving the solar device response and expanding our knowledge of how to overcome the problem of low solar energy use.

Manipulation of light intensities and spectra using this type of design optics may aid in our understanding of the effects of light in general. In photovoltaics, light is, in most cases, only discussed in the form of particles or photons, neglecting its wave nature.[1-4] However, by using optics and the fact that light passes through different environments, we have all the right to consider the phenomenon from a wave point or the photon as a wave. Furthermore, in the conclusion, through a short historical review, the right to justify the passage of light through different environments through its wave nature is explained. Next, we noticed that the V_{oc} and I_{sc} without the use of the WFL system mostly obeyed the role that decreases with decreasing light intensity independently of spectra. It should be noted that there are a lot of experimentally proved and reported exceptions to the mentioned behavior in the scientific literature, as well as those described and listed here, which primarily refer to artificial light and lower light intensities, which should not be the case according to general postulates. Additionally, that role drastically changes after passing the light through the optical system. That should not be the case if we look at light only in the form of photons as a particle. I will try to simply as possible (without going deeper into theory because I am not a theoretical physicist) connect our results with the used optics with the light wave and photon theory and the facts, because the wave theory separately, as the only theory that failed, to see where that connection can logically lead. When I say wave nature (due to the wave character of light in performed experiments), we primarily mean in terms of amplitude or intensity, wavelength, and frequency as basic characteristics of light waves. These are also the fundamental properties of light intensities and spectra, the changes of which we demonstrate in the book using developed optics.

Historically, to explain the photoelectric effect in general, 19th-century physicists proposed that the incoming light wave's oscillating electric field heated the electrons and caused them to vibrate, eventually freeing them from the metal surface. This hypothesis was based on the assumption that light moved through space solely as a wave. Scientists also thought that the energy of a light wave was proportional to its brightness, which is related to the amplitude of the wave. They conducted experiments to investigate the effects of light amplitude and frequency on the rate of electron ejection as well as the kinetic energy of the photoelectrons in order to test their hypotheses. Huygens' theory of light refraction, based on the idea that light is wave-like, held that the velocity of light in any substance was inversely proportional to its refractive index. Huygens hypothesized that the more light was "bent" or refracted by a substance, the slower it would move while traversing that substance. It took over 150 years for the speed of light to be measured accurately enough to prove that Huygens' theory was correct. Huygens, despite his intuition, proposed in his 1690 treatise “Traité de la Lumière” that light waves be mediated by the “ether”, a mystical, weightless substance that exists as an invisible entity throughout air and space.[5-7] During the nineteenth century, the search for ether consumed a significant amount of resources before being abandoned. As evidenced by Charles Wheatstone's proposed model demonstrating that ether carried light waves by vibrating at an angle perpendicular to the direction of light propagation, and James Clerk Maxwell's detailed models describing the construction of the invisible substance, the ether theory lasted at least until the late 1800s.[8-11] It is interesting to mention here and make a small digression by saying that we need three hundred years before scientific papers containing different proofs that the ether exists and that the speed of light is anisotropic, or that it is not the same in all directions, appear. We emphasized these last developments further in the text. In general, when a light beam travels between two media with different refractive indices (as is the case with the WFL system through which light passes before falling on the surface of a solar cell or module), the beam refracts and changes direction. At that time, in order to determine whether a light beam is composed of waves or particles, a model was designed for both the natures of light in order to explain the phenomenon. Huygens' wave theory states that a small portion of each angled wavefront should impact the second medium before the rest of the front reaches the interface. This portion of the wave will begin to move through the second medium while the rest of the wave remains in the first medium, but at a slower rate due to the higher refractive index of the second medium. Because the wavefront is now moving at two different speeds, it will bend into the second medium, causing the angle of propagation to change. Particle theory, on the other hand, has a difficult time explaining why light particles change direction when they pass from one medium to another. According to proponents of the theory, a special force acting perpendicular to the interface changes the speed of the particles as they enter the second medium. The precise nature of this force has remained unknown, and no evidence to support the theory has ever been gathered.[12-14]

It is generally accepted that the photoelectric effect could not be rationalized based on existing wave theories of light, as an increase in the intensity of light did not lead to the same outcome as an increase in the energy of light. The key distinction between the wave and particle natures of light is that the wave nature of light states that light behaves as an electromagnetic wave and hence fails to explain the photoelectric effect, while the particle photon theory can explain the mentioned effect. Based on the classical description of light as a wave, the following predictions were made: that the kinetic energy of emitted photoelectrons should increase with the light amplitude, as well as that the rate of electron emission, which is proportional to the measured electric current, should increase as the light frequency is increased. When experiments were performed due to which the wave theory failed, the following results were observed: the kinetic energy of photoelectrons increases with light frequency, the electric current remains constant as light frequency increases, the electric current increases with light amplitude, and the kinetic energy of photoelectrons remains constant as light amplitude increases. On the basis of these results, it is concluded that the predictions based on the classical description of light as a wave are not possible to explain. It was concluded that an entirely new model of light was needed. The model proposed that light sometimes behaves like particles of electromagnetic energy, which we now call photons. In general, wave-particle duality is both a fundamental property of matter and one of modern physics' greatest mysteries, because it confuses the status of the nature of light. Light was undeniably a wave phenomenon; there were numerous examples of interference effects, wave signatures, and a well-developed electromagnetic wave theory. There was, however, undeniable evidence that light is made up of particles with well-defined energies and momenta. This perplexing wave-particle duality was quickly discovered to be shared by all elements of the physical world. The American physicist Richard Feynman said that, in a wholly unexpected fashion, quantum mechanics resolved the long wave-particle debate over the nature of light by rejecting both models. The behavior of light cannot be fully accounted for by a classical wave model or by a classical particle model. These images are useful in their respective regimes, but they are ultimately approximate, complementary descriptions of an underlying reality described quantum mechanically. The Dutch mathematician-astronomer Christiaan Huygens, who formulated the first detailed wave theory of light, said: "Demonstrations in optics, as in every science where geometry is applied to matter, are based upon experimental facts." Most writers on optical subjects have been satisfied with assuming these facts. But others, of a more investigative turn of mind, have tried to find the origin and the cause of these facts, considering them in themselves interesting natural phenomena. And although they have advanced some ingenious ideas, they are not such that the more intelligent readers do not still want the further explanation to be completely satisfied." It seems that we are still not satisfied with the theories of light, and we are still looking for satisfactory answers. Before returning to Huygens, it should be noted that by the end of the nineteenth century, the debate over whether light is a wave or a collection of particles appeared to be over. Heinrich Hertz's discovery of electromagnetic waves and James Clerk Maxwell's synthesis of electric, magnetic, and optical phenomena were both theoretical and experimental triumphs of the first order.[15-17] Maxwell's electromagnetism joined Newtonian mechanics and thermodynamics as a foundational element of physics. However, just as everything seemed to be coming to a close, a period of revolutionary change was ushered in at the turn of the twentieth century. A new interpretation of the emission of light by heated objects, combined with new experimental methods that allowed for the study of the atomic world, resulted in a radical departure from Newton's and Maxwell's classical theories. Quantum mechanics was born. The problem of interpreting wave-particle duality has been exacerbated by the advent of quantum mechanics. We should note that, in the end, the interpretation of quantum mechanics is reduced to attempts to explain the wave-particle duality. One could argue that the various interpretations of quantum mechanics are, in fact, different explanations of wave-particle duality. The nature of light was raised once more. The quantum mechanics embodied in the 1926–27 formulation is nonrelativistic, which means it only applies to particles traveling at speeds significantly slower than the speed of light.[18] The quantum mechanical description of light was not fully realized until the late 1940s, when quantum electrodynamics appeared.[18] The electric and magnetic fields described by Maxwell's equations are quantized, and photons appear as quantized field excitations. In quantum electrodynamics, photons are used as carriers of electric and magnetic forces. This theory provides a theoretical framework for processes involving matter-to-photon and photon-to-matter conversions. A photon that interacts with an atomic nucleus (to conserve momentum) disappears during pair creation, and its energy is converted into an electron and a positron (a particle-antiparticle pair). An electron-positron pair is destroyed in pair annihilation, and two high-energy photons are produced. By delving deeper into the history of various light theories, it appears that the most recent scientific papers (the last fifteen years) concerning experimental proofs and polemics that radiation does not consist of particles, light speed anisotropy, gravitational waves, or ether existence[19-23] bring us closer to and return us to the initial theories and postulates established hundreds of years ago. We will make a small digression here and say that as long as new theories and views on problems emerge, there will always be scientists who are not satisfied with the current explanations. It is the same with the problem I present in this book and the fact that everyone in photovoltaics knows that higher efficiencies can be obtained at lower light intensities with just minor changes in the spectra of the light sources, without involving light manipulation and without deepening the problem, but no one knows the explanation of the same. It seems that space is a medium that can flow, and that light (and matter) are waves that flow with respect to this medium. Other important consequences follow from this. The most recent experiments appear to have confirmed that the prevailing physics belief system holds that the speed of light is isotropic, that there is no preferred frame of reference, that absolute motion has never been observed, and that 3-space does not, and cannot, exist. This is the essence of Einstein's 1905 postulate that the speed of light is unaffected by the observer's choice. This postulate has shaped the course of physics over the last century. It seems that after more than three hundred years, we are again returning to the first officially stated light theory of Huygens, in which light as a wave is produced by a certain motion (or can be said vibration), that the medium in which this motion propagates is called ether, and that the speed of light is not constant in different media. Additionally, it seems quite justified that none of the parameters mentioned are constant, even if they are influenced by the change of speed, amplitude, intensity, frequency, wavelength, and energy. In contrast, our results with light manipulation and a changeable current output will be difficult to explain.

Furthermore, we try to make a comment on our results, such as that the electric current increases with light amplitude or light intensity, according to the photon light model. According to our results, this is not true even for measurements performed without the use of the WFL system, because it was observed that different light spectra can generate different efficiencies (lower light intensities produced higher efficiencies than the higher light intensities by changing at least the light spectra). Next, we confirmed that this is also not true after light passes through the designed optical WFL system. It has been shown that, independently of the light intensity, the photocurrent can increase and decrease by light manipulation, an effect that we attribute to the spectra effect, or frequency and wavelength wave changes, which are connected and conditioned. To be more precise, it seems that an increase in the light amplitude or light intensity doesn’t lead to an increase in the current. Further, another result to which the particle nature of light was applied is that the electric current remains constant as light frequency increases. Again, according to the fact that when waves travel from one medium to another (in our case, light passing through different environments like air, glass, and water), the frequency never changes, the experimental results reveal that electric current can go in both directions, decreasing as well as increasing the values. So, according to the mentioned results, the statement that electric current remains constant as light frequency increases failed. Hence, changes in electrical current should again be associated with electromagnetic light spectra, frequency, and wavelength changes. Because we have designed optics with different mediums and with different refractive indexes of these mediums, the explanation would be more complex due to the fact that many boundary behaviors of waves should be taken into account. We should take into account that the wave speed is always greatest in the least dense medium, that the wavelength is always greatest in the least dense medium, as well as that the frequency of a wave is not altered by crossing a boundary. In general, the higher efficiency of solar devices at lower light intensities can be explained only by the presence of an additional energy source, which can be light ether. Any deeper or more daring conclusions will not be drowned out here. It has been tried and wanted to comment on some basic postulates and compare them with our results in order to expand our knowledge concerning unclear light phenomena.

At the end of this chapter and book, I would just like to return to the beginning and the fact that we mentioned here that, so far, only 11% of global primary energy has come from renewable technologies, and around 1% of global energy has come from solar technologies. It has been already stated that it is not realistic that there is such a powerful source of energy as the Sun without us being able to use it better than the existing one. The development of new solar materials and devices is certainly one of the steps towards progress, but it is certainly not a step with which we will be able to make significant progress (in any case, for the last fifty years we have not shown it). Only by manipulating light spectra and intensity through innovative design, we can make significant progress toward better solar energy utilization and further light understanding through additional light effects. Even if someone disagrees with the conclusions presented here, they should agree with the fact that this method of research through innovative design offers useful insights into many unsolved and hot problems in PV applications. Further, it should be mentioned that investigations at low or weak light intensity are very important, but unfortunately, comparable data for the most tested solar cells is somehow lacking. There should be sufficient reasons presented here (higher efficiency of designed solar devices at lower light intensities without and with light manipulation) for setting the standard conditions related to weak or low light because the efficiency of PV cell performance is not constant and depends on the light intensity, technology, and spectra used. To achieve this task, it is important to combine the outdoor and indoor results and develop a model for calculating the efficiency of commercial solar cells at low and weak light intensities that includes the modified light distribution.

References

[1] Husain, A. A. F., Hasan, W. Z. W., Shafie, S., Hamidon, M. N., Pandey, S. S., A review of transparent solar photovoltaic technologies (2018), Renewable and Sustainable Energy Reviews, 94, pp. 779-791.

[2] Tyagi, V. V., Rahim, N. A. A., Rahim, N. A., Selvaraj, J. A. L., Progress in solar PV technology: research and achievement (2013) Renewable and Sustainable Energy Reviews, 20, pp. 443-461.

[3] Parida, B., Iniyan, S., Goic, R., A review of solar photovoltaic technologies (2011) Renewable and Sustainable Energy Reviews, 15, pp. 1625-1636.

[4] Holmes-Siedleb, A., van Lint, V. A. J., Radiation effects in electronic materials and devices (2003) Encyclopedia of Physical Science and Technology (Third Edition), pp. 523-559.

[5] Huygens, C., (translated by Silvanus P. Thompson, 1912), Treatise on Light, Project Gutenberg (2005), gutenberg.org/ebooks/14725.

[6] Dijksterhuis, F. J., Lenses and Waves: Christiaan Huygens and the Mathematical Science of Optics in the Seventeenth Century (2004) Archimedes. Springer Netherlands. ISBN 978-1-4020-2697-3.
[7] Ziggelaar, A., How did the wave theory of light take shape in the mind of Christiaan Huygens? (1980) Annals of Science, 37, pp. 179–187.
[8] Newton, I., Opticks (1704), Fourth edition of 1730. (Republished 1952 (Dover: New York), with commentary by Bernard Cohen, Albert Einstein, and Edmund Whittaker).
[9] Maxwell, J. C., A dynamical theory of the electromagnetic field (1865) (Part 1), https://upload.wikimedia.org/wikipedia/commons/1/19/A Dynamical Theory of the Electromagnetic Field.pdf.
[10] Maxwell, J. C., Ether (1878) in Baynes, T. S. (ed.), Encyclopædia Britannica, 8 (9th ed.), New York: Charles Scribner's Sons, pp. 568–572.
[11] Einstein, A., Zur Elektrodynamik bewegter Körper (1905) Annalen der Physik, 322 (10), pp. 891–921.
[12] https://micro.magnet.fsu.edu/primer/lightandcolor/particleorwave.html
[13] Aspect, A., From Huygens' waves to Einstein's photons: Weird light (2017) Comptes Rendus Physique, 18, pp. 498-503.
[14] https://en.wikipedia.org/wiki/Corpuscular_theory_of_light
[15] Baird, D., Hughes, R. I. G., Nordmann, A., Heinrich Hertz: Classical physicist, modern philosopher (1998) New York: Springer-Verlag. ISBN 0-7923-4653-X. pp. 49.
[16] Longair, M., …a paper …I hold to be great guns': a commentary on Maxwell (1865) A dynamical theory of the electromagnetic field (2015) Philosophical Transactions of the Royal Society A – Mathematical Physical and Engineering Sciences, 373, pp. 20140473.
[17] Qadir, A., Mason, D. P., Sesquicentennial of the presentation by James Clerk Maxwell of his paper "A dynamical theory of the electromagnetic field" to the Royal Society of London (2015) International Journal of Modern Physics: Conference Series, 38, pp. 1560070.
[18] https://www.britannica.com/science/light/Quantum-mechanics
[19] Lamb, W. E. Jr., Anti-photon (1995) Applied Physics B, 60, pp. 77-84.
[20] Cahill. R. T., A new light-speed anisotropy experiment: absolute motion and gravitational waves detected (2006) Progress in Physics, 4, pp. 73-92.
[21] Cahill, R. T., Brotherton, D., Experimental investigation of the Fresnel Drag effect in RF coaxial cables (2011) Progress in Physics, 1, pp. 43-48.
[22] Cahill, R. T., Combining NASA/JPL one-way optical-fiber light-speed data with spacecraft earth-flyby doppler-shift data to characterize 3-Space Flow (2009) Progress in Physics, 4, pp. 50-64.
[23] Cahill, R. T., Dynamical 3-Space: A Review, in: Ether space-time and cosmology: New insights into a key physical medium (2009) Duy M. and L´evy J. (Editors), Apeiron, pp. 135-200.